Université de Franche-Comté, Besançon
Laboratoire de Mécanique Appliquée Raymond Chaleat

University of Debrecen
Department of Solid State Physics

Effect of the Applied Stress on Shape Memory Alloys

Effet des contraintes appliquées sur le comportement des Alliages à Mémoire de Forme

CO-DIRECTED PHD THESIS
FRANCE-HUNGARY

Presented by
Zoltán Palánki

For the degree of
DOCTOR OF PHILOSOPHY

In the subject of:
MATERIAL SCIENCE

Jury de thèse:
Rapporteurs:
Dr. Christian LICHT, directeur de recherche CNRS LMGC, Montpellier (France)
Dr. János GINSZTLER, professeur titulaire, BME-MTA Group d'étude de technologie des métaux, Budapest (Hongrie)
Examinateurs:
Dr. Jean BERNARDINI, directeur de recherche CNRS L2MP, Marseille (France)
Dr. Lajos DARÓCZI, maître assistant DSSP, Debrecen (Hongrie)
Directeurs de thèse:
Dr. Christian LEXCELLENT, professeur ENSMM, Besançon (France)
Dr. Dezső L. BEKE, professeur DSSP, Debrecen (Hongrie)

Date de soutenance :
24 avril 2009

Acknowledgments

First of all, I thank my directors, Christian Lexcellent and Dezső Beke, for their confidence in me and all the support given by them. They always judged me according to my effort, which I must confess was not so intensive all the time. Nevertheless their scientific knowledge led always in the right direction finish this thesis.

On the other hand, I was so lucky to meet Lajos Daróczi whose leadership I started my work in the great world of material science with. Furthermore, I want to thank him all the conversations which revealed a lot of secrets not only of the physics but of engineering, too. He taught me the correct approach: if you can't buy it (or it does not exist), build it!

I don't have a sentimental temper but I should thank to someone or something for finding great fellows during the school years and joining to a research team which always cheered me up or it is just a wonderful case of the billions.

Additionally, I have to thank the French Government for Decree of 6th January 2005 about the international codirection of thesis (NOR: MENS0402905A), which allowed me to get know another country, another language, another culture and for meeting such people who I wouldn't have ever met without this scholarship.

At last but not least I must express my gratitude to my family who created the opportunities and supported me in all the decision I had to make to achieve this amazing result. So my success belongs to them, too.

Contents

Introduction

Introduction

The shape memory effect since its discovery has attracted the attention of scientist and engineers with its amazing phenomena and the micro mechanisms allowing a lot of promising applications. During the years a number of model descriptions were created to understand better the behaviour of different alloys making also possible to tailor the critical parameters important for technology.

In this thesis two models will be concerned. The one developed earlier in Debrecen enabled to calculate the non-chemical energy terms at the start and at the end of martensitic transformation. Nevertheless not only theses points are relevant but the knowledge of the dependence of the dissipative and elastic terms on the transformed martensitic fraction in the whole transformation range is important too. Consequently an extension of the model was needed. This new model was used to evaluate the data measured on polycrystalline and single crystalline CuAlNi shape memory alloys.

The results of the measurements on single crystalline samples could be explained only if two types of martensitic phases were taken into account. Indeed the Besançon-model developed for simulation of the martensitic transformation counts with two different martensitic phases, too, namely temperature and stress induced ones. After finding the connection between these two models and took them also into account in the Debrecen-model the determination of the input parameters for the simulations became possible and comparison between the measured and calculated hysteresis loops had been made.

Introduction

L'effet mémoire de forme, depuis sa découverte, a attiré l'attention des chercheurs et ingénieurs grâce à ses spécificités et aux mécanismes microscopiques associées. La connaissance de ces alliages a permis de développer beaucoup d'applications prometteuses. Pendant des années, de nombreuses expériences en ont été faites afin de mieux comprendre le comportement spécifique de ces alliages.

Dans cette thèse, deux modèles ont été utilisés. Celui développé à Debrecen (Hongrie) a permis de calculer les termes d'énergie non-chimique au début et à la fin de transformation martensitique. Nonobstant, non seulement ces termes sont indispensables mais la connaissance de la dépendance des termes dissipatifs et élastiques à la fraction de martensite transformée est, elle aussi, importante. En conclusion, une extension du modèle s'est avérée nécessaire. Ce nouveau modèle a été utilisé afin de rationaliser les mesures effectuées sur des alliages à mémoire de forme CuAlNi poly et monocristallins.

Les résultats de mesures sur l'échantillon monocristallin n'ont pu être interprétés que si le concept de deux types de phase martensitique est introduit. Le modèle de Besançon (France), développé pour expliquer la transformation martensitique, introduit ces deux martensites différentes (la martensite auto-accommodante et la martensite induite par la contrainte). On verra que cette partition n'a aucun sens crystallographique mais est simplement utile dans une approche phénoménologique. Après qu'un lien ait été établie entre ces deux modèles et que deux phases martensitiques aient été prises en compte dans le modèle de Debrecen, la détermination des paramètres nécessaires aux simulations devient possible, et la comparaison a pu être réalisée entre les boucles hystérésis mesurées et calculées.

Bevezetés

Az alakmemória effektus a felfedezése óta tudósokat és mérnököket nyűgözött le bámulatos jelenségeivel és az ezeket lehetővé tevő mikroszintű mechanizmusaival. Az évek során sok modell leírás született, a különböző típusú ötvözetek viselkedéseire lehetővé téve, hogy és végső soron tervezhetővé váljanak a technikailag fontos kritikus paraméterek.

Eben a dolgozatban két modellel foglalkoztam. A Debrecenben korábban kidolgozott lehetővé tette, hogy kiszámoljuk a nem-kémiai energiatagokat a martenzites átalakulás elején és végén. Azonban nem csak a végpontok a lényegesek, hanem a disszipativ és rugalmas energiatagoknak az átalakult martenzit hányadtól való függésének ismerete a teljes tartományban is fontos. Tehát a szükségessé vált a modell továbbfejlesztése. Ezt az új modellt használtuk polikiristályos és egykristályos CuAlNi alakmemória ötvözeteken mért adatok kiértékelésére.

Az egykristályos mintákon végzett kísérlet eredményeit csak úgy lehetett magyarázni, ha kétfajta marteznitfázist veszünk figyelembe. A martenzites transzformáció szimulációjára kifejlesztett besançoni model is kétfajta martenzittel számol, nevezetesen hőmérséklet és feszültségindukáltakkal. Miután a két modell közötti kapcsolat tisztáztuk és debreceni modellben is kétféle járulékkal számoltunk, lehetővé vált, hogy a mérési adatok alapján meghatározzuk a szimulációhoz szükséges paramétereket és végezetül pedig összehasonlítsuk a számolt és mért hiszterézis hurokokat.

Chapter I

Overview: Shape memory alloys, martensitic transformation

I. Overview: Shape memory alloys, martensitic transformation

The shape memory effect was discovered in 1951 in Au-Cd system, which was followed by Cu based alloys in 1956-57 and by TiNi in 1963 [O&W]. The last one is the most widely used shape memory alloy, because it has excellent mechanical properties and can also be applied in human bodies. Although the TiNi shape memory alloy is very useful in functional applications, it is expensive and, due to the research efforts, the cheaply producible Cu based systems can replace it in some cases.

I.1. Martensitic transformation

Martensite, the product of decomposition of the austenite, or a high temperature parent phase, through a martensitic transformation, was named after Adolf Martens (1850-1914), an engineer bringing significant contribution to the field of metallography and describing firstly the above mentioned transformation in steel.

The martensitic transformation takes place between two solid phases: the high symmetry (mostly cubic) lattice structure, stable at high temperature, – called parent or austenitic phase (A) – transforms into a structure with low symmetry (possessing several variants with different orientations) stable at low temperature – martensitic phase (M). Since only the lattice structure changes during these transitions, the displacements of atoms are less than the lattice constant, i.e. it is a diffusionless transformation and the velocity of interface shift is in the order of the speed of sound, which means that the propagation of the transformation is very similar to the propagation of shock waves in meterials. [Nishiyama, Funakubo, Otsuka and Waymann]

I.2. Thermodynamic aspect

I.2.1. Energy contributions

In general from austenite to martensite phase transformations the change of the Gibbs free energy can be written (if we neglect the interface term for nucleation) as [F, C&H]:

$$\Delta G = \Delta G_c + \Delta G_{nc} \qquad \text{with} \qquad \Delta G_{nc} = \Delta G_e + \Delta G_d \tag{I.1}$$

Here ΔG_c is the change in the *chemical* Gibbs-free energy of the two phases (the driving force for the transformation), and there is a non-chemical contribution, ΔG_{nc}, composed of elastic (ΔG_e) and dissipative (ΔG_d) terms. The elastic energy accumulates as well as releases during the processes down and up just because the formation of different variants of the martensite phase usually is accompanied by a development of an elastic energy field (due to the transformation strain). The dissipative energy is always positive in both directions and results in the hysteretic behaviour.

Fig. I.1 shows schematically the chemical free energies of the two different phases and the position of the equilibrium transformation temperature, below and above of which the martensitic and austenitic phases are stable, respectively.

$$G_c^{\ A}(T_0) = G_c^{\ M}(T_0)$$

Denoting the transformed fraction by ξ (ξ =1, and ξ=0 correspond to pure martensite and austenite phases, respectively) Fig. I.2. illustrates the hysteretic behaviour of the transformation: a) is the transformation without elastic and dissipative contributions, b) no elastic contribution is present (during cooling, due to the dissipative energy assumed to be independent of ξ, the transformation starts only at a certain undercooling, and in the opposite direction it starts only at a certain overheating), c) general case: the elastic energy, which is usually ξ-dependent, is positive in cooling down and negative in the heating up branches).

In *thermoelastic* transformations the interface term is generally negligible, but the elastic term plays a determining role. For example at a given under-cooling for further growth of the martensite an additional under-cooling is required. Thus if the sample is further cooled the particle of the M phase will grow further, while if the sample is heated it will become smaller. Indeed in *thermoelastic* materials it was observed that once a particle formed and reached a certain size its growth was stopped and increased or decreased as the temperature was decreased or raised. This is *the thermoelastic behaviour* (the thermal and elastic terms are balanced).

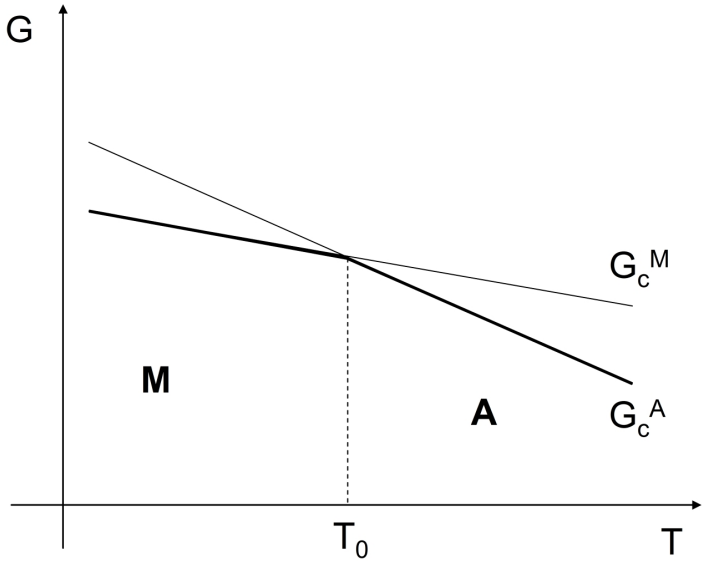

Figure I.1: Chemical free energies and the position of the equilibrium temperature

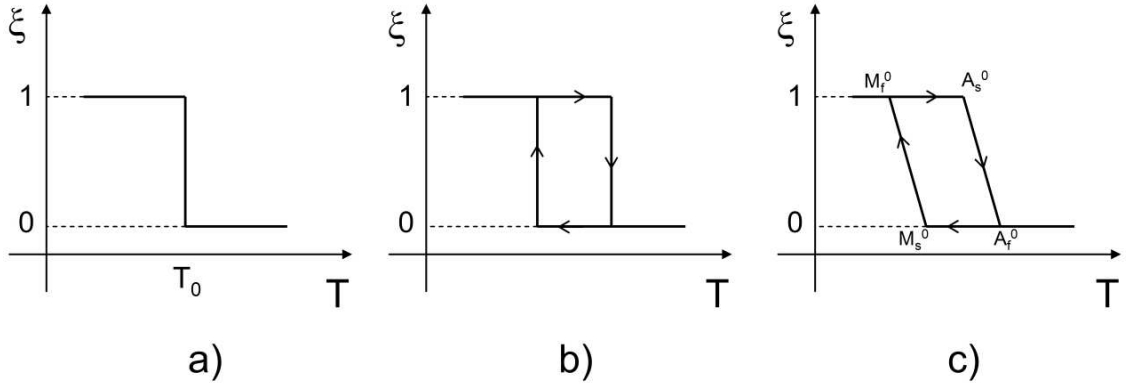

Figure I.2: Martensitic fraction (ξ) vs. temperature (T) considering the chemical and non-chemical contributions

I.2.2. Characteristic temperatures

Four temperatures are used to characterize the martensitic transformation (at external stress free state) which can be determined from a measured full hysteresis curve:

- M_s^0 – martensite start
- M_f^0 – martensite finish
- A_s^0 – austenite start and
- A_f^0 – austenite finish

temperatures as it can bee seen in Fig. I.2/c. For example the martensite and austenite start temperatures indicate the beginning of the formation of the martensitic and austenitic phases, respectively. The above temperatures depend on the equilibrium transformation temperature and, in general, they contain contributions from the non-chemical energies: this dependence will be analyzed in Chapter II and III.

The characteristic temperatures are measurable, but the most important one, the equilibrium temperature, T_0, cannot be directly determined from a usual hystersis loop measurement. Tong and Wayman [Tong Wayman] proposed that taking the arithmetic mean value of M_s and A_f can be a good approximation for T_o. However, Salzbrenner and Cohen [S&C] have shown that in general this is not a correct approximation. Furthermore these authors have also indicated that under special circumstances (using single crystalline specimens and special gradient heating technique) the T_0 can be determined even from this approximate relation.

It is worth to note that the knowledge of the equilibrium transformation temperature is very important for the simulations of martensitic transformations.

I.3. Mechanical properties of shape memory alloys

I.3.1. Shape memory effect

The shape memory alloys are really interesting and widely used in a wide variety of technological application because, as it is included in their names, they remember their shapes. This kind of memory effect arises from the martensitic transformation, precisely from the fact that the low temperature phase has more variants while the high temperature one exists in only one form.

Let us consider a 2D case when the austenitic phase is a square lattice and the martensite is a rhomboid one. Cooling the austenite without any external stress, the martensite evolves randomly and it can transform back to austenitic phase reversibly during heating. But if an external stress is applied, the variants with preferred orientations will grow in expense of the un-preferred ones. Furthermore, increasing the applied stress the balance between the two types of martensite shifts further toward the preferred variant and finally the whole sample transforms to a one variant state with a well measurable deformation. But, reheating the sample it returns to the austenitic phase, having only one variant, and thus the sample recovers to its original shape. (Fig. I.3); this is the so called one *way shape memory effec*t. If the shape memory material is trained, i.e. the above forward and reverse transformations are repeatedly applied several times, the sample will deform in the same way, changing only the temperature (although the magnitude of the deformation will be less); this phenomenon is called *two way shape memory effect*.

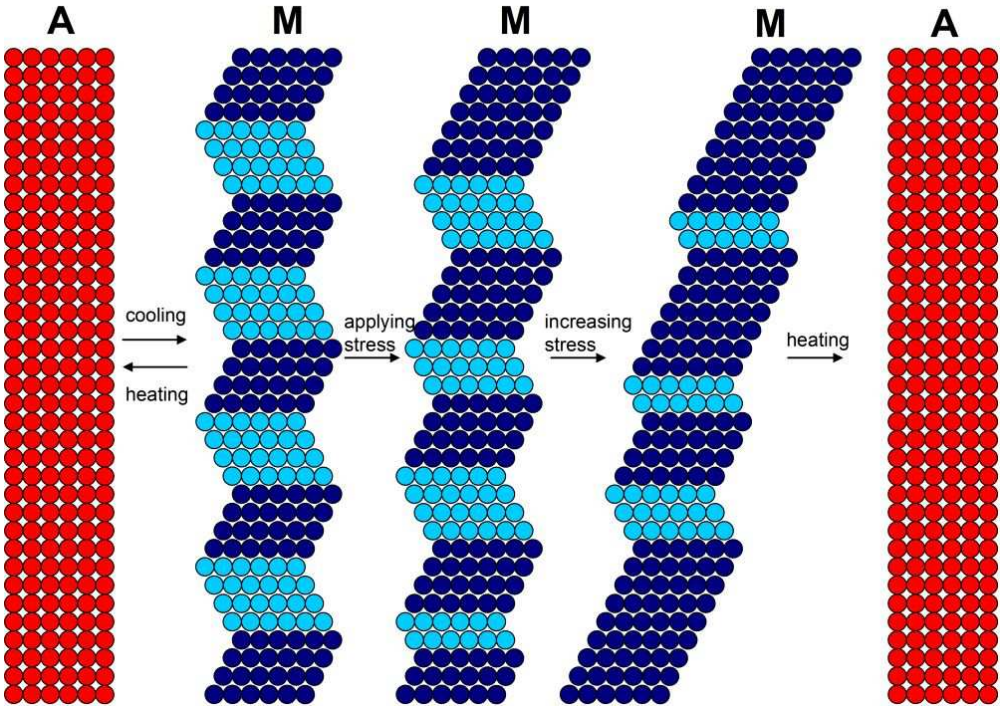

Figure I.3: Demonstration of the one way shape memory effect

After austenite/martensite transformation, due to the deformation strain, a characteristic surface pattern (surface relief) can be observed as it is illustrated in Fig. I.3 in the event the presented piece of material is at the surface. For the investigation of this phenomenon a piece of material has to be polished mechanically or electrically in austenitic or martensitic phase, and then it has to be cooled down or heated up. Although Fig. I.3 shows only the cooling down case one can easily imagine that the relief can be seen after the "reverse" process, too. Such kind of pattern can be seen in Fig. I.4.

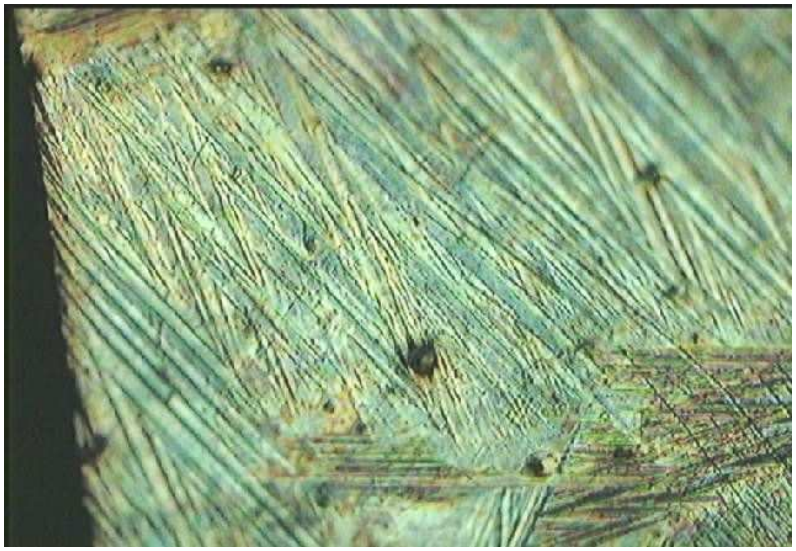

Figure I.4: The characteristic relief on the surface of a CuAlNi sample

The appearance and disappearance of the surface relief are also indications of the start and the end of the forward and reverse martensitic transformation, respectively. Unfortunately, using this method one can only determine the start and the end of the transformation. However, not only this method is appropriate to follow the transition. Since the values of different physical quantities (e.g. specific electrical resistance, strain) of the austenite and the martensite phases are different from each other, measuring on of them versus the temperature a hysteresis loop will be formed. The shape of the hysteresis usually characterizes the shape memory alloy itself; Fig. I.5 and Fig. I.6 show examples for the case of TiNi and CuZnAl alloys, respectively.

I.3.2. Pseudo-plasticity (Superplasticity)

Another feature of the shape memory materials comes from that fact that small loading force is enough to reorient the martensite variants and thereby to deform the alloy. Depending on the shape memory alloy this behaviour can result in a plateau on the stress-strain curves (Fig. I.7).

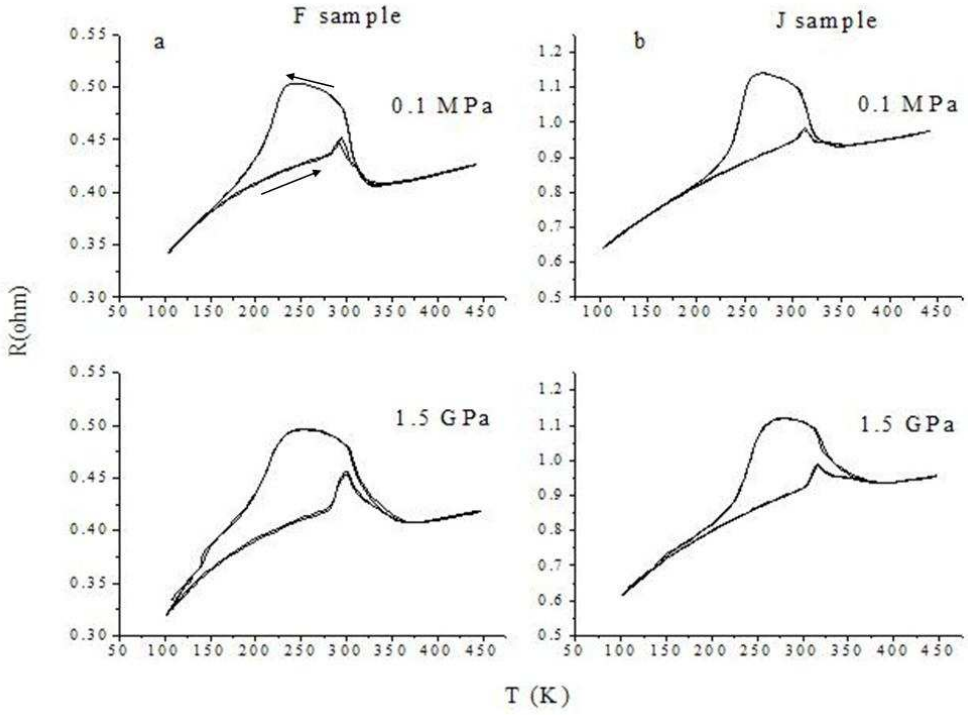

Figure I.5: Measured hysteresis loops on near equiatomic NiTi under constant hydrostatic pressure (Figs. 2/a and 2/b of Ref. [Detal02])

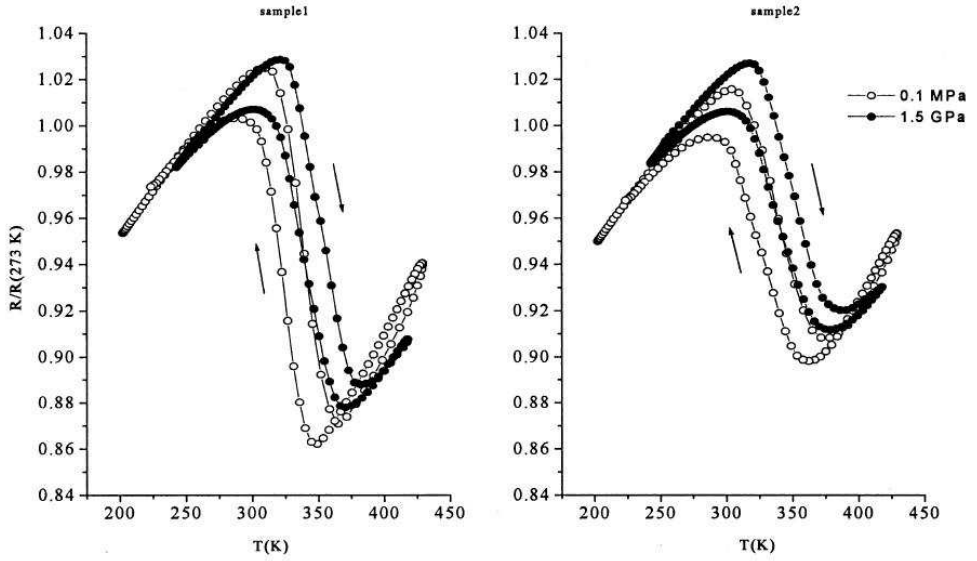

Figure I.6: Measured hysteresis loops on CuZnAl(Mn) under constant hydrostatic pressure (Fig. 1 of Ref. [Detal00])

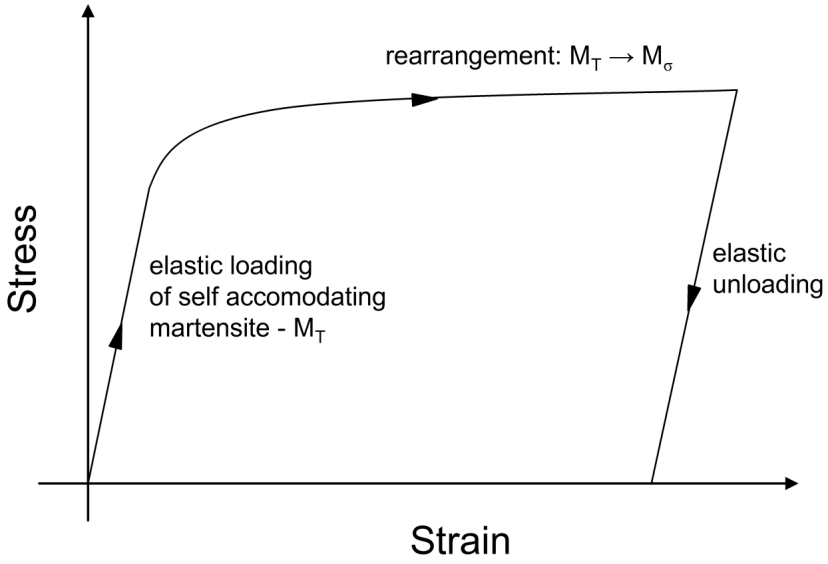

Figure I.7: The pseudo-plasticity behaviour (schematic curve)

I.3.3. Pseudo-elasticity (Superelasticity)

So far only stress free, thermally induced martensitic transformations, like the one- and two-way shape memory effects, were considered. Stress induced martensitic transformations exist, too. This phenomenon can be explained by the stress dependence of the martensitic transformation. As illustrated in Fig. I.8, although the temperature of the sample doesn't change, at a certain level of the applied stress the phase transformation takes place in the alloy.

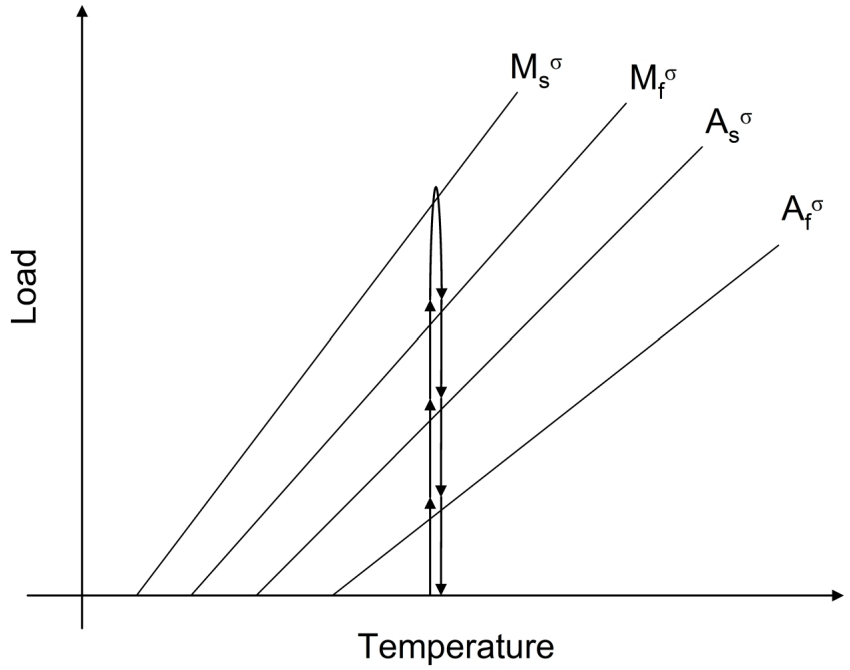

Figure I.8: Stress dependence of the transformation temperatures and the way of the stress induced martensitic transformation schematically

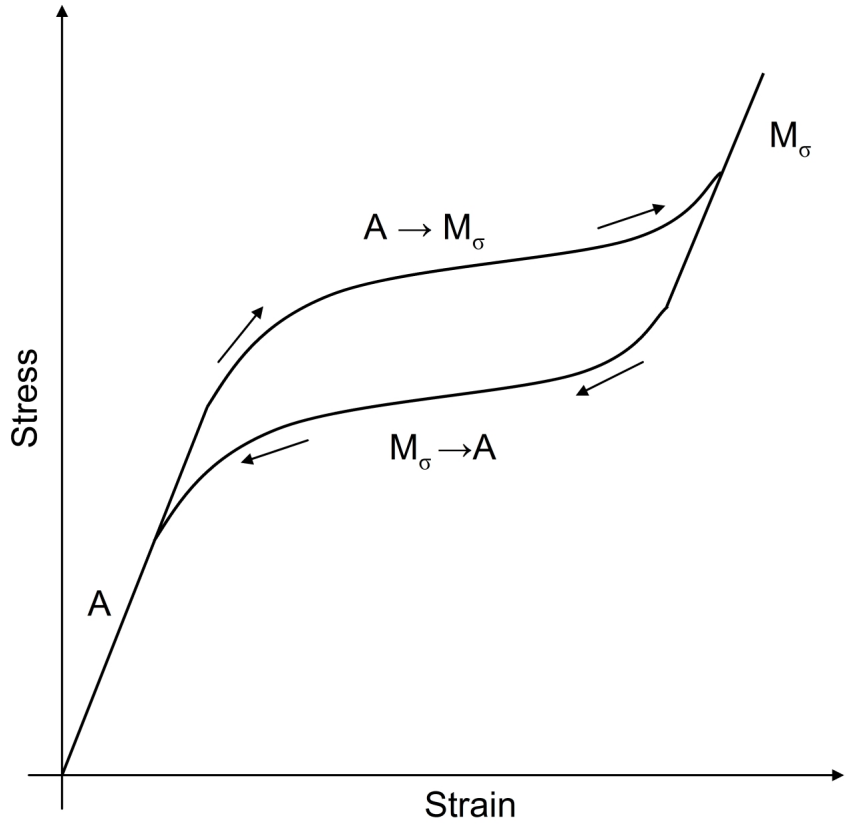

Figure I.9: Typical stress-strain curves of a stress induced martensitic transformation (schematic figure)

The pseudo-elasticity, similarly to the pseudo-plasticity, occurs at a constant temperature, but in this case at the beginning the specimen is completely composed of austenite (above A_f). Loading the shape memory alloy it is deformed and the martensitic transformation starts. If the loading is ceased, the reverse transition begins and finally the sample recovers its original shape. So it traces such a way like in Fig. I.8. This behaviour expressed in the stress-strain diagrams characteristically with a hysteresis effect (Fig. I.9).

I.4. Applications

Nowadays the shape memory alloys are widely applied even in every day life. For example one receives a wire of NiTi as orthodontic material at the dentist, or the eyeglass frame (Fig. I.10) is made also of NiTi [W&S]. In these two applications different features of the shape memory alloys are used.

Figure I.10: Glass frames made of NiTi (Fig. 2 of Ref. [W&S])

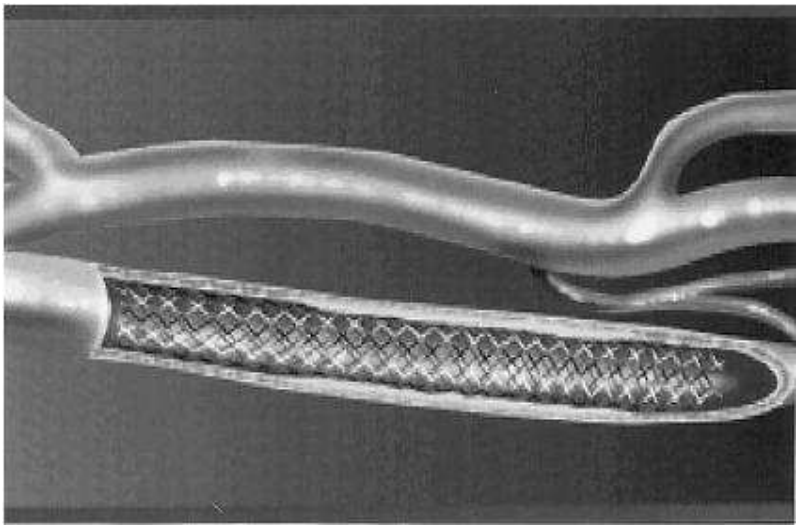

Figure I.11: Vascular stent (Fig. 1 of Ref. [Detal00])

In orthodontic applications of NiTi alloys the one way shape memory effect is used: cooling down the shape memory wire is fixed to the denture and in the mouth it is heated up, so it retransforms to austenite, recovers its original shape and in this way provides a constant tensional load (without any recalibration). Furthermore, this effect works e.g. in thermostats or in vascular stents too (Fig. I.11) [Detal00].

Thanks to the superelasticity the eyeglass frame can regain its original shape, and the same feature is utilized for example in bra underwires [W&S] or in some medical tools (Fig. I.12) [Detal00].

Besides the commercial applications the shape memory alloys are present in the modern technologies like the space shuttles [R&C] and do theirs bit from the science research like micro-manipulators.

Furthermore, the shape memory alloys start to be very important in the building trade, because thanks to the superplasticity they can applied as energy dissipaters or dumpers, so they can be very useful against earthquakes or the vibrations caused by wind. [Getal]

I.5. Magnetic shape memory alloys

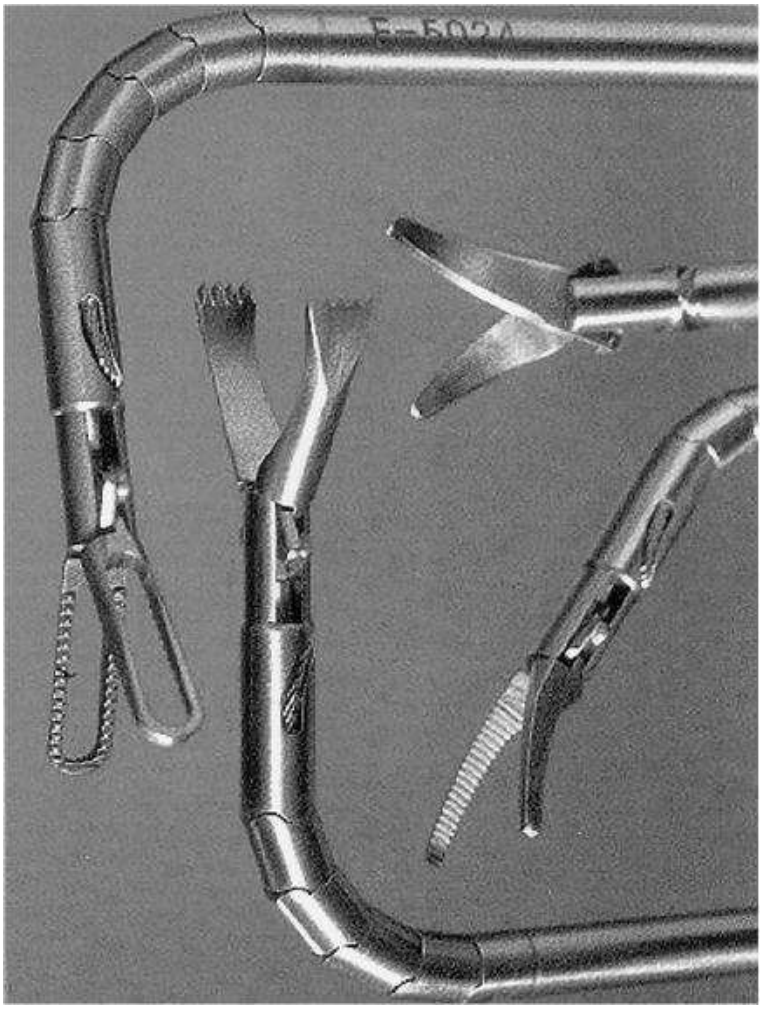

Figure I.12: Surgical innovations endoscopic instruments use nitinol rods to actuate scissors, graspers, etc. (Fig. 7 of Ref. [Detal99])

Nowadays the magnetic shape memory alloys stand in the centre of the many investigations, because they can be switched by magnetic field due to the coupling between the mechanical and the magnetic fields. For example very fast actuators can be constructed using them. The most promising magnetic shape memory alloy is NiMnGa, but it has very high switching field and it is hardly treatable because of its weak mechanical properties (brittleness). Hence, in some laboratories scientists and engineers are searching for a new magnetic shape memory alloy or for an appropriate modification (e.g. by microalloying) of it.

References

[O&W98] K. Otsuka and C. M. Wayman: *Shape Memory Materials*, 1998 Cambridge University Press
[F87] H. Funakubo: *Shape Memory Alloys*, 1987 Gordon and Breach Science Publisher
[N78] Z. Nishiyama: *Martensitic transformation*, 1978 Academic Press
[C&H96] R. W. Cahn, and P. Hasen, (Eds.) *Physical Metallurgy* North Holland, Amsterdam, 1996
[S&C79] R. J. Salzbrenner and M. Cohen: *On the thermodynamics of thermoelastic martensitic transformation* Acta Metallurgica **27** (1979) p. 739
[Detal02] L. Daróczi, D.L. Beke, C. Lexcellent and V. Mertinger: *Effect of hydrostatic pressure on the martensitic transformation in near equiatomic TiNi alloys*, Philos. Mag. B **82** (2002) p. 105
[Detal00] L. Daróczi, D.L. Beke, C. Lexcellent and V. Mertinger: *Effect of hydrostatic pressure on the martensitic transformation in CuZnAl(Mn) shape memory alloys*, Scripta materialia **43** (2000) p. 691
[Getal06] G. Song, N. Ma, H.-N. Li: *Applications of shape memory alloys in civil structures*, Engineering Structures **28** (2006) p. 1266
[R&C03] A. Razov and A. Cherniavsky: *Application of SMAs in modern spacecraft and devices*, Journal de physique. IV **112** (2003) p. 1173
[W&S00] Ming H. Wu and L. McD. Schetky: *Industrial applications for shape memory alloys*, Proceedings, SMST-2000, Pacific Grove, California, p. 171-182
[Detal99] T. Duerig, A. Pelton and D. Stöckel: An overview of nitinol medical applications Material Science and Engineering A **273-275** (1999) p. 149-160
[Setal06] O. Söderberg, A. Sozinov, Y. Ge, S-P. Hannula and V.K. Lindroos: *Giant magnetostrictive materials*, Handbbok of magnetic materials **16** (2006) p. 1

Chapter II

Summary of literature: motivation of my work

II. Summary of the literature: motivation of my work

In this chapter two models, describe the martensitic transformation, will be presented. For the reason that one can always know which model is talking about, I kept the original notations of the authors as well as in the Chapter IV, too.

II.1. Analysis of hysteresis loops and results of DSC measurements

II.1.1. Model for the description of the hysteretic behaviour

The model (Beke-Daróczi, in Refs. [Detal00] and [Detal02]) provides a suitable way for the determination of the non-chemical energy contributions from a measured thermal hysteresis loop. It starts from the Gibbs free energy change of the system during forward and reverse transformations, provides expressions for the transformation temperatures at the start and finish temperatures. For the determination of the non-chemical terms, however one has to know the value of T_0, where the chemical free energies of the parent and product phases are equal to each other; in the absence of this the elastic energy contributions can only be estimated exclusive a term containing T_0. Its generalization for obtaining the ξ-dependence of the non-chemical terms and for the comparison of the integrals of the results obtained form the hysteresis loops with DSC data will be described in Chapter III.

II.1.1.1. Basic equations for the start and finish temperatures

The equilibrium line during the austenite→martensite (A→M or forward) transformation – using superscript down arrows to indicate the cooling down process ($\downarrow$ for A→M) – is defined by the following equation:

$$\frac{\partial\left(\Delta G^{\downarrow}\right)}{\partial\xi} = \Delta g_c^{\downarrow} + e^{\downarrow}(\xi) + d^{\downarrow}(\xi) = 0\,, \qquad \text{(II.1)}$$

where it is assumed that the change in the chemical free energy per mole, $\Delta g_c^{\downarrow}$, is independent of the transformed fraction, ξ ($0 \le \xi \le 1$), and

$$\Delta g_c^{\downarrow} = \Delta h_c^{\downarrow} - T\Delta s_c^{\downarrow}\,. \qquad \text{(II.2)}$$

In (II.1) *e* and *d* denote the derivatives of the elastic and dissipative energies.

Here $\Delta h_c^{\downarrow} = h^M - h^A$ (<0) and $\Delta s_c^{\downarrow} = s^M - s^A$ (<0) (the M phase is the low temperature phase) are the free enthalpy and entropy changes, respectively. Furthermore, at the "equilibrium transformation temperature", T_0 (the temperature of zero-change in the chemical free energy)

$$\Delta g_c^{\downarrow}(T_0) = 0\,, \qquad \text{i.e.} \qquad T_0 = \Delta h_c^{\downarrow} / \Delta s_c^{\downarrow} = \Delta h_c^{\uparrow} / \Delta s_c^{\uparrow}\,, \qquad \text{(II.3)}$$

and e.g. at any temperature different from T_0

$$\Delta g_c^{\downarrow}(T) = (T_0 - T)\Delta s_c^{\downarrow}. \qquad \text{(II.4)}$$

If $T<T_o$ then there is an under-cooling and $\Delta g_c^{\downarrow}(T)$ is negative.

The temperature at which (II.1) is equal to zero for $\xi=0$ as well as for $\xi=1$ is the martensite start (M_s) and finish (M_f) temperature, respectively.

Similar considerations are valid for the martensite→austenite (M→A or reverse) transformation, but since now $\Delta h_c^{\uparrow}=-\Delta h_c^{\downarrow}$ and $\Delta s_c^{\uparrow}=-\Delta s_c=-\Delta s_c^{\downarrow}$ – according to (II.4) – $\Delta g_c^{\uparrow}<0$ can be fulfilled only if $T>T_0$. Indeed again the temperature at which (II.1) is zero for $\xi=1$ as well as for $\xi=0$ are the austenite start ($A_s>T_0$, i.e. an overheating is necessary) and austenite finish temperatures (A_f).

Thus

$$M_s = T_0 - \frac{d_0^{\downarrow} + e_0^{\downarrow}}{-\Delta s_c}$$

$$M_f = T_0 - \frac{d_1^{\downarrow} + e_1^{\downarrow}}{-\Delta s_c}$$

$$A_f = T_0 + \frac{d_0^{\uparrow} + e_0^{\uparrow}}{-\Delta s_c} \qquad \text{(II.5)}$$

$$A_s = T_0 + \frac{d_1^{\uparrow} + e_1^{\uparrow}}{-\Delta s_c}.$$

where the 0 and 1 subscripts mean the pure austenite and pure martensite phases (e.g. $d^{\downarrow}_0=d^{\downarrow}(\xi=0)$ and $e^{\uparrow}_1=e^{\uparrow}(\xi=1)$). Obviously if one measures the thermal hysteresis loop at fixed external field (e.g. at a fixed uniaxial stress, σ, or at a fixed hydrostatic pressure, p) in relation (II.5) all quantities on the right hand side in principle will be the function of σ (or p), too. In this case however, we have an additional relation for the derivative of the equilibrium transformation temperature: this is the Clausius-Clapeyron equation.

II.1.1.2. Clausius-Clapeyron equation

This relation can be derived from (II.2), if it is extended by the form(s) of the energy contributions to Δg_c, related to the effect of the field(s) in question. For example for the effect of uniaxial stress:

$$\Delta g_c^{\downarrow} = \Delta u_c^{\downarrow} - T_0 \Delta s_c - V_0 \sigma \varepsilon^{tr} = 0, \qquad \text{(II.6)}$$

or for the presence of hydrostatic pressure

$$\Delta g_c^{\downarrow} = \Delta u_c^{\downarrow} - T_0 \Delta s_c + pV^{tr} = 0\,, \qquad \text{(II.7)}$$

where ε^{tr} or V^{tr} are the transformation strain and the relative volume change due to the transformation, respectively and V_0 denotes the volume of the sample.

For the effect of uniaxial stress (σ) field

$$\frac{\partial}{\partial \sigma}\left(\Delta g_c^{\downarrow}\right) = 0 \qquad \text{(II.8)}$$

gives (assuming that Δu_c is independent of σ)

$$\frac{\partial(\Delta s_c T_o)}{\partial \sigma} = -\frac{\partial\left(\sigma V_0 \varepsilon^{tr}(\sigma)\right)}{\partial \sigma} \qquad \text{(II.9)}$$

If one also considers that $\varepsilon^{tr}(\sigma)$=const and Δs_c=const, i.e. they don't depend on the stress, the (II.9) equation leads to the usual form:

$$\frac{\partial T_o}{\partial \sigma} = -\frac{V_0 \varepsilon^{tr}}{\Delta s_c}\,. \qquad \text{(II.10)}$$

Similarly, in case of hydrostatic pressure (p) and taking again that Δs_c=const and V^{tr}=const,

$$\frac{\partial T_0}{\partial p} = \frac{V^{tr}}{\Delta s_c}\,, \qquad \text{(II.11)}$$

and for external magnetic field (B)

$$\frac{\partial T_0}{\partial B} = -\frac{M^{tr}}{\Delta s_c}\,, \qquad \text{(II.12)}$$

where M^{tr}, the change in magnetization due to the transformation (and M^{tr}=const.).

II.1.1.3. Integral quantities

The heats ($Q^{\downarrow}$ and $Q^{\uparrow}$) of the forward and reverse transformations can be measured in a calorimeter, e.g. in case of a heat compensation differential scanning calorimeter (DSC) measurement they will be equal to the area of the peaks during A→M and M→A transitions, respectively. (Fig. II.1) This heat emission or absorption originates from the latent heat (ΔH_c<0) – whose magnitude is the same for both directions and only its sign is different – and the non-chemical free energies.

$D^{\downarrow}$ and $D^{\uparrow}$ mean the energy dissipated mainly due to the friction stresses required to move interface during forward and reverse transformation, respectively, as well as $E^{\downarrow}$ is the whole stored energy by the formation of the martensite phase and $E^{\uparrow}$ releases during

martensite/austenite transition and so helps the transformation. From this one can see that the assumptions, which will be discussed in the next section, have physical background.

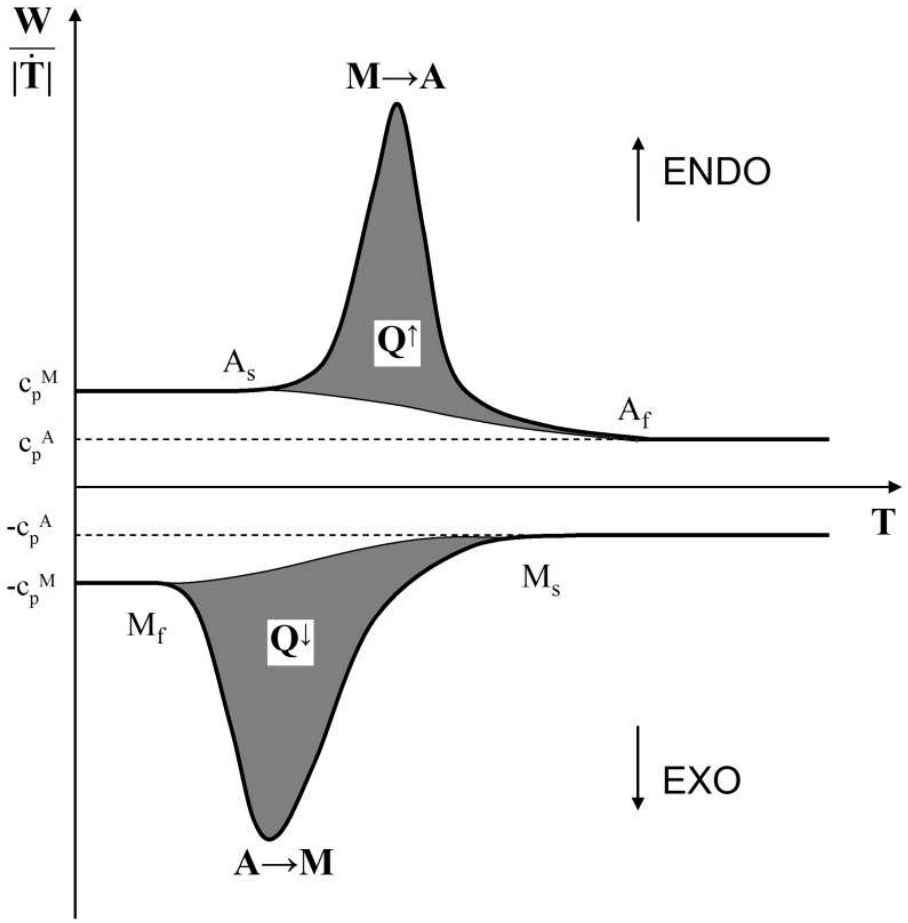

Figure II.1: Schematic figure of a DSC curve corresponding to martensitic transformation (modified version of Fig. 7 of Ref. [O&P88])

$$Q^{\downarrow} = \Delta H_c + E^{\downarrow} + D^{\downarrow}$$
$$Q^{\uparrow} = -\Delta H_c + E^{\uparrow} + D^{\uparrow} \qquad \text{(II.13)}$$

One can compose the sum and the difference of these heats:

$$Q^{\downarrow} - Q^{\uparrow} = 2\Delta H_c + E^{\downarrow} - E^{\uparrow} + D^{\downarrow} - D^{\uparrow}$$
$$Q^{\uparrow} + Q^{\downarrow} = E^{\uparrow} + E^{\downarrow} + D^{\uparrow} + D^{\downarrow}. \qquad \text{(II.14)}$$

II.1.1.4. Typical assumptions used in the evaluations

In order to determine the elastic and dissipative contributions from hysteresis loops additional assumptions are needed. It is usually assumed for shape memory alloys, that

$e_o=e_o^{\downarrow}=-e_o^{\uparrow}$ (and $e_1=e_1^{\downarrow}=-e_1^{\uparrow}$). Similarly it can also be assumed that $d_o=d_o^{\downarrow}=d_o^{\uparrow}$ (and $d_1=d_1^{\downarrow}=d_1^{\uparrow}$). Then from (II.5)

$$M_s = T_0 - \frac{d_0 + e_0}{-\Delta s_c} = T_0 - T_{d0} - T_{e0},$$

$$M_f = T_0 - \frac{d_1 + e_1}{-\Delta s_c} = T_0 - T_{d1} - T_{e1},$$

$$A_f = T_0 + \frac{d_0 - e_0}{-\Delta s_c} = T_0 + T_{d0} - T_{e0}, \qquad \text{(II.15)}$$

and

$$A_s = T_0 + \frac{d_1 - e_1}{-\Delta s_c} = T_0 + T_{d1} - T_{e1}$$

result, where the T_{d0}, T_{d1}, T_{e0} and T_{e1} are the "non-chemical" temperatures corresponding to the derivatives of dissipative and elastic terms. They can be written as:

$$T_{d0} = \frac{d_0}{-\Delta s_c} \quad (\geq 0) \quad ; \qquad T_{d1} = \frac{d_1}{-\Delta s_c} \quad (\geq 0)$$

$$T_{e0} = \frac{e_0}{-\Delta s_c} \quad (\geq 0) \quad ; \qquad T_{e1} = \frac{e_1}{-\Delta s_c} \quad (\geq 0) \qquad \text{(II.16)}$$

Evaluating thermal hysteresis cycles the transformation temperatures, i.e. the left sides of (II.15), can be determined but terms on the right sides – except of the entropy change – all are unknown; we have five unknowns and four equations, so not all of unknowns can be calculated The evaluation is usually done by using these equations, but as one can see the elastic term cannot be determined exactly, if the value of the T_0 isn't known from an independent measurement (as it is so in many cases). Anyway from the right combination of the (II.15) equations the dissipative terms can be exactly determined but the expressions of the elastic ones contain the value of T_0.

According to the above assumptions and due to the fact that in relations (II.14) the E and D quantities are the integrals of the differential quantities treated above one can also assume: $E^{\downarrow}=-E^{\uparrow}=E(>0)$ and $D^{\downarrow}=D^{\uparrow}=D(>0)$ and so:

$$Q^{\uparrow} - Q^{\downarrow} = -2\Delta H_c - 2E$$

$$Q^{\uparrow} + Q^{\downarrow} = 2D. \qquad \text{(II.17)}$$

It is important to note that the last equations are strictly valid only in that case if the system comes back to the same thermodynamic state after a cycle, i.e. it does not evolve from cycle to cycle. Ortin and Planes [O&P88] showed that (II.14/b) is only valid if the heat

capacities of the phases (c_p^A and c_p^M) are equal to each other, but in general the next relation is true:

$$Q^{\uparrow} + Q^{\downarrow} = 2D - (c_p{}^M - c_p{}^A)(T_A - T_M) \qquad \text{(II.17)}$$

where T_A and T_M are the corresponding peak temperatures.

II.1.2. Effect of Hydrostatic pressure and tensile stress

II.1.2.1. Effect of hydrostatic pressure

II.1.2.1.1. CuZnAl(Mn) alloys from Ref. [Detal00]

The authors investigated the effect of the hydrostatic pressure on the martensitic transformation in two samples of a polycrystalline Cu-22at%Zn-12at%Al-1at%Mn alloy. They followed the transformation by the measurement of the electrical resistance (as it can be seen in the Fig. I.6. in Chapter I) and the transformation temperatures were determined from 0.1MPa to 1.5Gpa (Fig. II.2).

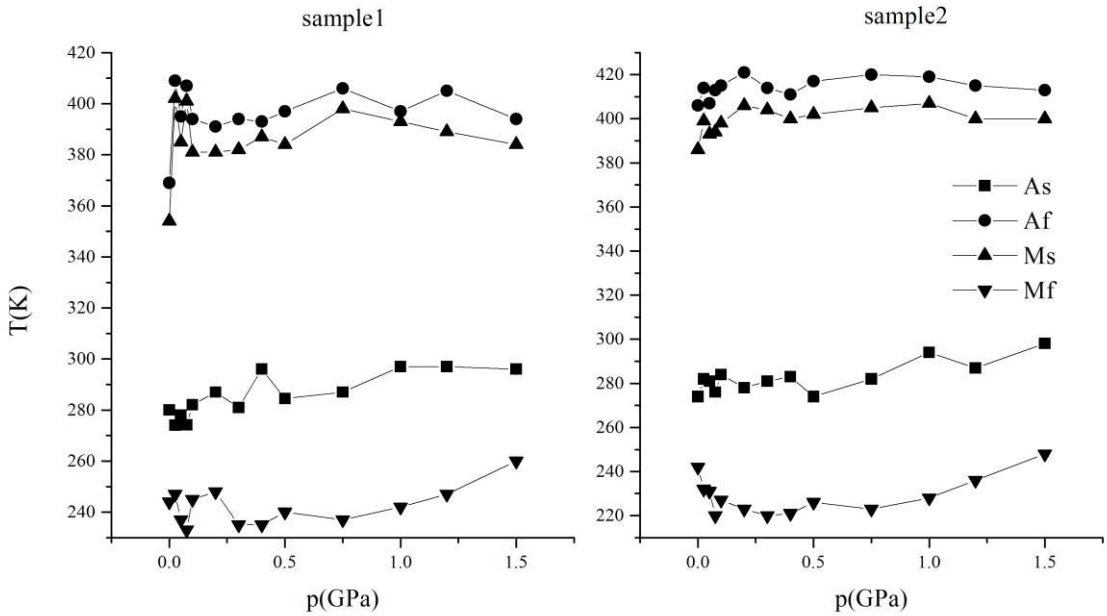

Figure II.2: The transformation temperatures as a function of hydrostatic pressure in CuZnAl(Mn) samples (Fig. 2 of Ref. [Detal00])

The (II.12) expressions were combined and the next relations were calculated for all pressure levels:

$$\frac{1}{2}(\mathrm{A_s} - \mathrm{A_f} + \mathrm{M_s} - \mathrm{M_f}) = \frac{\Delta g_{di}^{*} - \Delta g_{di}}{-\Delta s_c} \qquad \text{(II.15)}$$

$$\frac{1}{2}(\mathrm{A_s} + \mathrm{A_f} - \mathrm{M_s} - \mathrm{M_f}) = \frac{\Delta g_{di}^{*} + \Delta g_{di}}{-\Delta s_c} \tag{II.16}$$

$$\frac{1}{2}(-\mathrm{A_s} + \mathrm{A_f} + \mathrm{M_s} - \mathrm{M_f}) = \frac{e_m - e_0}{-\Delta s_c} \tag{II.17}$$

and

$$\frac{1}{2}(\mathrm{M_s} + \mathrm{A_f}) = T_0 - \frac{e_0}{-\Delta s_c} \tag{II.18}$$

$$\frac{1}{2}(\mathrm{M_f} + \mathrm{A_s}) = T_0 - \frac{e_m}{-\Delta s_c}, \tag{II.19}$$

where $\Delta g_{di}=d_0$, $\Delta g_{di}^{*}=d_1$, $e_m=e_1$ and e_0 has the same meaning.

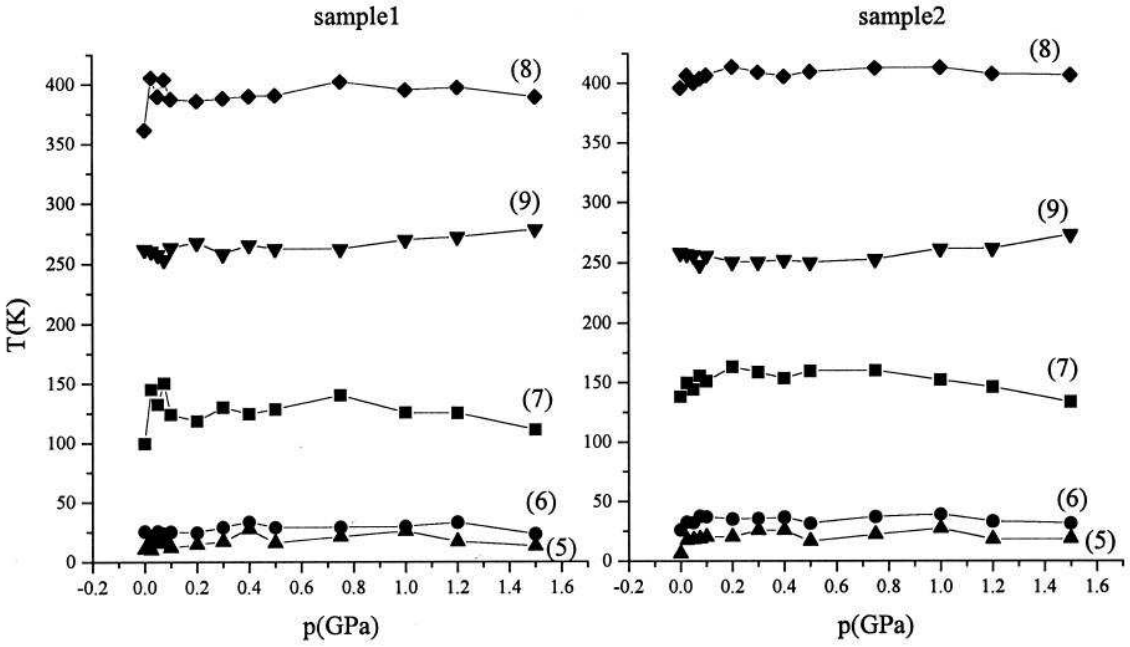

Figure II.3: The pressure dependence of the (II.15)-(II.19) expressions in CuAlNi(Mn) samples (The (5)-(9) equations of Ref. [Detal00] are the (II.15)-(II.19) in order.)

They different behaviour in the low pressure range observed for e_0 between the two samples ((8) in the Fig. II.3 (appearing also on curve (7) in Fig. II.3), was interpreted by the differences of the microstructure and the history of the specimens. Additionally, they found that the dissipative energy terms are much smaller than the corresponding elastic ones.

Furthermore, from power compensation DSC measurement the specific entropy change was calculated: $\Delta sc = -1.14$ J/molK, therewith the knowledge of the volume change during the transformation is also necessary to calculate the hydrostatic pressure dependence of the equilibrium temperature, T_0. They found that there is no any shape change related to the phase transformation (or at least it is less than 0.05%) in this material. Hence, according to the Clausius-Clapeyron equation, T_0 is independent of the hydrostatic pressure.

II.1.2.1.2. NiTi alloys from Ref. [Detal02]

Daróczi et al. have performed the same procedure (thermal cycling under constant hydrostatic pressure from 0.1MPa to 1.5Gpa on two samples–F and J), similarly as in the case of CuZnAl(Mn), but now the compositions (and the origin) of the two specimens were a little bit different. Moreover, they had to take into account the R transient phase, i.e. two martensitic phase transformation took place one after another; namely B2→R and R→B19' during cooling and B19'→R and R→B2 during heating. Like before the resistance vs. temperature curves (Fig. I.5. in the Chapter I) were used to follow the transition and determine the transformation temperatures (Fig. II.4).

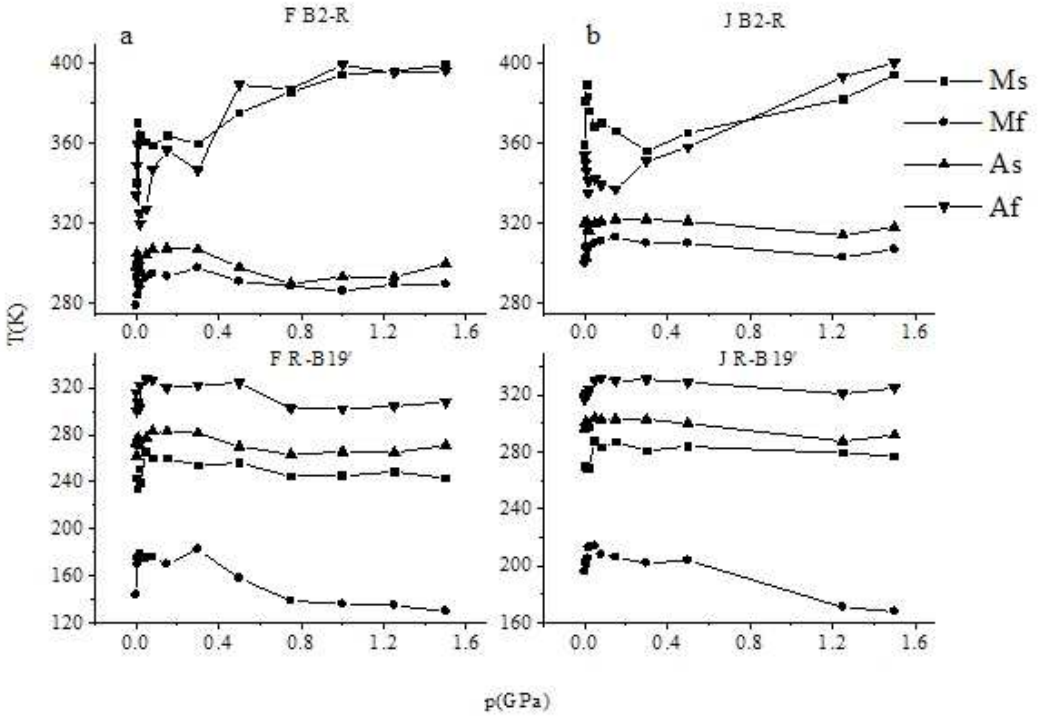

Figure II.4: Transformation temperatures vs. hydrostatic pressure in NiTi alloys (Fig. 3/a and b of Ref. [Detal02]

It can be seen that in the 0.2-1.5 GPa range the tendencies are similar in both types of samples, but in the low pressure range there are relatively strong changes which are even slightly different for the two specimens.

Furthermore, according to (II.15)-(II.19) the combinations of the corresponding temperatures were calculated (Fig. II.5) and similar tendencies were observed between the two samples. The sum and the difference of the dissipative contributions are approximately zero, i.e. the dissipative contributions are negligible in B2/R transition, and at the same time the difference of the elastic terms (II.17) and the difference (II.15) and the sum (II.16) of the dissipative ones have the same order of magnitude in R/B19' transformation.

The authors added two further equations to calculate the dissipative energies from the transformation temperatures:

$$\frac{1}{2}(A_s - M_f) = \frac{\Delta g_{di}^{*}}{-\Delta s_c} \tag{II.20}$$

$$\frac{1}{2}(A_f - M_s) = \frac{\Delta g_{di}}{-\Delta s_c} \tag{II.21}$$

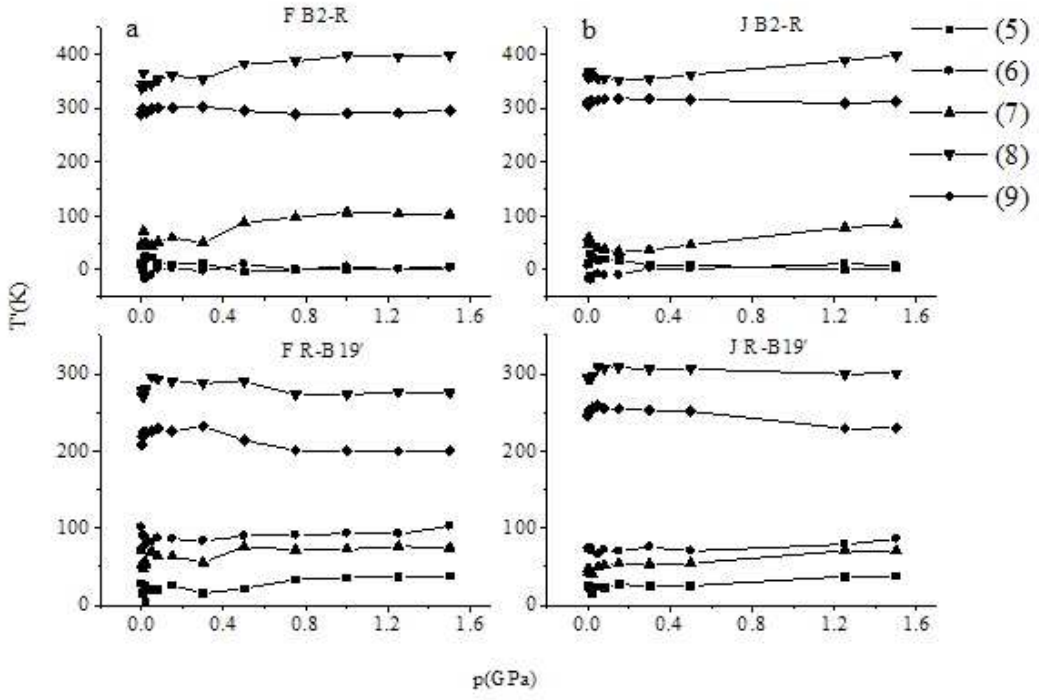

Figure II.5: The pressure dependence of the (II.15)-(II.19) expressions in NiTi alloys(The (5)-(9) equations of Ref. [Detal02] are the (II.15)-(II.19) in order.)

The entropy (Δs_c) and volume (V^{tr}) changes accompanied with the martensitic transformations were determined at stress free state from DSC and elongation-temperature curve measurements, respectively. Supposing the $\Delta s_c/V^{tr}$ is independent of pressure (p) the Clausius-Clapeyron equation (II.8) leads to

$$T_0(p) = \frac{V^{tr}}{\Delta s_c} p + T_0(0). \tag{II.22}$$

Thus T_0 can be replaced in (II.18) and (II.19):

$$V_0 e_0 + \Delta H_c(0) = -\frac{1}{2}(\mathrm{M_s} + \mathrm{A_f})(-\Delta S_c) + V^{tr} p \tag{II.23}$$

$$V_0 e_m + \Delta H_c(0) = -\frac{1}{2}(\mathrm{M_f} + \mathrm{A_s})(-\Delta S_c) + V^{tr} p, \tag{II.24}$$

where $\Delta H_c(0)=T_0(0)\Delta S_c(<0)$ is the enthalpy difference between the two phases at $T_0(0)$ and $\Delta S_c=\Delta s_c V_0$.

Accordingly the authors were able to determine the dissipative terms and the tendency of elastic ones. Fig. II.6 shows the pressure dependence of the dissipative energies. It can be seen that it (Δg_{di}*) increases with the pressure for R/B19' transformation, and it is practically constant for the reverse (B19'/R) transformation (Δg_{di}).

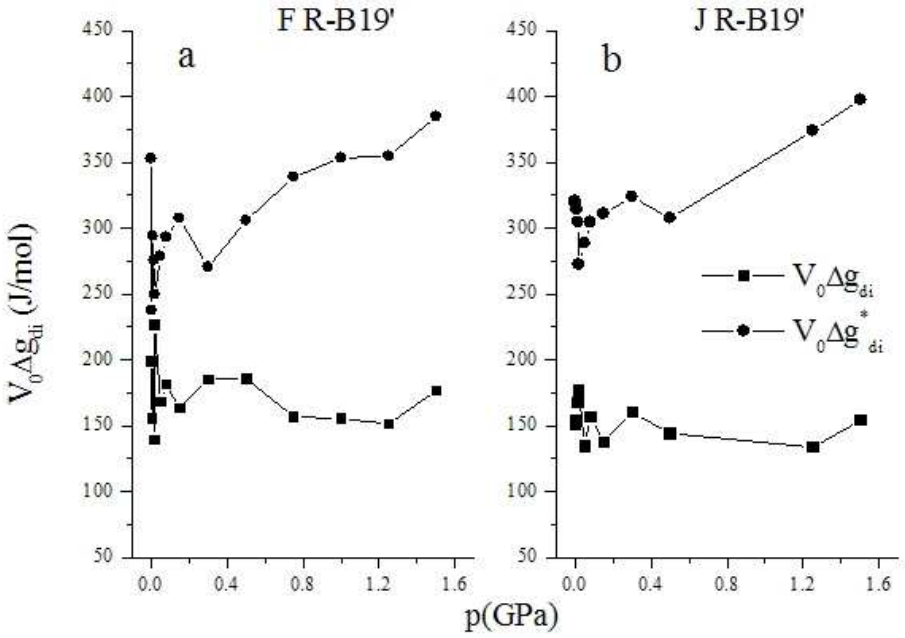

Figure II.6: Pressure dependence of the dissipative energies for R/B19' transformation in two NiTi samples (Fig. 9a-b of Ref.[Detal02])

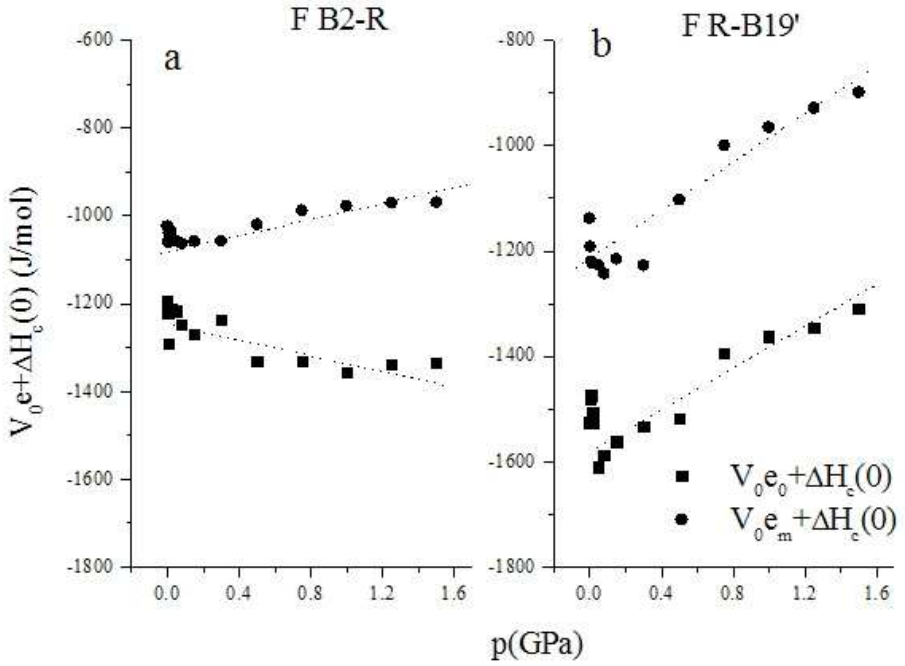

Figure II.7: Elastic energies vs. pressure in sample F (Fig. 7a-b of Ref.[Detal02])

Figs. II.7 and II.8 show the elastic contributions versus hydrostatic pressure for both transformations and both specimens. It can be seen, that not only the tendencies but the slopes of all four energies of F and J samples are similar. The exclusive differences are the values of $V_0e_0+\Delta H_c(0)$ and $V_0e_m+\Delta H_c(0)$, but they come from the difference of the additive constant ($\Delta H_c(0)$) of the two specimens. Moreover only the B2-side elastic energy (e_0 in case of B2/R transformation) decreases with increasing hydrostatic pressure, and there is an opposite tendency for the reverse transformation.

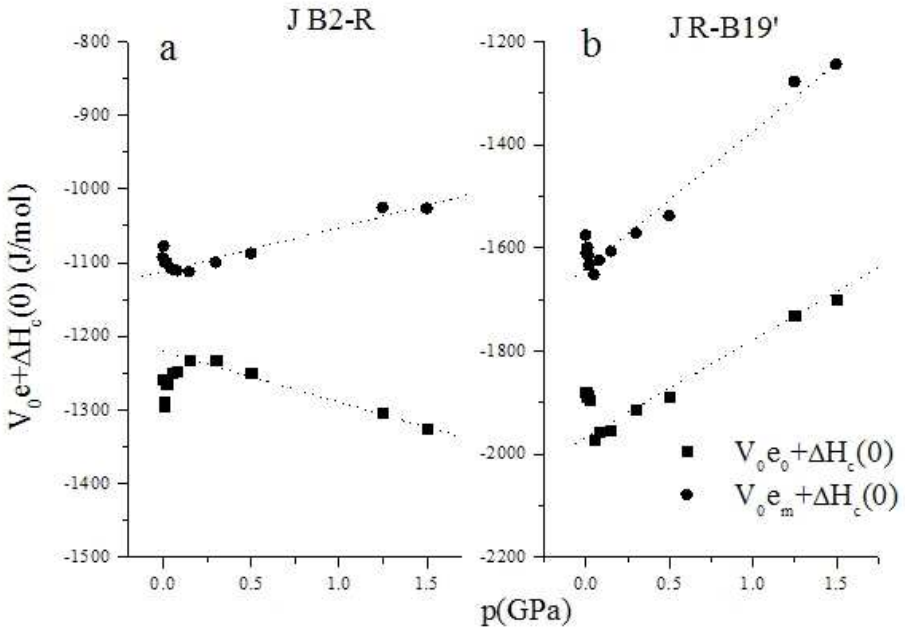

Figure II.8: The effect of hydrostatic pressure on the volume derivatives of elastic energy in sample J (Fig. 8a-b of Ref.[Detal02])

II.1.2.2. Effect of tensile stress

II.1.2.2.1. NiTi alloys from Ref. [Betal04]

The procedure presented above was generalized for the determination of the stress dependence of the dissipative and elastic energy terms using the results of measurements of Tanaka et al. [Tetal99]. The authors investigated three transformations: for set1 both B2/R and R/B19' transitions and in case of set2, only the B2/R one. The transformation temperatures vs. applied stress can be seen in the Figs. II.9 and II.10, as well as Fig. II.11 shows the stress dependence of the transformation strains.

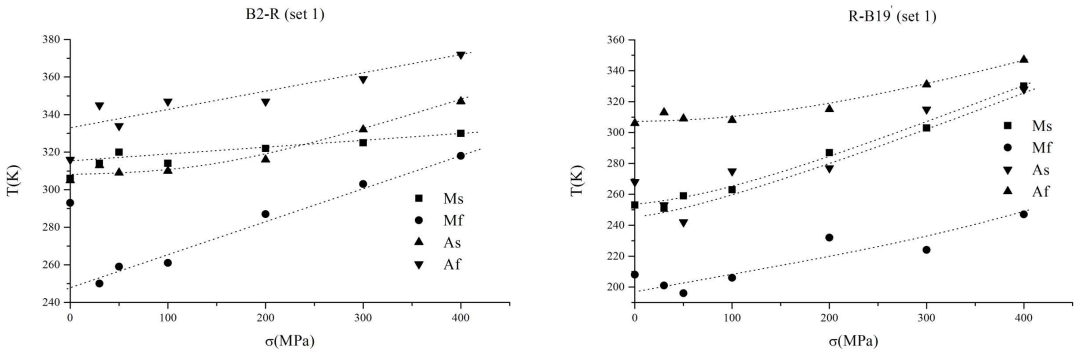

Figure II.9: Transformation temperatures in case of set1 (Figs. 1a and 1b of Ref. [Betal04])

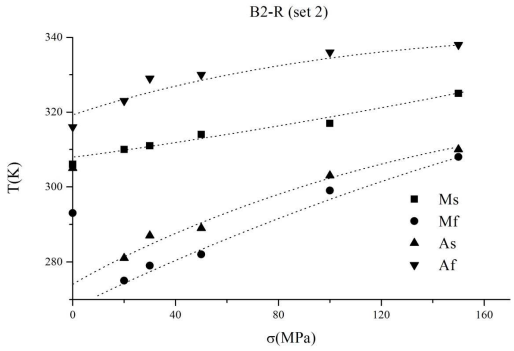

Figure II.10: Start and finish temperatures of B2/R transition of set2 (Fig. 2 of Ref. [Betal04])

Again the analysis was based on equations (II.5) and the general form of the Clausius-Clapeyron equation (II.6), valid in case of external stress, was used to determine the shift of T_0 because the strain accompanied by the transformation depends on the external stress. Since T_0 appears only in the elastic contributions, the dissipative energies can be expressed from the (II.20) and (II.21) equations without any changes:

$$\Delta g_{di}(\sigma) = -\Delta s_c[A_f(\sigma) - M_s(\sigma)]/2 \qquad \text{(II.25)}$$

$$\Delta g_{di}^{*}(\sigma) = -\Delta s_c[A_s(\sigma) - M_f(\sigma)]/2 \qquad \text{(III.26)}$$

but expressions for the elastic ones include an additional term which describes the stress dependence of T_0:

$$e_0(\sigma) = \sigma V \varepsilon^{tr}(\sigma) + \Delta s_c[\mathrm{M_s}(\sigma) + \mathrm{A_f}(\sigma)]/2 - \Delta s_c T_0(0) \qquad \text{(II.27)}$$

$$e_m(\sigma) = \sigma V \varepsilon^{tr}(\sigma) + \Delta s_c[\mathrm{M_f}(\sigma) + \mathrm{A_s}(\sigma)]/2 - \Delta s_c T_0(0)\,. \qquad \text{(II.28)}$$

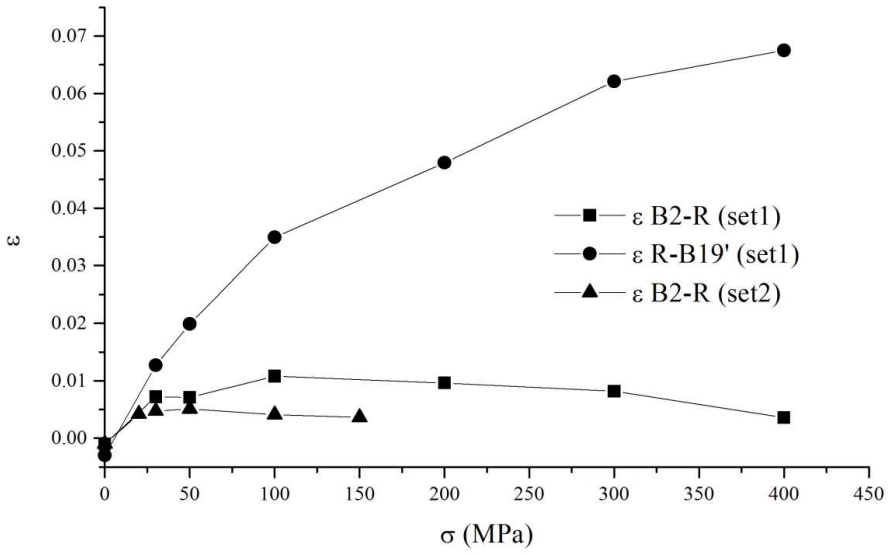

Figure II.11: Transformation strains vs. stress for all three transitions (Fig. 3 of Ref. [Betal04])

Using these equations the stress dependence of the derivatives of the non-chemical free energies can be calculated. It can be seen that the magnitude of the elastic terms could not be determined because the value of $T_0(0)$ was not known.

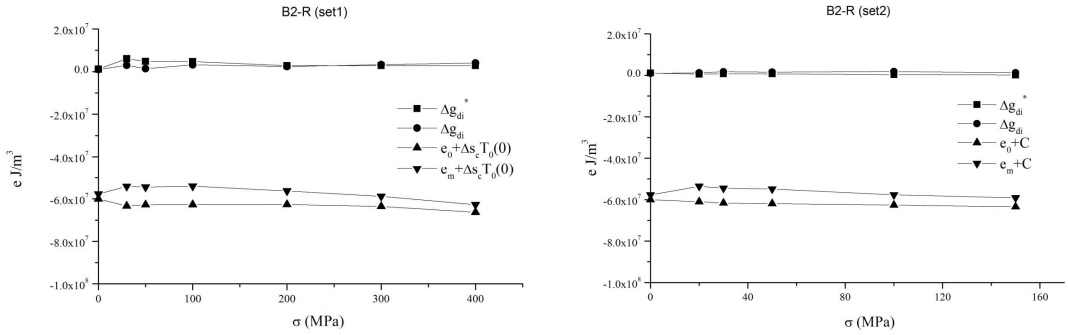

Figure II.12: The calculated non-chemical energy contributions as functions of external stress for B2/R transformations (Figs. 4a and 5 of Ref. [Betal04])

One can see in the Fig. II.12, that the calculated energy terms for B2-R transformation show very similar tendency in both series. The dissipative energies are really close to zero corresponding to the results obtained when the effect of hydrostatic pressure was investigated on NiTi [Detal02]. Furthermore, neither elastic terms show stress dependence and their values are similar, but at every stress levels $e_m > e_0$ is valid.

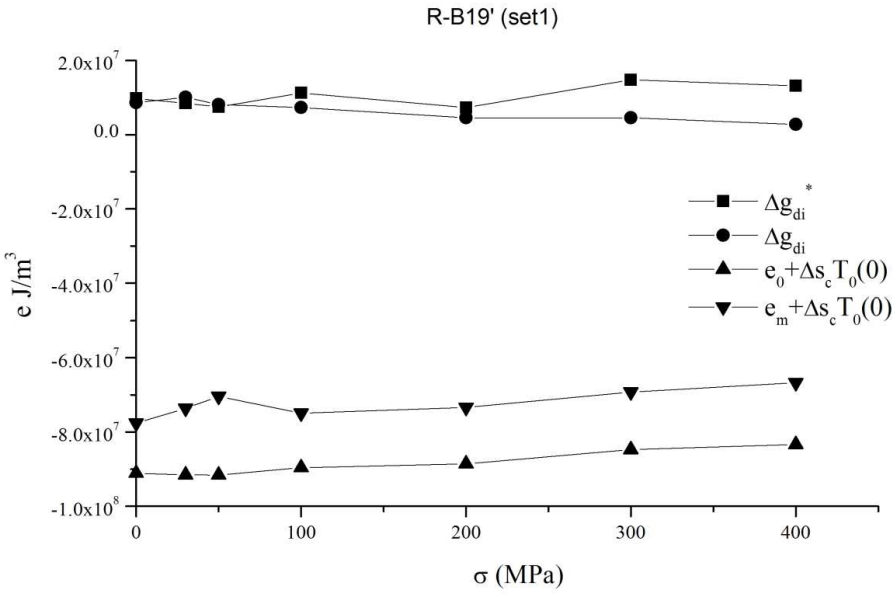

Figure II.13: Stress dependence of non-chemical energies during R/B19' transition (Fig. 4b of Ref. [Betal04])

For R/B19' transformation both the dissipative and the elastic energies have stress dependence. Even the two dissipative terms have different tendency: Δg_{di}^{*} increases while Δg_{di} shows a decreasing tendency with increasing stress (Fig. II.13). On the other hand the both elastic contributions are increasing functions of the stress and e_m is bigger than e_0, like before, but the difference between them are higher than for B2/R transition.

II.1.2.3. Open questions

It is clear from the above examples that the analysis is capable to determine the derivatives of the non-chemical free energies of martensitic transformation only at the beginning and at the end of the martensitic transition. The derivatives were calculated only at the start and finish temperatures, whereas the hysteresis loop inevitably contains the information on the whole forward and reverse transformations.

Furthermore one has to keep in mind that while the magnitude of the dissipative terms could be determined, for the elastic ones only the tendency could be estimated, because their expressions contain the equilibrium transformation temperature, T_0, whose value was unknown.

II.2. Simulation of hysteresis curves

II.2.1. Model for two-phase system

The R_L model ([Retal92], [R&L94], [R&L98]) provides us a way to describe the evolution of martensitic fraction during pseudoelastic test after some parameters are determined from the experimental curves. In all three articles the authors consider the stress and strain fields very generally; it means three dimensional stress and strain matrices were used; now I will present a simpler version in which both the stress and the strain are uniaxial.

II.2.1.1. Free energy

Consider a piece of shape memory alloy (representative volume element – RVE) which at a reference state ($\sigma=0$ and $T=T_0$) is in austenite state. As soon as the applied increasing stress reaches a certain level the martensite phase appears, then it grows and the after a given stress only martensite phase can be found in that piece of shape memory alloys (forward transformation); and if the stress decreases, then a reverse process will take place, i.e. firstly the austenite phase accommodates then the whole RVE turns into austenite phase. The Helmholtz free energy of such a mixture:

$$\Phi = (1-z)\Phi^1 + z\Phi^2 + z(1-z)\Phi_{it} \qquad \text{(II.29)}$$

where the Φ^α ($\alpha=1,2$) is the free energy of
the austenite phase (A) if $\alpha=1$ and
the martensite phase (M) if $\alpha=2$.
Furthermore the last term describes the interaction between the austenite and the martensite phases, and Φ_{it}, so called configurational free energy is defined as

$$\Phi_{it} = \bar{u}_0 - T\bar{s}_0 \qquad \text{(II.30)}$$

where $\bar{u}_0$, $\bar{s}_0$ are the configurational internal energy and entropy, respectively, and Φ_{it} is expected non negative. Finally z is the martensitic fractions which must comply with

$$0 \le z \le 1. \qquad \text{(II.31)}$$

The sign of the uniaxial description appears firstly in the expressions of the Helmholtz free energies of the phases:

$$\Phi^\alpha = {u_0}^\alpha - T{s_0}^\alpha + \frac{E}{2\rho}(\varepsilon_\alpha - {\varepsilon_\alpha}^{tr} - {\varepsilon_\alpha}^{T})^2 + c_V\left[T - T_0 - T\ln\frac{T}{T_0}\right] \qquad \text{(II.32)}$$

where ${u_0}^\alpha$ and ${s_0}^\alpha$ are the internal energy and the entropy of the α phase, E, ρ and c_V are the Young modulus, the mass density and the heat capacity in order (supposing they are the same for each phase). Furthermore ε_α, ${\varepsilon_\alpha}^{tr}$ and ${\varepsilon_\alpha}^{T}$ are the total intrinsic, the transformation and the

thermal strain and so the expression in the parentheses is the elastic strain of the α phase (ε_α^e) and due to the same Young modulus $\varepsilon_1^e=\varepsilon_2^e$. The thermal strains can be given as

$$\varepsilon_1^T = \varepsilon_2^T = \alpha_0(T - T_0) \tag{II.33}$$

where α_0 is the thermal expansion coefficients supposing the same for both phases. Whatever this strain contribution is practically negligible comparing to the transformation one which has a value different from zero only for α=2:

$$\varepsilon_1^{tr} = 0; \qquad \varepsilon_2^{tr} = \gamma; \tag{II.34}$$

where γ is the total pseudoelastic uniaxial strain (Fig. II.14). Moreover the total strain of RVE can be written as

$$\varepsilon = (1-z)\varepsilon_1 + z\varepsilon_2 . \tag{II.35}$$

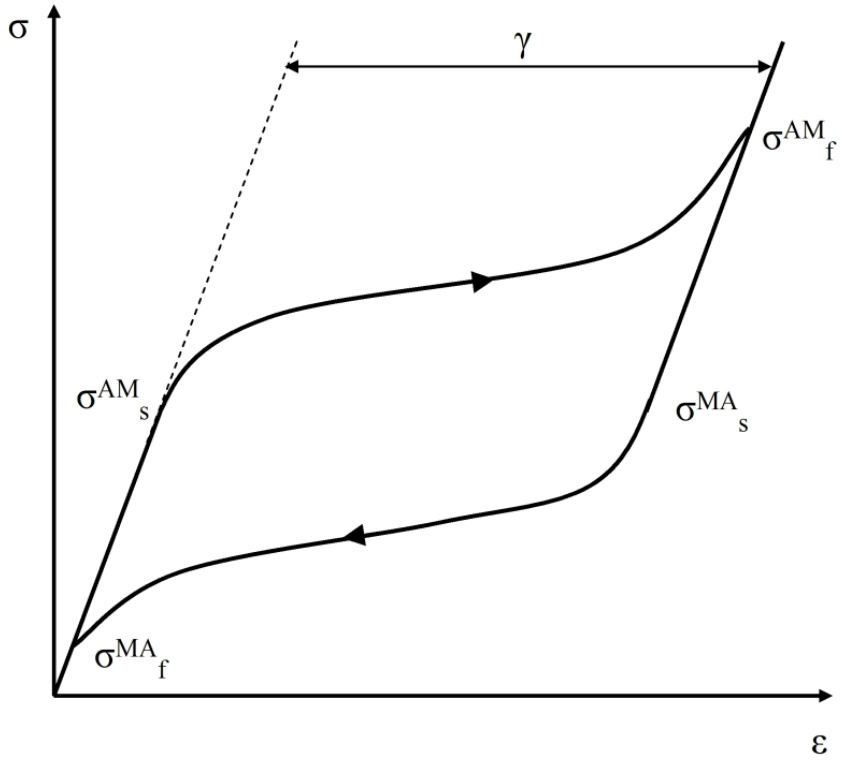

Figure 14: Determination of γ from a stress-strain curve of martensitic transformation measured during isothermal experiment and the characteristic stresses

Substituting (II.32) expressions (α=1,2) into (II.29) the Helmholtz free energy of this two-phase system is obtained:

$$\begin{aligned}\Phi = u_0^{\,1} - Ts_0^{\,1} - z\pi_0^{\,f}(T) + \frac{E}{2\rho}(\varepsilon - z\gamma - \alpha_0(T-T_0))^2 + \\ + c_V\left[T - T_0 - T\ln\frac{T}{T_0}\right] + z(1-z)\Phi_{it}\end{aligned} \tag{II.36}$$

where u_0^1 and s_0^1 are the internal energy and the entropy of the austenite phase, respectively, as well as $\pi_0^f(T)$, the chemical potential of phase transformation, contains the internal energy and entropy changes of the system because of the evolved martensite phases:

$$\pi_0^{\,f}(T) = \Delta u^* - T\Delta s^*$$
$$\Delta u^* = u_0^{\,1} - u_0^{\,2} \qquad \text{(II.37)}$$
$$\Delta s^* = s_0^{\,1} - s_0^{\,2}$$

Furthermore it is worth to examine the (II.36) expression. The partial derivatives of it according to three variables (z,T and ε) provide the next thermal equations:

$$\sigma = \rho\frac{\partial\Phi}{\partial\varepsilon} = E(\varepsilon - z\gamma - \alpha_0(T - T_0)) \qquad \text{(II.38)}$$

$$s = -\frac{\partial\Phi}{\partial T} = s_0^{\,1} - z\Delta s^* + \frac{\alpha_0 E}{\rho}(\varepsilon - z\gamma - \alpha_0(T - T_0)) + c_V \ln\frac{T}{T_0} + z(1-z)\bar{s}_0 \qquad \text{(II.39)}$$

and

$$\pi^f = -\frac{\partial\Phi}{\partial z} = \pi_0^{\,f} + \frac{\gamma E}{\rho}(\varepsilon - z\gamma - \alpha_0(T - T_0)) - (1-2z)\Phi_{it} \qquad \text{(II.40)}$$

where σ, s and π^f are the stress, the specific entropy of RVE and the thermodynamic force associated to the phase transformation and if the expression for stress is substituted into (II.39) and (II.40), then one will receives simplified forms:

$$s = -\frac{\partial\Phi}{\partial T} = s_0^{\,1} - z\Delta s^* + \frac{\alpha_0\sigma}{\rho} + c_V \ln\frac{T}{T_0} + z(1-z)\bar{s}_0 \qquad \text{(II.41)}$$

and

$$\pi^f = -\frac{\partial\Phi}{\partial z} = \pi_0^{\,f} + \frac{\gamma\sigma}{\rho} - (1-2z)\Phi_{it} \qquad \text{(II.42)}$$

where now the three variables are z,T and σ.

II.2.1.2. Transformation kinetics

Let us consider the first and second laws of thermodynamics:

$$du = -\delta q + \frac{\sigma d\varepsilon}{\rho} \qquad \text{(II.43)}$$

$$Tds + \delta q \geq 0 \qquad \text{(II.44)}$$

where u=Φ+Ts is the specific internal energy, δq is the heat exchange and σdε/ρ is the work done on the system by the uniaxial loading. Hence (II.43) can be written as

$$\frac{\partial \Phi}{\partial T} dT + \frac{\partial \Phi}{\partial z} dz + \frac{\partial \Phi}{\partial \varepsilon} d\varepsilon + s dT + T ds = -\delta q + \frac{\sigma d\varepsilon}{\rho} \qquad \text{(II.45)}$$

which is simplified easily having regard to (II.38), (II.39) and (II.40) as well as the heat exchange is expressed and it substituted into (II.44). So one obtained finally:

$$\pi^f dz \geq 0 \qquad \text{(II.46)}$$

Thus, it is understandable the meaning of thermodynamic force: The sign of π^f determines the direction of the martensitic transformation, if it is non negative, then dz≥0, i.e. the martensitic fraction can increase only – forward transformation – and the martensite phase can shrink (dz≤0) if π^f less than or equal to zero – reverse transformation.

Neglecting the thermal expansion effect there are six parameters (γ, ρ, Δu*, Δs*, $\bar{u}_0$, $\bar{s}_0$) which are necessary to know to determine the thermodynamic force using (II.42). The total pseudoelastic uniaxial strain and the mass density can easily measured and the other four parameters can determined taking into account that π^f is equal to zero at the start of the forward and reverse transformations. In fact, there are more ways to calculate these constants, e.g. let us take stress-strain cycles measured at different temperatures, and it will be true at for every hysteresis:

$$\pi^f(\sigma^{AM}{}_s, T, z=0) = \frac{\gamma \sigma^{AM}{}_s}{\rho} + (\Delta u^* - \bar{u}_0) - T(\Delta s^* - \bar{s}_0) = 0 \qquad \text{(II.47)}$$

$$\pi^f(\sigma^{MA}{}_s, T, z=1) = \frac{\gamma \sigma^{MA}{}_s}{\rho} + (\Delta u^* + \bar{u}_0) - T(\Delta s^* + \bar{s}_0) = 0 \qquad \text{(II.48)}$$

and considering the slopes of $\sigma^{AM}{}_s(T)$ and $\sigma^{MA}{}_s(T)$ (Fig. II.14):

$$\frac{d\sigma^{AM}{}_s}{dT} = \frac{\rho}{\gamma}(\Delta s^* - \bar{s}_0) \qquad \text{(II.49)}$$

$$\frac{d\sigma^{MA}{}_s}{dT} = \frac{\rho}{\gamma}(\Delta s^* + \bar{s}_0) \qquad \text{(II.50)}$$

So we have four unknowns and four independent equations, i.e. the parameters can be calculated from the start stresses ($\sigma^{AM}{}_s$ and $\sigma^{MA}{}_s$) which are known at least at two different temperatures. Another way could be to measure the start temperatures (M_s and A_s) at least at two different stress levels, nevertheless in this case one has to make a stress-strain curve measurement to determine γ as well.

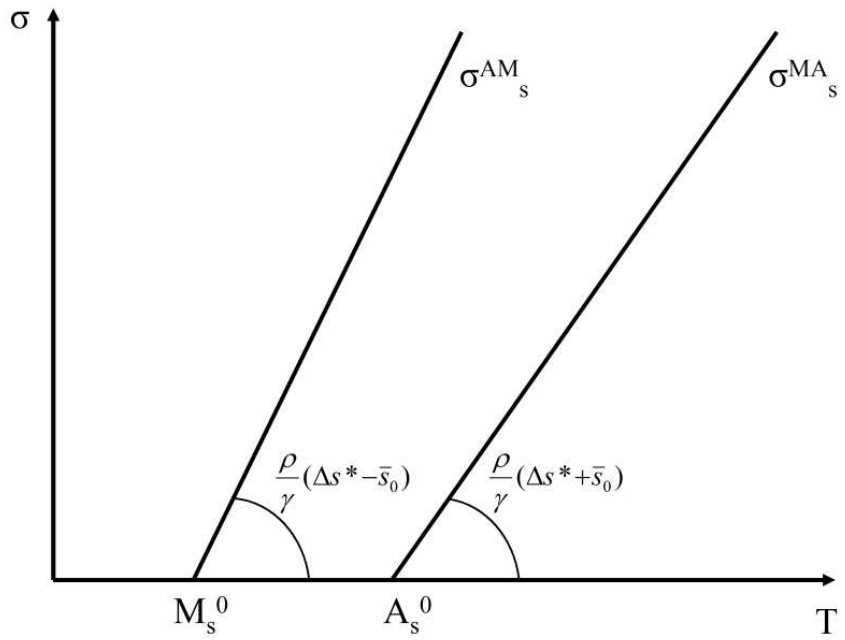

Figure II.15: The temperature dependence of the start stresses

Nevertheless, the (II.46) inequality cannot determine the transformation kinetics, but it decides what kind of process can take place. To describe the evolving of martensitic fraction the authors presumed that two functions exist: $\Psi^1(\pi^f,z)$ and $\Psi^2(\pi^f,z)$ which are constant for partial and zero for external cycle during the forward and reverse transformation, respectively (Figs. II.15 and II.16):

$$\Psi^1 = \pi^f - k^1(z)$$
$$\Psi^2 = -\pi^f + k^2(z) \qquad \text{(II.51)}$$

and the authors assumed that the $k^\alpha(z)$ (α=1,2) functions have the following mathematical properties:

$$k^1(0)=0; \quad \lim_{z\to 1} k^1 = +\infty; \quad \lim_{z\to 1}(1-z)k^1 = 0; \quad k^1 \geq 0;$$
$$k^2(1)=0; \quad \lim_{z\to 0} k^2 = -\infty; \quad \lim_{z\to 0} zk^2 = 0; \quad k^2 \leq 0; \qquad \text{(II.52)}$$
$$dk^\alpha / dz > 0 \ \ for \ \ 0 < z < 1$$

and take

$$k^1 = -(A_1 + B_1 z)\ln(1-z) + C_1 z$$
$$k^2 = [A_2 - B_2(1-z)]\ln z - C_2(1-z) \qquad \text{(II.53)}$$

where A_α, B_α and C_α are constants ($A_\alpha>0$, $C_\alpha\geq 0$) and their values can be determined from the branches of martensitic transformation.

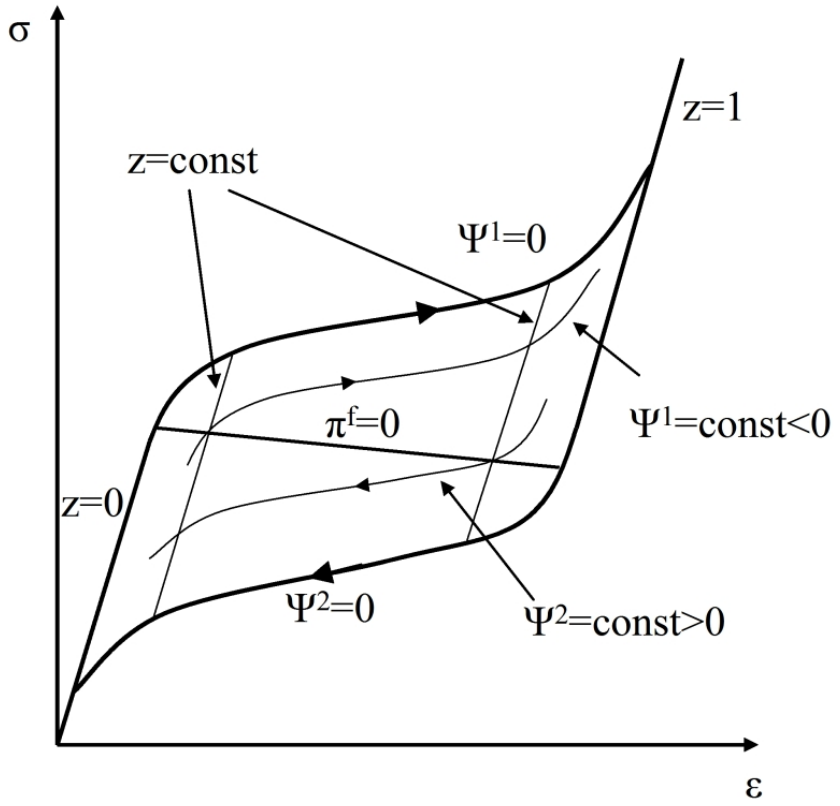

Figure II.16: Schematic figure about the stress induced martensitic transformation

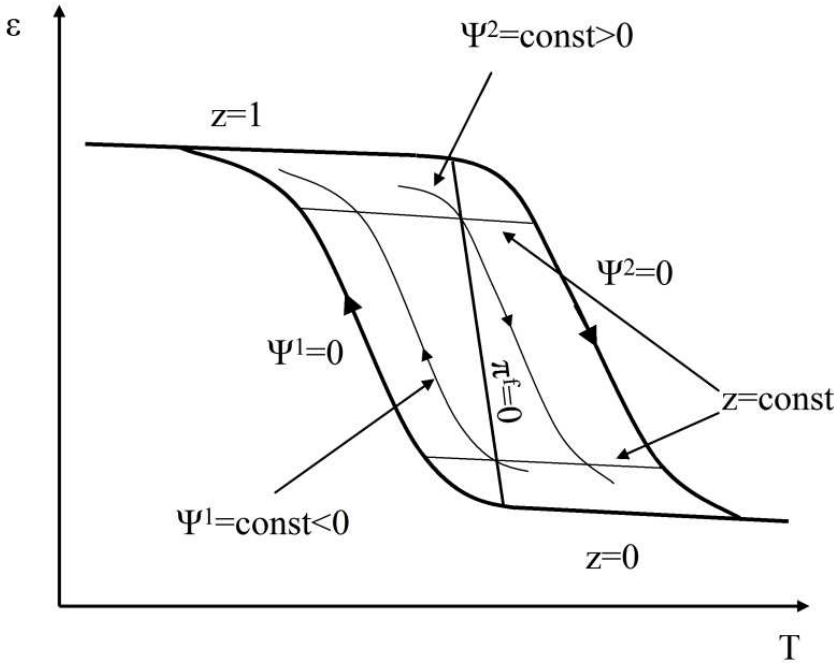

Figure II.17: Schematic figure about thermal cycle hysteresis loop

II.2.2. Model for three-phase system

The above written model is appropriate to describe the martensitic transformation if either only self accommodated (thermal induced) or only oriented (stress induced) martensite shows up, and it is true for example in case of isothermal process, where only the oriented one can evolve under external load, or in case of stress-free anisothermal experiment, where the martensite phase accommodates randomly. But it can easily happen during thermal induced martensitic transformation under stress that these two martensite variants form simultaneously.

Hence one has to take into account the possibility of appearing more than one martensite variant, i.e. now we have a three phase system. The details of this improved R_L model and general, three-dimensional case can be found in Refs. [L&L96, Getal00] and now I present the one dimensional version as above.

II.2.2.1. Free energy

First of all it is worth to discuss about the martensite variants, let us assume the total martensite fraction, z, is split into

z_T, self-accommodated, which obtained under pure thermal process, and each variant has its own complement, hence appearing of this martensite doesn't draw down macroscopic phase transition strain; and

z_σ, oriented, result of external mechanical loading and associated macroscopic transformation strain.

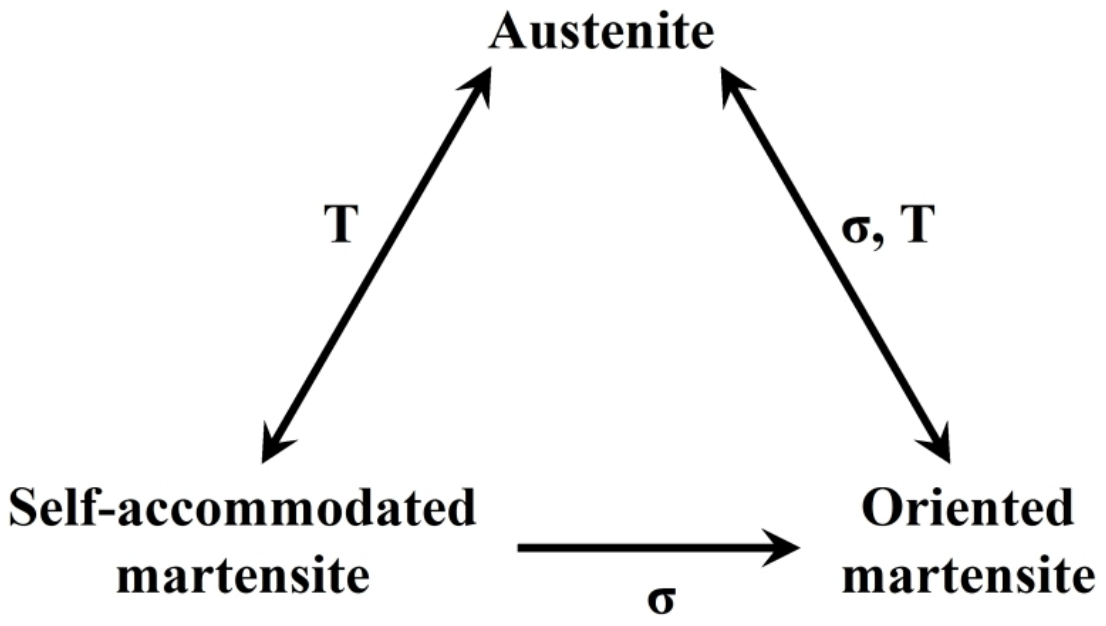

Figure II.18: Interrelations between the parent and product phases (Fig. 1 of Ref. [L&L96])

Fig. II.18 shows the interrelations between the austenite and martensite phases and the martensitic fractions must comply with

$$0 \le z = z_T + z_\sigma \le 1 \qquad \text{and} \qquad \begin{cases} 0 \le z_T \le 1 \\ 0 \le z_\sigma \le 1 \end{cases}. \tag{II.54}$$

Of course the Helmholtz free energy is similar like (II.29) but now there are two additional terms: one concerns the plus martensite and another one describes the interaction between the martensite variants.

$$\Phi = (1-z)\Phi^1 + z_T\Phi^2 + z_\sigma\Phi^3 + z(1-z)\Phi_{it} + z_T z_\sigma \Phi_{it}{}^m \tag{II.55}$$

where the Φ^α (α=1,2,3) is the free energy of
the austenite phase (A) if α=1,
the self-accommodated martensite phase (M_T) if α=2 and
the oriented martensite phase (M_σ) if α=3.
The $z(1-z)\Phi_{it}$ has the former meaning and $z_T z_\sigma \Phi_{it}{}^m$ describes the interaction between the two types of martensite variants, now together these two terms are called configurational energy. The free energy expressions of the pure phases are the same like before (II.32) (α=1,2,3). However the situation of Φ_{it} and $\Phi_{it}{}^m$ is not so clear, it means that either they are considered as non-negative constants [L&L96] or only $\Phi_{it}{}^m$ is constant and Φ_{it} has a temperature dependence like (II.30) [Getal00] or both of them depend on the temperature [Letal06]. Now the first case will be presented.

Let us regard the strains of all three phases. Everyone's strain is composed of an elastic, a transformation and a thermic part.

$$\varepsilon_\alpha = \varepsilon_\alpha{}^e + \varepsilon_\alpha{}^{tr} + \varepsilon_\alpha{}^T \tag{II.56}$$

The elastic term and the thermal expansion, which can be written as (II.33), are the same for all phases. Furthermore, as it was assumed only the oriented martensite has transformation strain different from zero:

$$\begin{aligned} \varepsilon_1{}^{tr} &= \varepsilon_2{}^{tr} = 0 \\ \varepsilon_3{}^{tr} &= \gamma \end{aligned} \tag{II.57}$$

As well as the total strain of RVE can be written consequently:

$$\varepsilon = (1-z)\varepsilon_1 + z_T\varepsilon_2 + z_\sigma\varepsilon_3 \tag{II.58}$$

And now following the analogy anyone can derive the Helmholtz free energy of this three-phase RVE:

$$\begin{aligned} \Phi = u_0{}^1 - Ts_0{}^1 - z\pi_0{}^f(T) + \frac{E}{2\rho}(\varepsilon - z_\sigma\gamma - \alpha_0(T-T_0))^2 + \\ + C_V\left[T - T_0 - T\ln\frac{T}{T_0}\right] + z(1-z)\Phi_{it} + z_T z_\sigma \Phi_{it}{}^m \end{aligned} \tag{II.59}$$

where now $\pi_0{}^f(T)$, the chemical potential of phase transformation is defined as

$$\pi_0{}^f(T) = \Delta u^* - T\Delta s^*$$
$$\Delta u^* = u_0{}^1 - u_0{}^2 = u_0{}^1 - u_0{}^3 \qquad \text{(II.60)}$$
$$\Delta s^* = s_0{}^1 - s_0{}^2 = s_0{}^1 - s_0{}^3$$

i.e. the same internal energy and the same entropy are considered for both martensite phases.

The next step is the composing the partial derivatives of the Helmholtz free energy of the system like before but now the Φ_{it} does not depend on T:

$$\sigma = \rho\frac{\partial\Phi}{\partial\varepsilon} = E(\varepsilon - z_\sigma\gamma - \alpha_0(T - T_0)) \qquad \text{(II.61)}$$

$$s = -\frac{\partial\Phi}{\partial T} = s_0{}^1 - z\Delta s^* + \frac{\alpha_0 E}{\rho}(\varepsilon - z_\sigma\gamma - \alpha_0(T - T_0)) + c_V \ln\frac{T}{T_0} \qquad \text{(II.62)}$$

and

$$\pi^f{}_T = -\frac{\partial\Phi}{\partial z_T} = \pi_0{}^f - (1-2z)\Phi_{it} - z_\sigma\Phi_{it}{}^m \qquad \text{(II.63)}$$

$$\pi^f{}_\sigma = -\frac{\partial\Phi}{\partial z_\sigma} = \pi_0{}^f + \frac{\gamma E}{\rho}(\varepsilon - z_\sigma\gamma - \alpha_0(T - T_0)) - (1-2z)\Phi_{it} - z_T\Phi_{it}{}^m \qquad \text{(II.64)}$$

where π^f_T and π^f_σ the thermodynamic forces associated to the forming of self-accommodated and oriented martensite phases, respectively. Analogously substituting the stress expression (II.61) into (II.62) the former expression (II.41) is reobtained and into (II.64) a simplified form is received:

$$\pi^f{}_\sigma = -\frac{\partial\Phi}{\partial z_\sigma} = \pi_0{}^f + \frac{\gamma\sigma}{\rho} - (1-2z)\Phi_{it} - z_T\Phi_{it}{}^m \qquad \text{(II.65)}$$

As one can see the dependence of the thermodynamic forces is in accord with Fig. II.18. i.e. π^f_T is independent from σ while in π^f_σ there are a thermal and a stress contribution as well.

II.2.2.2. Transformation kinetics

The initial point is the first two laws of thermodynamics, and after a similar derivation one obtains:

$$\pi^f{}_T dz_T + \pi^f{}_\sigma dz_\sigma \geq 0 \qquad \text{(II.66)}$$

and this inequality determines the processes can take place. For example it explains the transition between the two martensite phases when a piece of thermal induced martensite becomes oriented, i.e. $dz_T = -dz_\sigma$ and so

$$(\pi^{f}{}_{\sigma} - \pi^{f}{}_{T})dz_{\sigma} = \pi^{f}{}_{T\sigma}dz_{\sigma} \geq 0$$

where

$$\pi^{f}{}_{T\sigma} = \frac{\gamma\sigma}{\rho} - (z_T - z_\sigma)\Phi_{it}{}^{m} \tag{II.67}$$

is referred to the thermodynamic force associated to the reorientation of the self-accommodated product phase, and it depends on only the stress really as Fig. II.18 shows.

The number of parameters (γ, ρ, Δu*, Δs*, Φ_{it} and $\Phi_{it}{}^{m}$) is six here too neglecting the thermal expansion, thanks that the configurational energy does not depend on the temperature, i.e. Φ_{it} is constant. The same holds true of γ and ρ and on the other four constant Leclercq and Lexcellent [L&L96] gave the next relations using the fact that the thermodynamic forces at the start of the transformations (austenite ↔ martensite and self-accommodated → oriented) are equal to zero:

$$\Phi_{it} = \frac{\rho(M_s{}^{0} - A_s{}^{0})}{2\gamma(M_s{}^{0} - T_{pe})}\sigma^{AM}{}_{s} \tag{II.68}$$

$$\Phi_{it}{}^{m} = \frac{\gamma\sigma^{T\sigma}}{\rho} \tag{II.69}$$

$$\Delta u^{*} = \frac{\gamma\sigma^{AM}{}_{s}}{2\rho}\left(\frac{M_s{}^{0} + A_s{}^{0}}{T_{pe} - M_s{}^{0}}\right) \tag{II.70}$$

$$\Delta s^{*} = \frac{\gamma\sigma^{AM}{}_{s}}{\rho T_{pe} - M_s{}^{0}} \tag{II.71}$$

where $M_s{}^{0}$ and $A_s{}^{0}$ are the martensite and austenite start temperatures at zero stress, $\sigma^{AM}{}_{s}$ is the yield stress on the isothermal martensitic transformation performed at $T_{pe} \geq A_f{}^{0}$ (austenite finish temperature at stress free state) temperature, as well as $\sigma^{T\sigma}$ is the yield stress for reorientation of self-accommodated martensite variants.

There are five different transitions, which can take place, so following the presumption of R_L model five functions exist which are constant for partial and zero for full transformation:

$$\begin{aligned}
&\Psi^{\sigma}{}_{f} = \pi^{f}{}_{\sigma} - k^{\sigma}{}_{f}; \qquad \Psi^{\sigma}{}_{r} = -\pi^{f}{}_{\sigma} + k^{\sigma}{}_{r};\\
&\Psi^{T}{}_{f} = \pi^{f}{}_{T} - k^{T}{}_{f}; \qquad \Psi^{T}{}_{r} = \pi^{f}{}_{T} - k^{T}{}_{r};\\
&\Psi^{T\sigma} = \pi^{f}{}_{T\sigma} - k^{T\sigma}
\end{aligned} \tag{II.72}$$

where σ, T and $T\sigma$ superscripts mean the A/M_σ, the A/M_T and the $M_T \rightarrow M_\sigma$ transitions, as well the f and r subscripts show the direction of martensitic transformation such as forward (A→M) and reverse (M→A). In contradistinction to R_L model the $k^{\sigma}{}_{f}$, $k^{\sigma}{}_{r}$, $k^{T}{}_{f}$, $k^{T}{}_{r}$ and $k^{T\sigma}$ functions don't depend only on the martensitic fraction, but on the stress and on the temperature and take zero value at the beginning of phase transitions. The functions, which

were published in Ref. [L&L96], are extended from the kinetic forms proposed by Koistinen and Marburger [K&M59] and Raniecki et al [Retal92].

$$k_f^{\sigma} = 2\Phi_{it}(z_{\sigma} - z_{\sigma}{}^{m}) - \frac{\Delta s^{*}}{a_f^{\sigma}} \ln\left(1 - z_{\sigma} + z_{\sigma}{}^{m}\right) - \Delta s^{*}\left[\left(T - T^{*}\right) + \frac{b_f}{b_m{}'}\exp\left(-b_m{}'\left(T - M_s^{0}\right)\right) - \exp\left(-b_m{}'\left(T^{*} - M_s^{0}\right)\right)\right] \tag{II.73}$$

$$k_r^{\sigma} = 2\Phi_{it}(z_{\sigma} - z_{\sigma}{}^{M} - 1) + \frac{\Delta s^{*}}{a_r^{\sigma}} \ln\left(z_{\sigma} - z_{\sigma}{}^{M}\right) + \Delta s^{*}\left[-\left(T - T^{*}\right) + \frac{b_r}{b_m}\exp\left(-b_m\left(T - A_s^{0}\right)\right) - \exp\left(-b_m\left(T^{*} - A_s^{0}\right)\right)\right] \tag{II.74}$$

$$k_f^{T} = 2\Phi_{it}(z_T - z_T{}^{m}) - \frac{\Delta s^{*}}{a_f^{T}} \ln\left(1 - z_T + z_T{}^{m}\right) \tag{II.75}$$

$$k_r^{T} = 2\Phi_{it}(z_T - z_T{}^{M} - 1) + \frac{\Delta s^{*}}{a_r^{T}} \ln\left(z_T - z_T{}^{M}\right) \tag{II.76}$$

and

$$k_r^{T} = 2\Phi_{it}{}^{m} z_{\sigma} - \frac{\Delta s^{*}}{a^{T\sigma}} \ln\left(1 - z_{\sigma}\right) \tag{II.77}$$

The parameters a_f^{σ}, a_r^{σ}, a_f^{T}, a_r^{T}, $a^{T\sigma}$, b_f, b_r, b_m' and b_m are identified from experimental tests. The temperature T^{*} is that for which a mechanical loading is ongoing, i.e. T^{*} can be the temperature at the beginning of an isothermal mechanical loading or the actual temperature in case of non-isothermal mechanical loading.

The z_{σ}^{m}, z_{σ}^{M}, z_T^{m} and z_T^{M} characterize the "memory" of the material, i.e. z_{σ}^{m} and z_T^{m} are the initial values of z_{σ} and z_T when a forward transformation begins and z_{σ}^{M} and z_T^{M} are the initial values of z_{σ} and z_T likewise when a reverse transformation commences. Hence these parameters are relevant in the case of partial hysteresis loop.

II.2.3. About the models

II.2.3.1. Results of simulation

Let me introduce one example of the application of the above two models: firstly a simulation of the pseudoelastic behaviour on equatomic NiTi using R_L model is presented and then the thermal induced martensitic transformation on NiTiCu and NiTi alloys will be investigated applying the L–L model.

II.2.3.1.1. NiTi alloy from Ref. [R&L98]

In this article Raniecki and Lexcellent took into account that the pseudoelastic properties are different in cases of tension and compression. This asymmetry is described by an *f(y)* function which has to comply with

$$f(y=0)=1 \quad \text{and} \quad \left.\frac{df}{dy}\right|_{y=0}=0 \tag{II.78}$$

where the value of y provides information about the state of external mechanical field; for example for pure tension $y=+1$, for pure compression $y=-1$ and for pure shear $y=0$. The total strain ($\bar{\gamma}$) can be calculated

$$\bar{\gamma}=\gamma\cdot f(y) \tag{II.79}$$

where γ is the total shear strain obviously. Thus, for tension (γ_T) and for compression (γ_C) the total uniaxial strain can be given as:

$$\gamma_T=\gamma\cdot f(+1); \qquad \gamma_C=\gamma\cdot f(-1) \tag{II.80}$$

To verify the validity of the predictions the authors used the experimental data published by Orgeas and Favier [O&F95] on NiTi. The calculated parameters can be found in Table II.1, practically they considered a constant Φ_{it} since $\bar{s}_0=0$.

Properties	Value
ρ [kg/m^3]	6500
E [MPa]	55000
ν (Poisson ratio)	0.29
Δu* [J/kg]	23800
$\bar{u}_0$ [J/kg]	1000
Δs* [J/kgK]	80
$\bar{s}_0$ [J/kgK]	0
γ	0.061
f(+1)	1.05
f(–1)	0.744

Table II.1: Values of parameters for equatomic NiTi (Table I. of Ref. [R&L98])

Finally in Fig. II.19 one can see that the correlation between the experimental data and the hysteresis loop calculated according to R_L model, and they show good agreement.

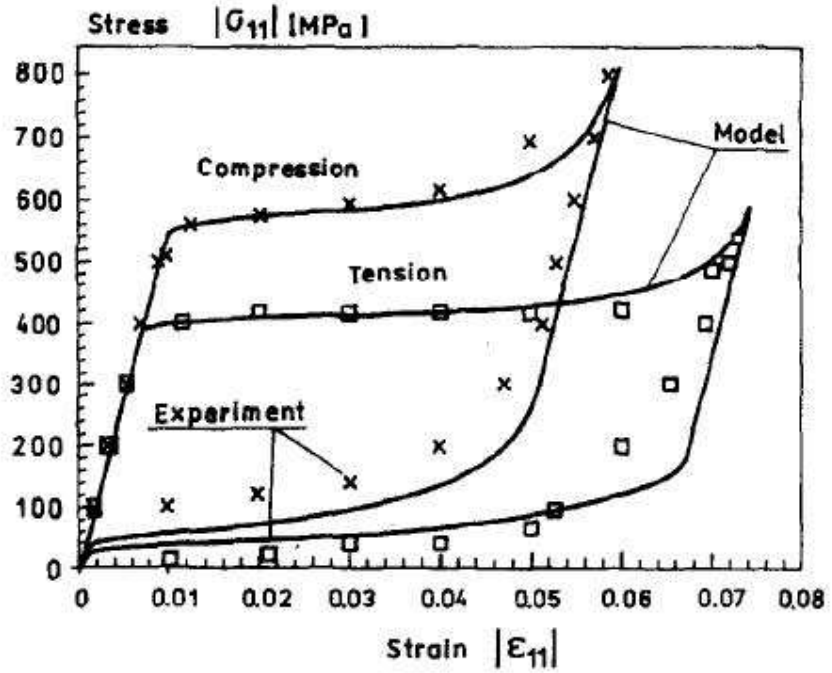

Figure II.19: The correlation between the experiment and model prediction at T=333K (Fig.3 of Ref. [R&L98])

II.2.3.1.2. NiTiCu alloy from Ref. [Getal00]

The authors investigated three shape memory alloy thin films and applying the L–L model they calculated the strain–temperature hysteresis loops at different stress levels which were compared to the experiments.

It was showed that at constant stress the reorientation of self-accommodated martensite doesn't take place but only the creation and the annihilation of martensite. Finally two-two relations were obtained for the forward and for the reverse transformations.

For A→M transformation:

$$z_\sigma = 1 - \exp\left[-\frac{\gamma a_f^{\ \sigma}}{\rho(\Delta s^* - \bar{s}_0)} \left\langle \sigma_0 - \rho \frac{\Delta s^* - \bar{s}_0}{\gamma} \left(T - M_s^{\ 0} \right) \right\rangle \right] \tag{II.81}$$

$$z_T = 1 - \exp\left(- a_f^{\ T} \left\langle M_s^{\ 0} - T \right\rangle \right) \tag{II.82}$$

In case of M→A transition:

$$z_\sigma = \exp\left[-\frac{\gamma a_r^{\ \sigma}}{\rho(\Delta s^* + \bar{s}_0)} \left\langle \rho \frac{\Delta s^* + \bar{s}_0}{\gamma} \left(T - A_s^{\ 0} \right) - \sigma_0 \right\rangle \right] \tag{II.83}$$

$$z_T = \exp\left(- a_r^{\ T} \left\langle T - A_s^{\ 0} \right\rangle \right) \tag{II.84}$$

The thirteen material parameters of the three alloys were determined by some appropriate isothermal and anisothermal tests, their values can be seen in Table II.2.

Parameters	Ti-43.0Ni-6.2Cu (at%)	Ti-48.7Ni (at%)	Ti-51.5Ni (at%)
E [GPa]	55.6	55.56	55.7
ρ [kg/m^3]	6500	6500	6500
M_s^0 [K]	324	338	160
A_s^0 [K]	341	360	215
Δu^* [J/kg]	38245	35931	10179
Δs^* [J/kgK]	113.71	102.5	52.85
$\overline{u}_0$ [J/kg]	17432	6515	3288
$\overline{s}_0$ [J/kgK]	49.57	15.45	9.78
Φ_{it}	1200	900	1600
γ	4.6	5	5.6
a_f^T	0.025	0.001	0.016
a_r^T	0.19	0.16	0.19
a_f^σ	0.07	0.05	0.03
a_r^σ	0.082	0.036	0.082

Table II.2: The values of the thirteen parameters for both three alloys (summary of Tables 2, 3 and 4 of Ref. [Getal00])

In the conclusions it is announced that the main hypothesis, i.e. distinguishing two types of martensite, is appropriate to NiTi based alloy films. However, at low stress levels the model didn't provide a good agreement with the experiment, and the authors mentioned that they had the same problem in the modelling of classical shape memory alloy.

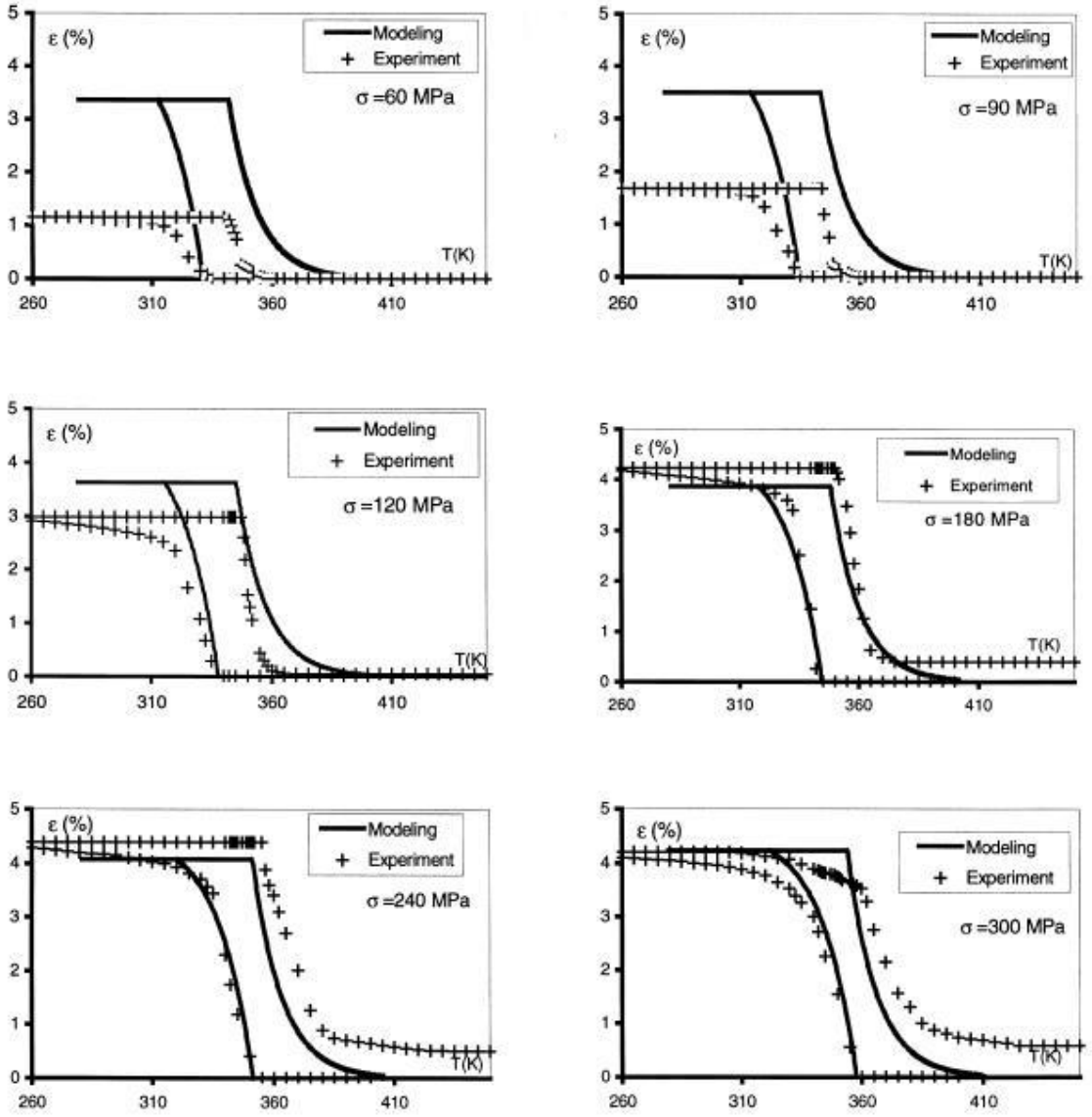

Figure II.20: Measured and calculated strain-temperature curves on Ti-43.0Ni-6.2Cu (at%) thin film at different stress levels (Fig. 4a of Ref. [Getal00])

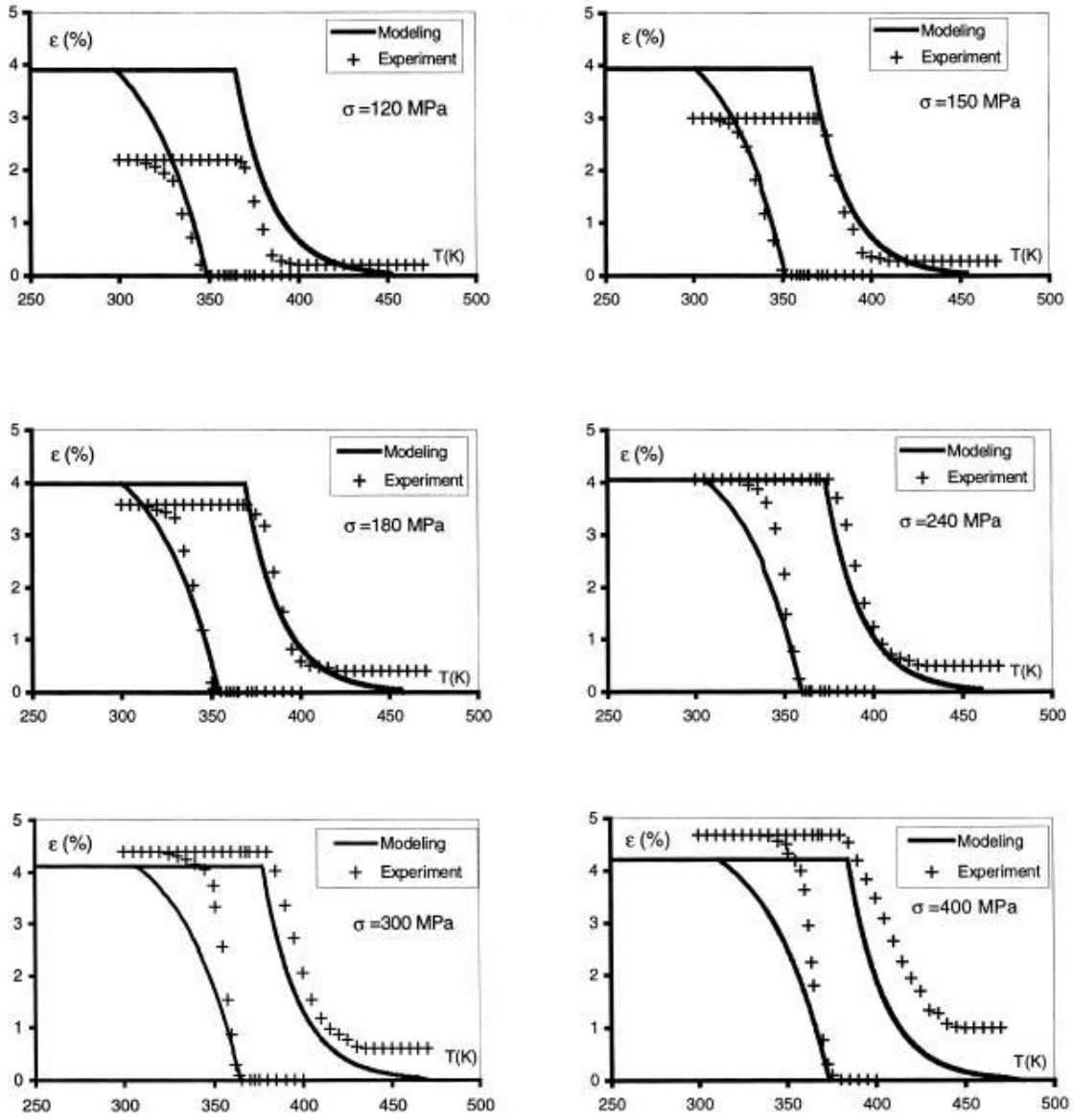

Figure II.21: Measured and calculated strain-temperature curves on Ti-48.7Ni (at%) thin film at different stress levels (Fig. 5a of Ref. [Getal00])

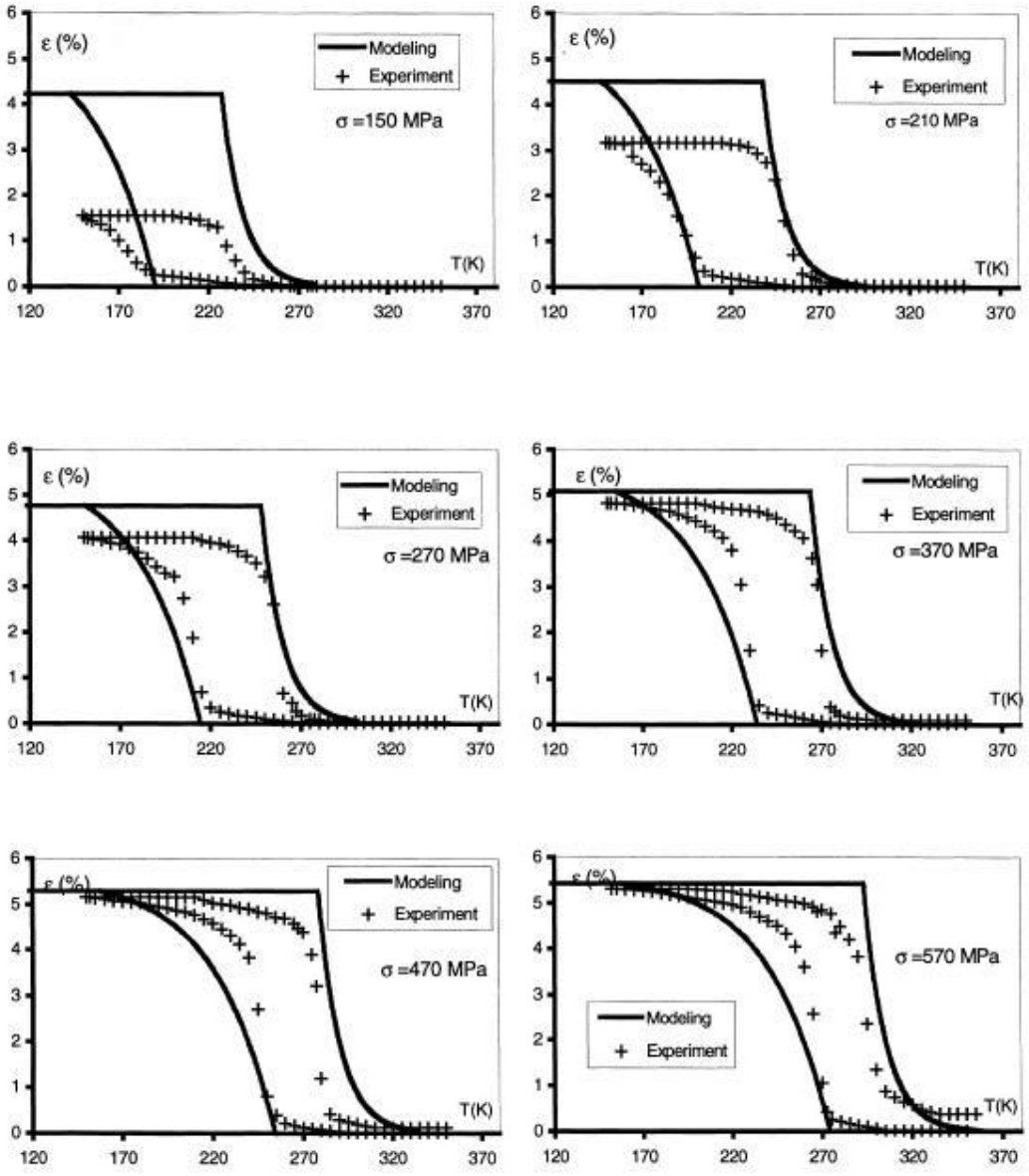

Figure II.22: Measured and calculated strain-temperature curves on Ti-51.5Ni (at%) thin film at different stress levels (Fig. 6a of Ref. [Getal00])

II.2.3.2. Validity of models

Although the R_L model was developed to describe the stress induced martensitic transformation behaviour of shape memory alloys when only oriented martensite can form, it allows us to calculate the thermal induced martensitic transformation case where the conditions are so that only one type of martensite can appear. It can be seen from the fact that the equations of L–L lead to the ones of R_L if only one martensite is considered and if it is the self-accommodated one, then the γ has to be equal to zero, i.e. the $\gamma\sigma/\rho$ term vanishes in expression of π^f. I must to note that at stress-free state this term vanishes automatically and so the R_L model works correctly without changing γ to zero.

References

[O&W] K. Otsuka and C. M. Wayman: *Shape Memory Materials*, 1998 Cambridge University Press

[Ketal06] J.-H. Kim, T. Fukuda, T. Kakeshita: *Effects of magnetic field and hydrostatic pressure on the martensitic transformation temperature of Ni–Mn–Ga ferromagnetic shape memory alloys*, Materials Science and Engineering A **438–440** (2006) p. 952

[Detal00] L. Daróczi, D.L. Beke, C. Lexcellent and V. Mertinger: *Effect of hydrostatic pressure on the martensitic transformation in CuZnAl(Mn) shape memory alloys,* Scripta materialia **43** (2000) p. 691

[Detal02] L. Daróczi, D.L. Beke, C. Lexcellent, V. Mertinger: *Effect of hydrostatic pressure on the martensitic transformation in near equiatomic Ti–Ni alloys*, Philosophical Magazine B **82/1** (2002) p. 105

[Betal04] D.L. Beke, L. Daróczi, C. Lexcellent, V. Mertinger: *Determination of stress dependence of elastic and dissipative energy terms of martensitic phase transformations in a NiTi shape memory alloy*, Journal de Physique IV (France) **115** (2004) p. 279

[O&P88] J. Ortin and A. Planes: *Thermodynamic analysis of thermal measurements in thermoelastic martensitic transformations*, Acta Metallurgica **36** (1988) p. 1873

[Tetal99] K. Tanaka, K. Kitamura, and S. Miyazaki: *Shape memory alloy preparation for multiaxial tests and identification of fundamental alloy performance Archives of Mechanics*, **51/6** (1999) p. 785

[Retal92] B. Raniecki, C. Lexcellent and K. Tanaka: *Thermodynamics models of pseudoelastic behaviour of shape memory alloys Archives of Mechanics*, **44/3** (1992) p. 261

[R&L94] B. Raniecki and C. Lexcellent: *Models of pseudoelasticity and their specification for some shape memory alloys*, European Journal of Mechanics and Solids **13** (1994) p. 21

[R&L98] B. Raniecki and C. Lexcellent: *Thermodynamics of isotropic pseudoelasticity in shape memory alloys*, European Journal of Mechanics and Solids **17** (1998) p. 185

[L&L96] S. Leclercq and C. Lexcellent: *A general macroscopic description of the thermo-mechanical behavior of shape memory alloys*, Journal of the Mechanics and Physics of Solids **44/6** (1996) p. 953

[Getal00] B. Gabry, C. Lexcellent, V. H. No, S. Miyazaki: *Thermodynamic modelling of the recovery strain of sputter-deposited shape memory alloys Ti-Ni and Ti-Ni-Cu thin films*, Thin Solid Films **372** (2000) p. 118

[K&M59] D. P. Koistinen and R. E. Marburger: *A general equation prescribing the extent of the austenite-martensite transformation in pure iron-carbon alloys and plain carbon steels*, Acta Metallurgica **7** (1959) p. 59

[O&F95] L. Orgeas and D. Favier: *Non-symmetric tension-compression behaviour of NiTi alloy*, Jornal de Physique IV Colloque (France) **5** C8 (1995) p. 605

Chapter III

Experiment and evaluation

III. Experiment and evaluation

III.1. Generalization of Beke-Daróczi model for the whole transformation

The anisothermal tests are usually made on different shape memory alloys to determine only the transformation temperatures from the measured hysteresis curves. Nevertheless these curves contain information about the whole martensitic transformation, i.e. one can follow up both the forward and the reverse transition as a function of transformed (martensitic) fraction, ξ, and even the ξ dependence of the non-chemical energies can be obtained. [Petal05]

III.1.1. Expressions for the up and down parts of the hysteresis loop

The starting relation is the (II.1) equation, which is pasted here as (III.1), because the derivatives of the Gibbs free energy changing according to the transformed fraction is equal to zero not only at the starts end finish temperatures but at any time during the transformation; namely the martensitic phase transition is diffusionless and so a balanced state can find an other equilibrium very fast after any temperature or loading force changes, i.e. the derivatives of the Gibbs free energy according to the martensitic fraction is equal to zero through A→M and M→A transitions:

$$\frac{\partial\left(\Delta G^{\downarrow}\right)}{\partial\xi} = \Delta g_c{}^{\downarrow} + d^{\downarrow}(\xi) + e^{\downarrow}(\xi) = 0 \qquad \text{(III.1)}$$

and a similar one is valid for M→A, too:

$$\frac{\partial\left(\Delta G^{\uparrow}\right)}{\partial\xi} = \Delta g_c{}^{\uparrow} + d^{\uparrow}(\xi) + e^{\uparrow}(\xi) = 0 \qquad \text{(III.2)}$$

Furthermore the expressions of the chemical terms don't change either, because the chemical free energy and the transformed fraction changes are linear to each other and the derivation keeps the slope only, which can be easily derived from the expression of chemical Gibbs free energy of the two phase system:

$$G_c = (1-\xi)G_c{}^{A} + \xi G_c{}^{M} \qquad \text{(III.3)}$$

Thus using the relation about the enthalpy and entropy changes one receives:

$$\Delta g_c{}^{\downarrow}(T) = -\Delta g_c{}^{\uparrow}(T) = (T_0 - T)\Delta s_c \qquad \text{(III.4)}$$

and $\Delta s_c = s^M - s^A$ (<0) like before. Writing it in (III.1) and in (III.2) two relations will be received:

$$(T_0 - T)\Delta s_c + d^{\downarrow}(\xi) + e^{\downarrow}(\xi) = 0 \qquad \text{(III.5)}$$

$$(T - T_0)\Delta s_c + d^{\uparrow}(\xi) + e^{\uparrow}(\xi) = 0$$

where T is the temperature at which the derivatives of the chemical and the non-chemical energies cancel each other and the direction and martensitic fraction dependence of non-chemical ones result the usual hysteretic behaviour, i.e. the temperature of the forward and the reverse transformation can be expressed by T_0 and the derivatives of non-chemical energies whose transformed fraction dependence appears in the temperature.

$$T^{\downarrow}(\xi) = T_0 + \frac{d^{\downarrow}(\xi) + e^{\downarrow}(\xi)}{\Delta s_c}$$

$$T^{\uparrow}(\xi) = T_0 - \frac{d^{\uparrow}(\xi) + e^{\uparrow}(\xi)}{\Delta s_c} \qquad \text{(III.6)}$$

The $T^{\downarrow}(\xi)$ and $T^{\uparrow}(\xi)$ functions are the inverses of the well known $\xi^{\downarrow}(T)$ and $\xi^{\uparrow}(T)$ which can be calculated from resistance-temperature or from strain-temperature curves using a normalizing process which includes the eliminating of thermal effect and the actual normalizing, i.e. $\xi=0$ at parent state and $\xi=1$ at martensitic state.

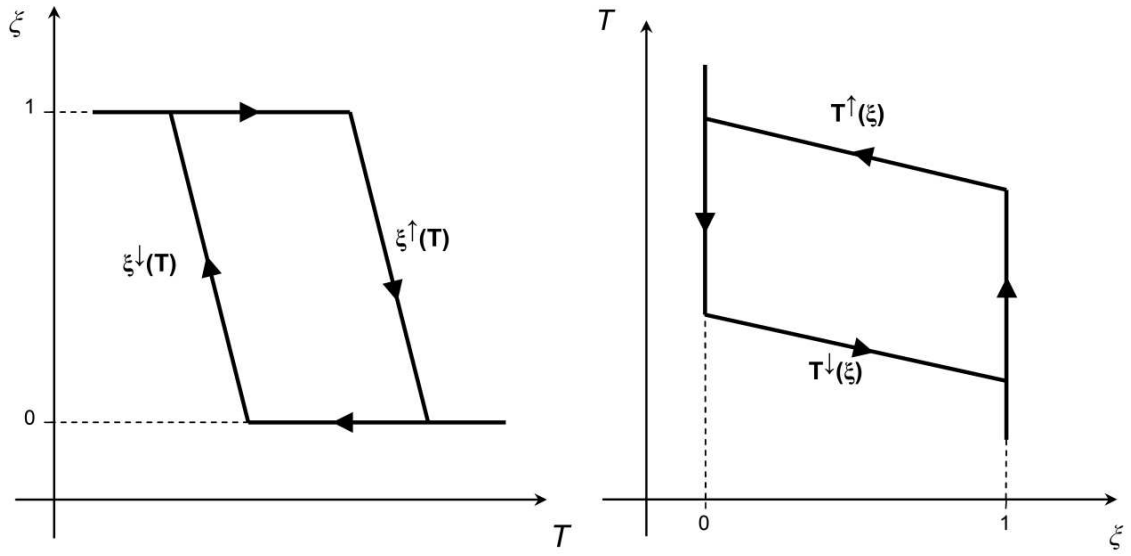

Figure III.1: The well known ξ(T) hysteresis loop and its inverse

Obviously the (III.6) equations give back the relations valid for start and finish temperatures (II.5), if one uses the next notifications:

$$M_s = T^{\downarrow}(0); \quad M_f = T^{\downarrow}(1); \quad A_s = T^{\uparrow}(1); \quad A_f = T^{\uparrow}(0)$$
$$d_0^{\downarrow} = d^{\downarrow}(0); \quad d_1^{\downarrow} = d^{\downarrow}(1); \quad d_0^{\uparrow} = d^{\uparrow}(0); \quad d_1^{\uparrow} = d^{\uparrow}(1) \qquad \text{(III.7)}$$
$$e_0^{\downarrow} = e^{\downarrow}(0); \quad e_1^{\downarrow} = e^{\downarrow}(1); \quad e_0^{\uparrow} = e^{\uparrow}(0); \quad e_1^{\uparrow} = e^{\uparrow}(1)$$

If thermal cycles is measured on shape memory alloys under different circumstances (applied pressure, stress, etc.), one will experience that the characteristic temperatures are shifted and even the shapes of the hysteresis branches are changed. Regarding the (III.6) relations, which are valid in stress-free and under-loading cases, the shape change can be derived only from the external field dependence of the elastic or the dissipative contributions, because only they depend on the transformed fraction. On the contrary, supposing the entropy change isn't sensible to external load, a reason of the temperature shifting is stress or pressure dependence of the equilibrium temperature, which dependence is described by the Clausius-Clapeyron equation, but the magnitude change of the non-chemical energies can do theirs bit from this shifting.

Let us compose the sum and the difference of the (III.6) expressions.

$$T^{\downarrow}(\xi)+T^{\uparrow}(\xi)=2T_0+[e^{\downarrow}(\xi)-e^{\uparrow}(\xi)+d^{\downarrow}(\xi)-d^{\uparrow}(\xi)]/\Delta s_c$$
$$T^{\downarrow}(\xi)-T^{\uparrow}(\xi)=[e^{\uparrow}(\xi)+e^{\downarrow}(\xi)+d^{\uparrow}(\xi)+d^{\downarrow}(\xi)]/\Delta s_c \qquad \text{(III.8)}$$

These relations will have roles in the next two sections.

III.1.2. Correlation between the differential and the integral quantities

As one can see there is an analogy between the corresponding (II.14) and (III.8) equations, and if the connection between the differential and integral quantities is cleared, this analogy will become relations.

Since the small letters mean the differential quantities the next equations are relevant:

$$\int_0^1 \Delta h_c{}^{\downarrow} d\xi = -\int_0^1 \Delta h_c{}^{\uparrow} d\xi = \int_0^1 T_0 \Delta s_c d\xi = \Delta H_c \ (<0)$$
$$\int_0^1 d^{\downarrow}(\xi)d\xi = D^{\downarrow} \ (>0) \qquad \int_0^1 d^{\uparrow}(\xi)d\xi = D^{\uparrow} \ (>0) \qquad \text{(III.9)}$$
$$\int_0^1 e^{\downarrow}(\xi)d\xi = E^{\downarrow} \ (>0) \qquad \int_0^1 e^{\uparrow}(\xi)d\xi = E^{\uparrow} \ (<0)$$

After all, one can get the next two equations which describe the correlation between the measurable "differential" ($T^{\downarrow}(\xi)$, $T^{\uparrow}(\xi)$) and "integral" ($Q^{\downarrow}$, $Q^{\uparrow}$) quantities.

$$\int_0^1 \Delta s_c (T^{\downarrow}(\xi)+T^{\uparrow}(\xi))d\xi = Q^{\downarrow}-Q^{\uparrow}$$
$$\int_0^1 \Delta s_c (T^{\downarrow}(\xi)-T^{\uparrow}(\xi))d\xi = Q^{\downarrow}+Q^{\uparrow} \qquad \text{(II.12)}$$

These equations allow us without any simplifier assumptions to examine the self consistency of this model.

III.1.3. Extending the typical assumptions

Like Chapter II we meet the same problem, namely the number of variables ($e^{\downarrow}(\xi)$, $e^{\uparrow}(\xi)$, $d^{\downarrow}(\xi)$, $d^{\uparrow}(\xi)$) is more than the number of equations and even if we forget the determination of T_0 is not possible in lots of cases. So similar assumptions have to be accepted like in case of pure-phase evaluation (section II.1.4.), i.e. the direction dependence has to be eliminated: $e^{\downarrow}(\xi)=-e^{\uparrow}(\xi)=e(\xi)\geq 0$ and $d^{\downarrow}(\xi)=d^{\uparrow}(\xi)=d(\xi)\geq 0$. Hence such relations are received which resemble to the (II.12) ones:

$$T^{\downarrow}(\xi)=T_0+\frac{d(\xi)+e(\xi)}{\Delta s_c}=T_0-T_d(\xi)-T_e(\xi)$$
$$T^{\downarrow}(\xi)=T_0-\frac{d(\xi)-e(\xi)}{\Delta s_c}=T_0+T_d(\xi)-T_e(\xi) \qquad \text{(III.13)}$$

where

$$T_d(\xi)=\frac{d(\xi)}{-\Delta s_c}\geq 0; \qquad T_e(\xi)=\frac{e(\xi)}{-\Delta s_c}\geq 0. \qquad \text{(III.14)}$$

Now, to express the derivatives of the non-chemical free energies the assumptions have to be applied to (III.8) and after a little arrangement one receives the next:

$$d(\xi)=-\Delta s_c\frac{T^{\downarrow}(\xi)-T^{\uparrow}(\xi)}{2}$$
$$e(\xi)=\Delta s_c\frac{T^{\downarrow}(\xi)+T^{\uparrow}(\xi)}{2}-\Delta s_c T_0 \qquad \text{(III.15)}$$

III.2. Measurements in polycrystalline samples

As continuance of the work of Beke and Daróczi [Detal00, Detal02, Betal04] I investigated the effect of tensile stress dependence on the derivatives of non-chemical energies during martensitic transformation on CuAlNi shape memory alloy. Firstly the dissipative and elastic terms were determined in pure phases [Detal04]; then the extended evaluation method was used to have information about the whole transformation [Petal05].

III.2.1. Anisothermal test under constant stress

III.2.1.1. Samples manufacturing

A copper based shape memory alloy was chosen for the further tests. The Cu-24.0at% Al-2.2at% Ni samples with 0.5at% B addition were melted in arc melting equipment from elemental components. Then the melt was snuffed up into an Al_2O_3 tube with 1.1 mm internal diameter, so-cast l_0=28.5mm length wires were used for the experiments. The composition was determined by energy dispersive X-ray spectrometry in a scanning electron microscope.

III.2.1.2. Experimental set-up

The equipments in which anisothermal test can be done under external constant stress are not so diffused than the ones which are built for isothermal tests. Hence we decided to develop our own machines and so we can construct it after our wishes, the Fig. III.2 illustrates the heating–cooling, the loading and the strain measurement systems.

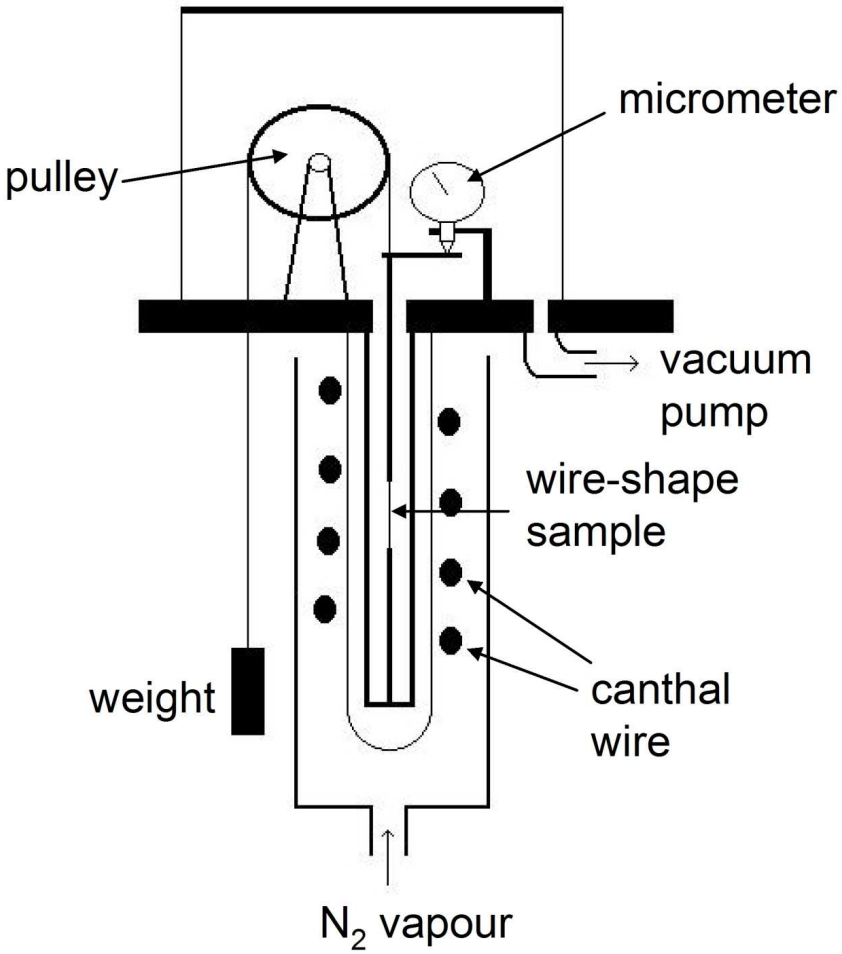

Figure III.2: Schematic figure about anisothermal test equipment

The sample was oriented vertically to be sure that the gravity can not bend it which can cause that the stress field won't be uniaxial. Furthermore the sample was fixed by its bottom and its other end was pull by a cord which was guided through a pulley for the direction

change and the appropriate weights for a certain stress hung on its other end. Actually the cord was used only on the pulley and the rest of the loading system was made by bar steel. At the boundary of the vacuum chamber and the outer atmosphere a packing-gland assured the hermetic sealing in which an oiled bar moved.

The equipment was designed so that it allows us to measure simultaneously the resistance and the change of length of the sample precisely as functions of temperature. A copper-constantan thermocouple fixed to the middles of sample gave the temperature information, the resistance of sample was determined using the four-wire method and a micrometer was used to measure the change of length. To avoid the oxidation of sample and the condensation of water on the sample, which could have changed its resistance, the specimen was placed in a small vacuum chamber.

External heating–cooling system was applied: a resistance furnace made by canthal wire heated up the part of the chamber where the specimen was located and vapour of liquid nitrogen was blown into the furnace, so the cooling was localised as well.

III.2.1.3. Hysteresis curves

Using this equipment we investigated the thermal cycles at constant stress up to 100 MPa[*], both the resistance-temperature and the elongation-temperature curves were measured. At low stresses the resistance hysteresis loops was rather usable to follow up the transformation (Fig. III.3/a) and the measurement of the change of length was important to determine the transformational strain $\varepsilon^{tr}=\Delta l/l_0$ (Fig. III.3/b).

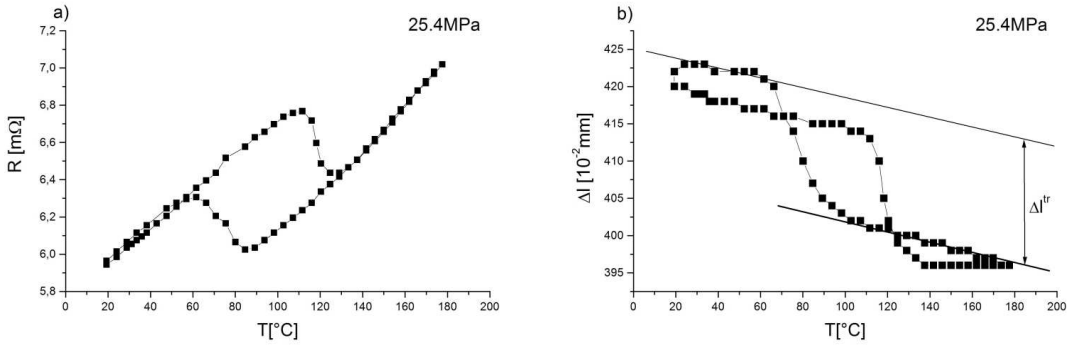

Figure III.3: a) Resistance and b) change of length hysteresis loops at 25.4MPa uniaxial stress (where Δl is the change of length accompanied to the transformation)[*]

Increasing the loading force both the resistance-temperature (Fig. III.4/a) and elongation temperature (Fig. III.4/b) hysteresis curves open the door to determine the transformation temperatures or even to perform the normalization process.

[*] Because of a calculation error the stress values were about 10 times smaller in the Refs. [Detal04] and [Petal05]. Here this error is corrected and the correct figures will be signed by a superscripted star.

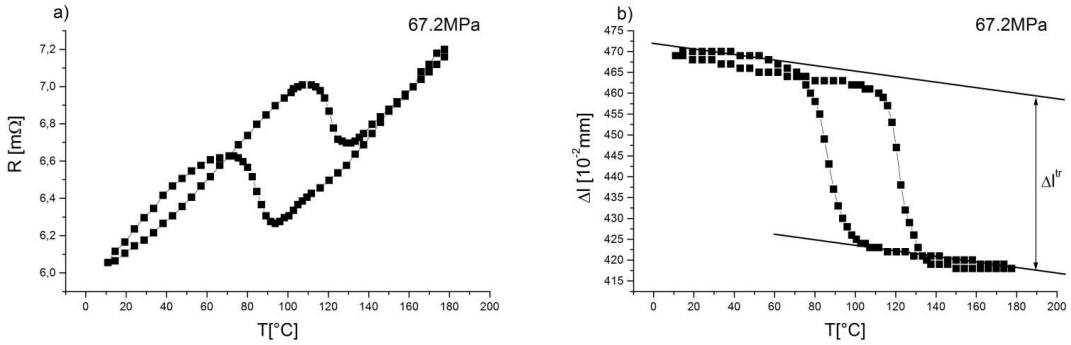

Figure III.4: a) Resistance vs. temperature and b) elongation vs. temperature hysteresis loops at 67.2MPa uniaxial stress[*]

As one can see that both on the resistance-temperature and on the elongation-temperature hysteresis curves there are loops besides of the hysteretic behaviour. In the case of elongation these artifacts are derived from the shifting of the cooling down and the heating up branches to each other this effect probably comes from the fact that the steel bar couldn't move easily, i.e. a limit force was needed to put it in motion, or the different hydrostatic pressure values cause the shifting. In the case of resistance the additional loop appears only in martensite state and even its size is different at different stress levels, for example at 78.2MPa its area is about the half of the hysteresis loop while at 25.4MPa any additional loop can not be experienced. In conclusion the elongation-temperature hysteresis loops are more appropriate to be the bases of the evaluation processes in spite of its weak resolution at low stresses.

All measured hysteresis loops can be found in Appendix A.

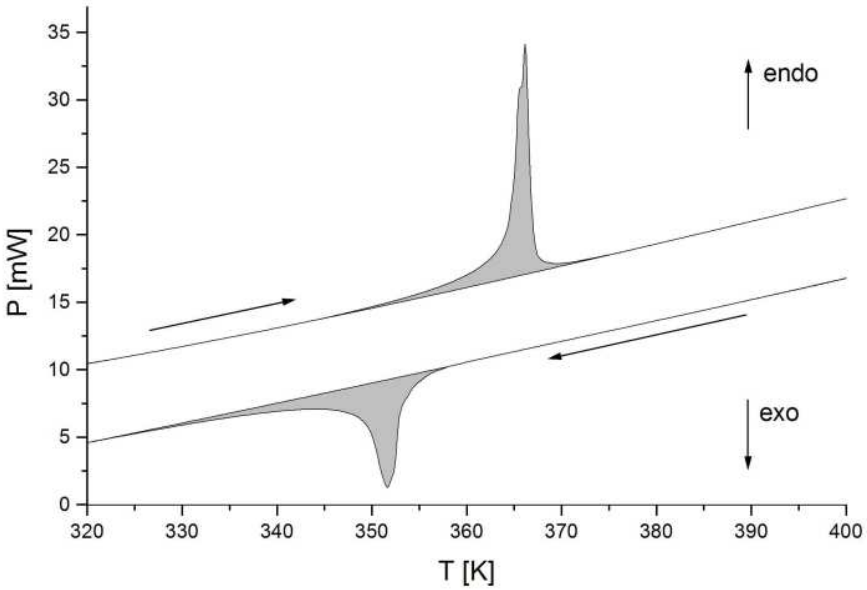

Figure III.5: DSC curves measured at zero stress

[*] See footnote at page 61.

III.2.1.4. DSC measurement

As it was cleared in the previous chapter the entropy change between the parent and the martensitic phase during the martensitic transformation is needed to the evaluation procedure. To obtain this information a Perkin-Elmer DSC 7 was used to measure the absorption and release of energy during the martensitic transformation at stress free state. (Fig. III.5)

III.2.2. Evaluation in accordance with B-D model

III.2.2.1. In the pure phases

III.2.2.1.1. Measured parameters

First of all the start and finish temperatures (M_s, M_f, A_s and A_f) were determined, we considered the start as well as the finish points where the hysteresis curve leaves as well as returns the linear fitted on the pure phases, respectively (Fig. III.6). However this temperature values are sensitive to the fitting and so ±5K error was considered. Finally the transformation temperatures vs. stress functions can be seen in the Fig. III.7.

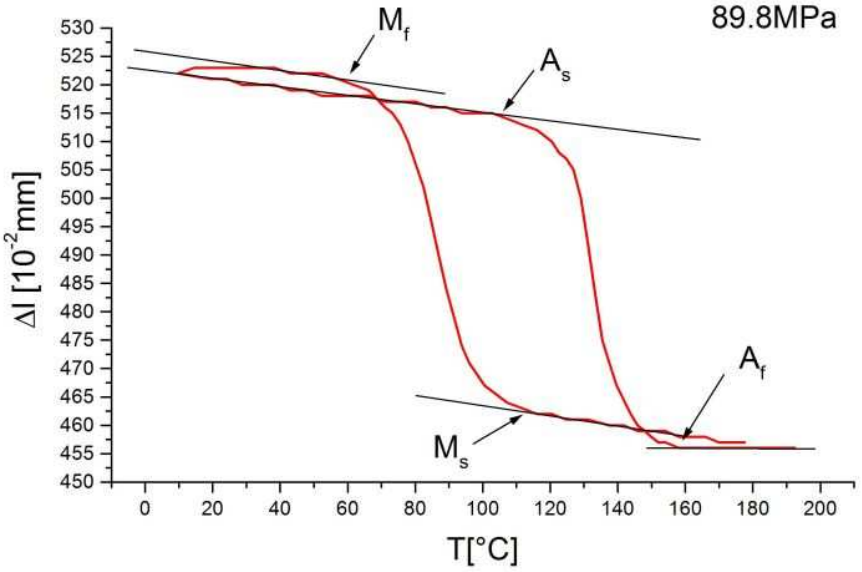

Figure III.6: Determination of transformation temperatures from elongation-temperature hysteresis curve[*]

- 63 -

[*] See footnote at page 61.

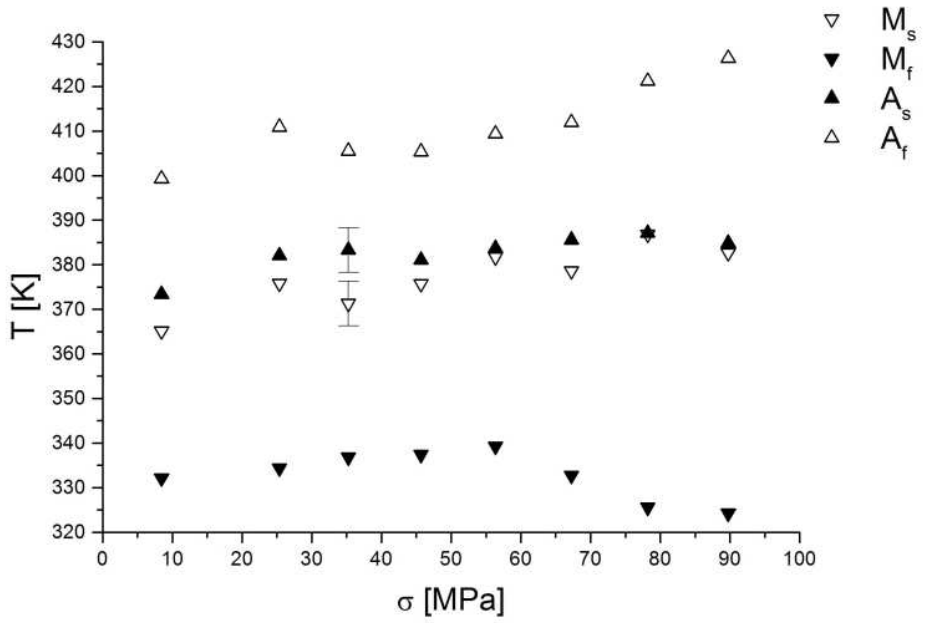

Figure III.7: Transformation temperatures at different stress levels stress[*]

Almost all transformation temperatures show increasing tendencies at the whole stress range except of the martensite finish temperature which becomes decreasing from 57MPa. The M_s and A_s temperatures are almost correspondent to each other; the biggest difference, where it is more than the error limit only, can be experienced at 35MPa.

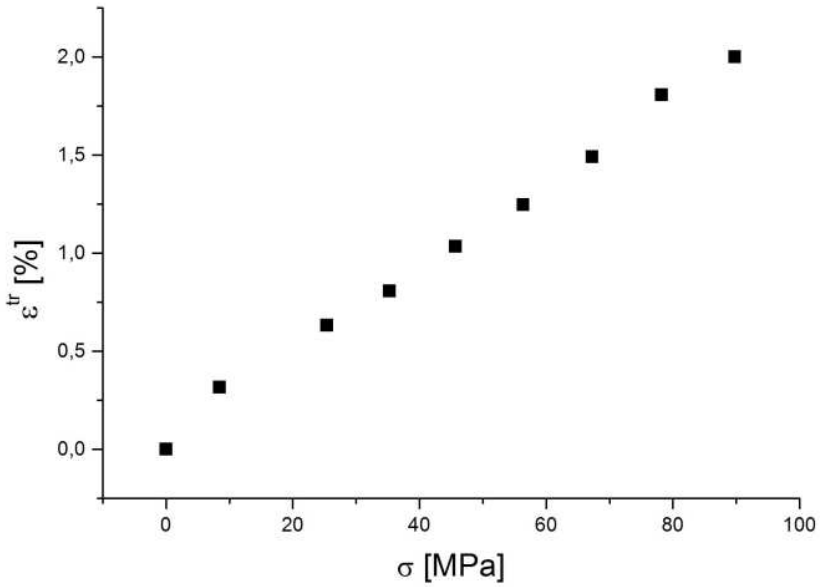

Figure III.8: Transformation strain as a function of stress[*]

- 64 -

[*] See footnote at page 61.

Due to the measurement of change of length the stress dependence of the transformational strain could be determined (Fig. III.8) and as it can be seen that it depends linearly on the uniaxial stress so the general form of Clausius-Clapeyron relation (II.9) has to be used to describe the stress dependence of the equilibrium transformation temperature.

Ortín and Planes [O&P88] showed that the entropy changes can be calculated from a DSC curve as follows:

$$\Delta s_c^{\downarrow} = \int_{M_s}^{M_f} \frac{dQ^{\downarrow}}{T}$$

$$\Delta s_c^{\uparrow} = \int_{A_s}^{A_f} \frac{dQ^{\uparrow}}{T} \qquad \text{(III.16)}$$

and if the heat capacity difference between the parent and the product phase is zero ($c_p^A = c_p^M$) the magnitude of the entropy change is independent from the direction of the transformation and it is negative for A→M and positive for M→A. Nevertheless, if $c_p^A \neq c_p^M$, then a correction term appears between the $\Delta s_c^{\downarrow}$ and $\Delta s_c^{\uparrow}$ likewise in case of dissipated energy (II.17):

$$\Delta s_c^{\downarrow} + \Delta s_c^{\uparrow} = (c_p^{\,M} - c_p^{\,A}) \ln \frac{T_M}{T_A} \qquad \text{(III.17)}$$

but now because of term $ln(T_M/T_A)$ this correction is negligible in most of case. Evaluating the data from the DSC measurement (Fig. III.5)

$\Delta s_c^{\downarrow} = -1{,}393 * 10^5\ J/Km^3$ and $\Delta s_c^{\uparrow} = 1{,}379 * 10^5\ J/Km^3$

are obtained. Since the difference of their magnitude is within error it is acceptable to neglect the heat capacity correction and during the evaluation

$\Delta s_c = 1/2(\Delta s_c^{\downarrow} - \Delta s_c^{\uparrow}) = -1{,}386 * 10^5\ J/Km^3 = -1.026\ J/Kmol$

is used.

III.2.2.1.2. Stress dependence of non-chemical free energies

Combining the relations of the transformation temperatures (II.12) one can obtain the next expressions taking into account the stress dependence of the transformation equilibrium temperature, T_0:

$$d_0(\sigma) = -\Delta s_c \frac{A_f(\sigma) - M_s(\sigma)}{2}$$

$$d_1(\sigma) = -\Delta s_c \frac{A_s(\sigma) - M_f(\sigma)}{2} \qquad \text{(III.18)}$$

and

$$e_0(\sigma) = \Delta s_c \frac{A_f(\sigma) + M_s(\sigma)}{2} + \sigma\varepsilon^{tr}(\sigma) - \Delta s_c T_0(0)$$
$$e_1(\sigma) = \Delta s_c \frac{A_s(\sigma) + M_f(\sigma)}{2} + \sigma\varepsilon^{tr}(\sigma) - \Delta s_c T_0(0) \qquad \text{(III.19)}$$

Now it is obvious that the derivatives of the dissipative energy can be determined exactly, but for lack of knowing $T_0(0)$ only the tendency of the elastic ones can be given.

The derivatives of the dissipative and of the elastic free energy calculated can be found in Figs. III.9 and III.10. The transformed fraction derivatives of the dissipative free energy contribution at ξ=0 (d_0) and at ξ=1 (d_1) are approximately constant at low stresses and they show small increasing above 55MPa and d_1 is bigger than d_0 for the whole stress range, however the difference between them is almost within error. In case of elastic contribution it is experienced that it is bigger at ξ=1 than ξ=0 just like by dissipated ones and both of them do not change significantly with the stress.

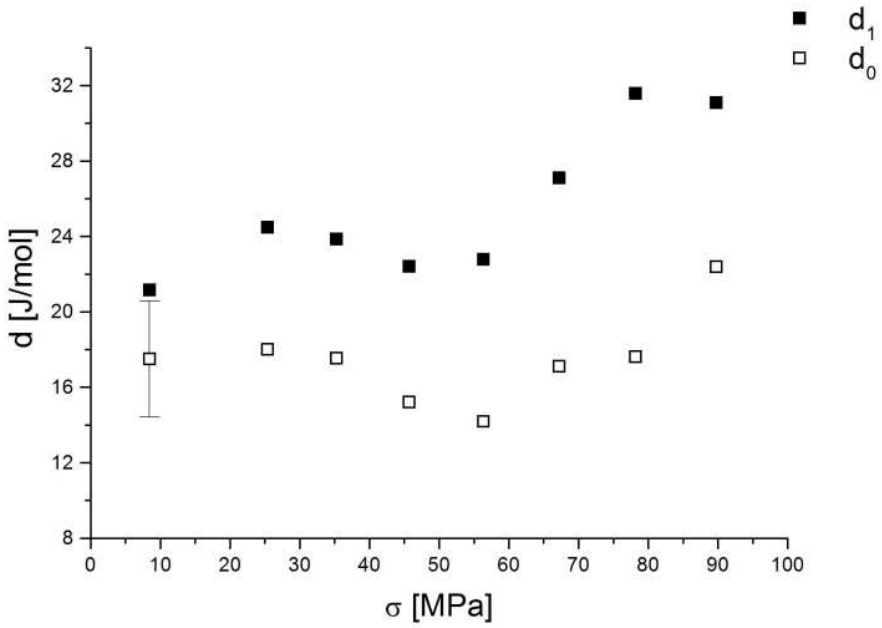

Figure III.9: The derivatives of dissipative free energies vs. uniaxial stress[*]

[*] See footnote at page 61.

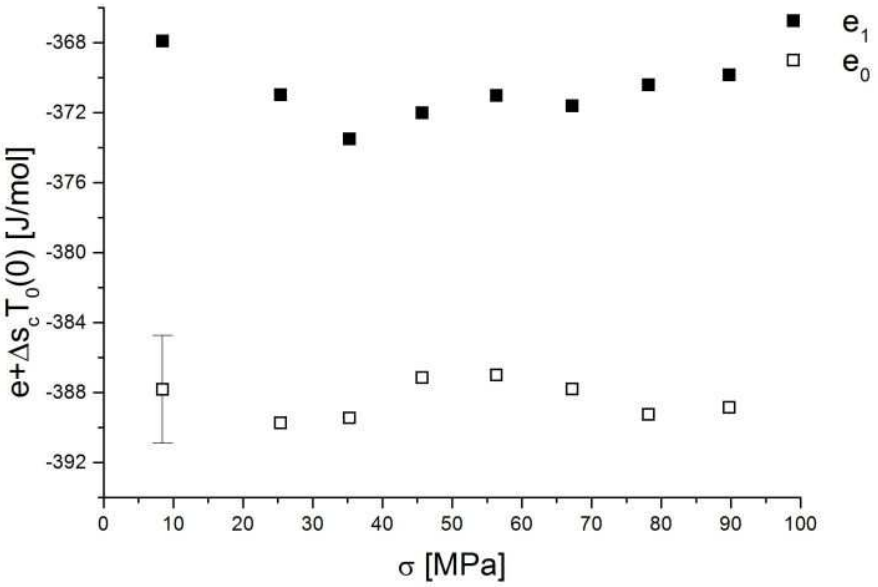

Figure III.10: Stress dependence of the derivatives of elastic free energies in austenite (e_0) and in martensite (e_1) phases[*]

III.2.2.2. During the whole transformation

III.2.2.1.1. Normalization of measured hysteresis

Regarding the (III.6) equations to calculate the non-chemical free energies one needs to know the temperatures of the down and high branches as a function of martensitic fraction, so a normalization process has to be done, which consist of two parts: eliminating the thermal effects and converting the hysteresis loop between 0 and 1.

As it follows from the section III.2.1.3. the elongation-temperature curves are more appropriate to perform the normalization process (Fig. III.11), but at the lowest stress levels the resolution of the elongation measurement does not allow us to follow the transformation. So in this case the resistance-temperature hysteresis loop was used to have the normalized one and fortunately in this case the above mentioned additional loop is treatable (Fig. III.12).

[*] See footnote at page 61.

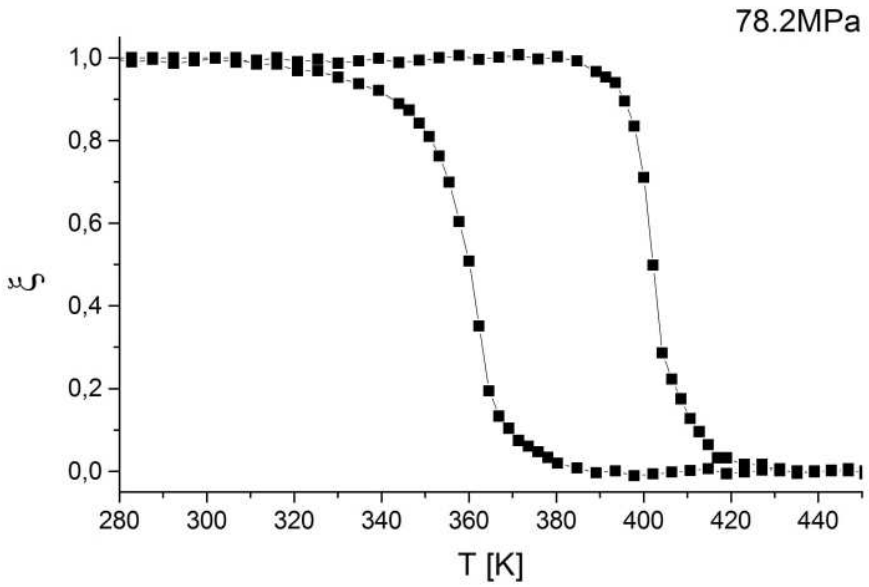

Figure III.11: Normalized hysteresis loop from measured elongation-temperature curve at 78.2MPa[*]

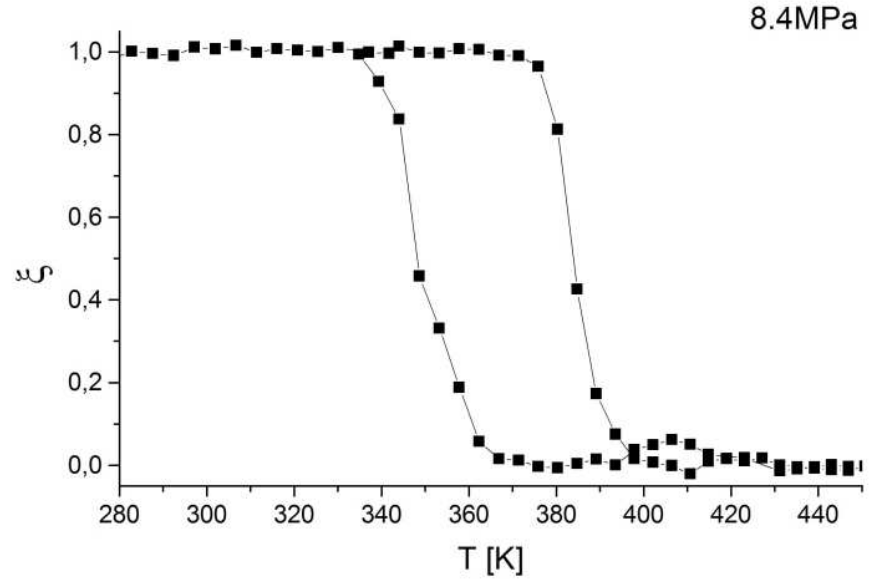

Figure III.12: Normalized hysteresis loop from measured resistance-temperature curve at 8.4MPa[*]

Performing this normalization process one receives ξ(T) functions of the down and up branches; then inverting them the $T^{\downarrow}(\xi)$ and $T^{\uparrow}(\xi)$ curves are obtained (Fig. III.13). It is worth to note that the determination of the down and up temperatures has bigger errors in the start

- 68 -

[*] See footnote at page 61.

(ξ=0) and finish points (ξ=1) than in the middle of the transformation between ξ=0.1 and ξ=0.9. It comes from that fact the start and finish temperatures are very sensitive to the base lines, so the normalization process is responsible for the different error bars (Fig. III.13).

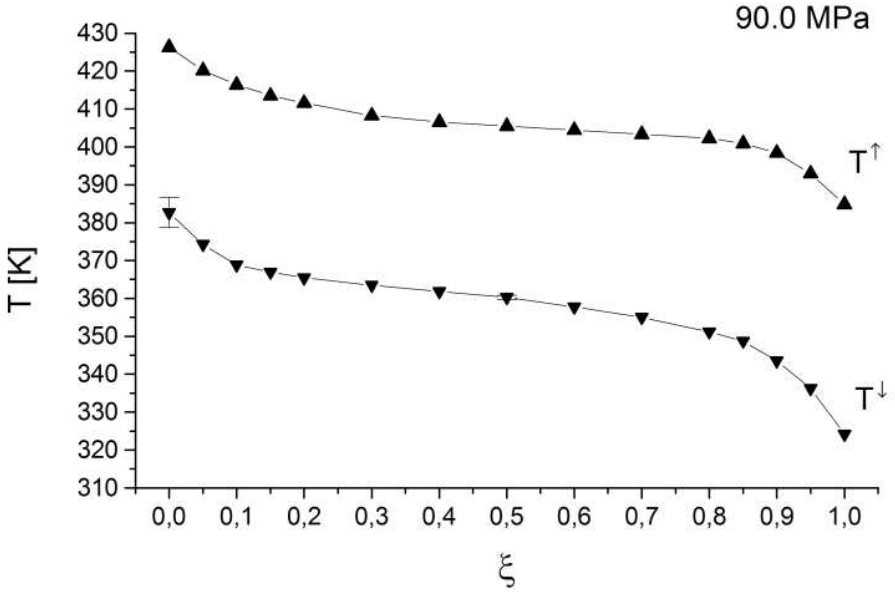

Figure III.13: The temperature of the up and low branches as a function of martensitic fraction (The size of error in the middle of transformation is equal to the size of the symbols and in the start and in the finish points it can be considered as the error bar at $T^{\downarrow}(\xi=0)$*)*[*]

III.2.2.1.1. Derivatives of the non-chemical free energies

Knowing the $T^{\downarrow}(\xi)$ and $T^{\uparrow}(\xi)$ temperatures, the specific entropy change and taking into account the Clausius-Clapeyron relation the (III.15) equations allow us to calculate the derivatives of the dissipative and elastic terms as a function of martensitic fraction. The summary of $T^{\downarrow}(\xi)$ and $T^{\uparrow}(\xi)$ is proportional to the derivatives of the elastic free energy, as well as their difference is proportional to the dissipative term, respectively; so the experienced parallel branches pre-indicate constant dissipative contribution during the martensitic transformation.

In the Fig. III.14 one can see that regarding the transformed fraction dependence of the derivatives of elastic term the differences between the different stress levels are within error limit and in the middle of the transformation the correspondence is perfect except of the lowest stress, where the resistance-temperature hysteresis loop was used for the normalization incidentally and it could cause the relatively big difference from the rest curves. Furthermore, it is worth to mention that the derivatives of the elastic energy contribution have singular points in the start and at the finish temperatures; and this behaviour leads thereto that the transformation paths tend tangentially to the base lines of the pure phases as Planes et al observed [Petal89].

In case of dissipative contribution the difference between the different stress levels are significant. It can be predicated that the derivatives of the dissipated free energy are constant

[*] See footnote at page 61.

independently of the uniaxial stress, only around the start and finish points one can experience different behaviour but where the error limit is bigger.

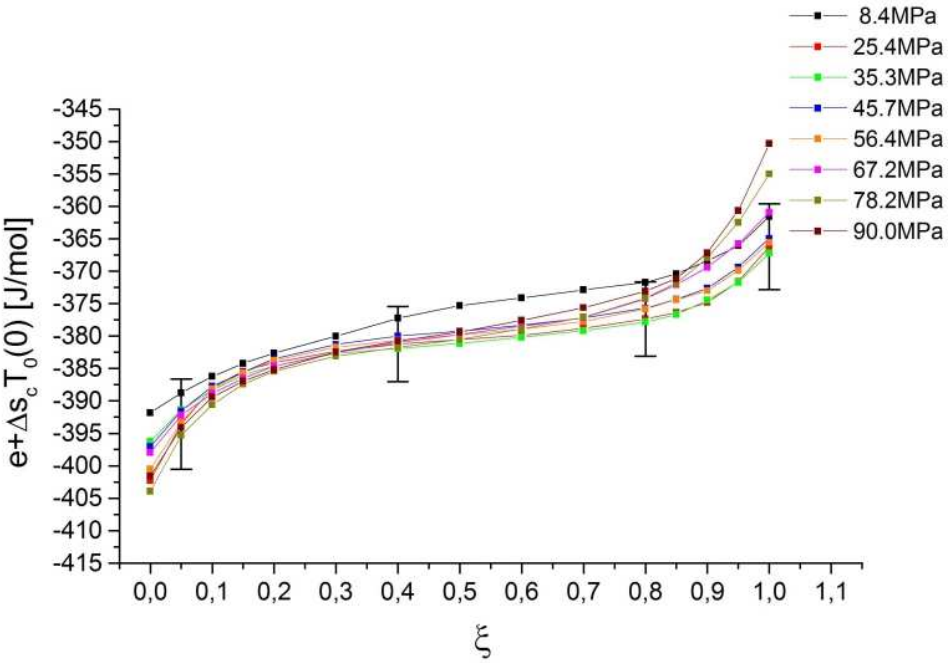

Figure III.14: Derivatives of elastic contribution determined irrespective of an additive constant vs. martensitic fraction[*]

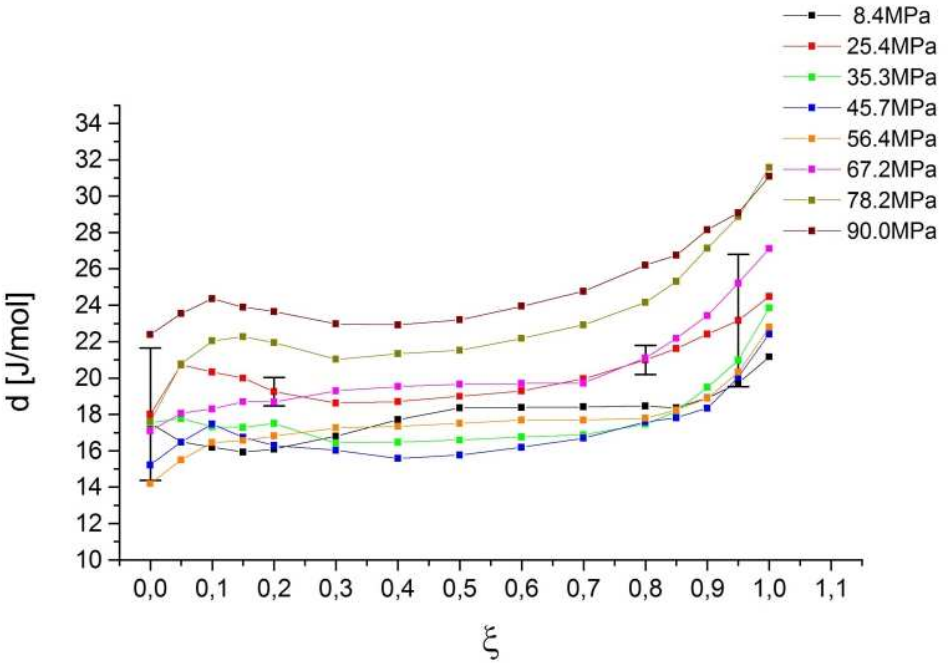

Figure III.15: Changing of the derivatives of the dissipative terms during the transformation[*]

- 70 -

[*] See footnote at page 61.

Using the fact that the derivative of the elastic free energy cannot be negative a lower bound can be given for $T_0(0)$ from (III.15) and using the Clausius-Clapeyron equation:

$$T_0(0) \geq \frac{T^{\downarrow}(\xi,\sigma) + T^{\uparrow}(\xi,\sigma)}{2} + \frac{\sigma\varepsilon^{tr}(\sigma)}{\Delta s_c}, \qquad \text{(III.20)}$$

and in the case of σ=78.2MPa and ξ=0 the left side of (III.20) is the biggest, so $T_0(0) \geq 393.8$K.

III.2.2.1.2. The non-chemical free energies

Until this point the derivatives of the different energy contributions were investigated, i.e. their slopes were determined as a function of transformed fraction. Nevertheless these data didn't provide us information about the amount of the dissipated energy and about the stored or released elastic one. However due to know the derivatives of these terms along the transformation one can calculate the transformed fraction dependence of the elastic and dissipative free energies:

$$D(\xi) = \int_0^{\xi} d(z)dz; \;\; E(\xi) = \int_0^{\xi} e(z)dz \qquad \text{(III.21)}$$

To calculate the elastic free energy one should know the exact value of its derivatives, i.e. the *$T_0(0)$*. If the above mentioned lower bound value is used, we could receive a good estimation (*E'*) for the elastic energy (Fig. III.16)

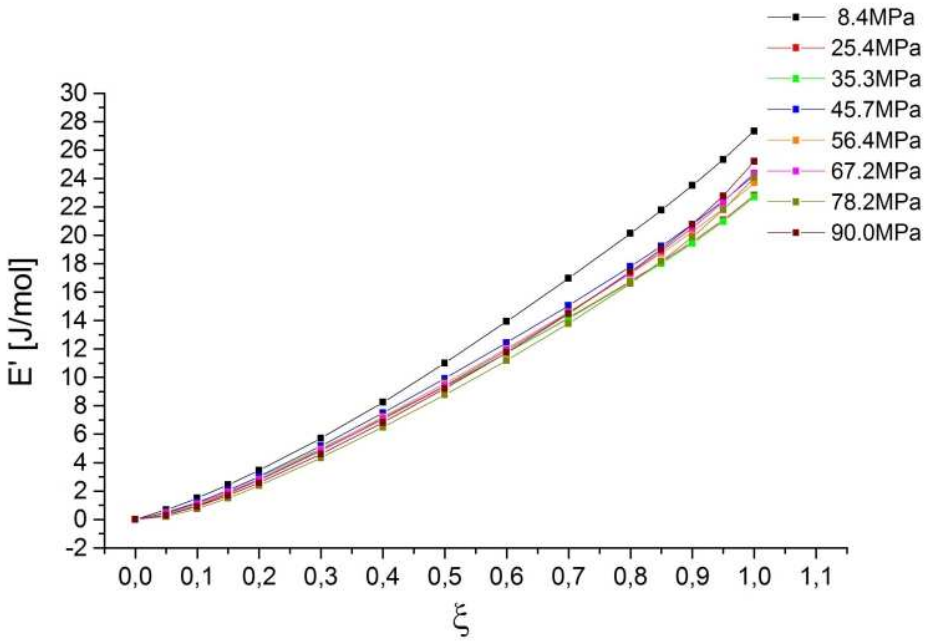

Figure III.16: The elastic energy vs. martensitic fraction (estimated result)[*]

[*] See footnote at page 61.

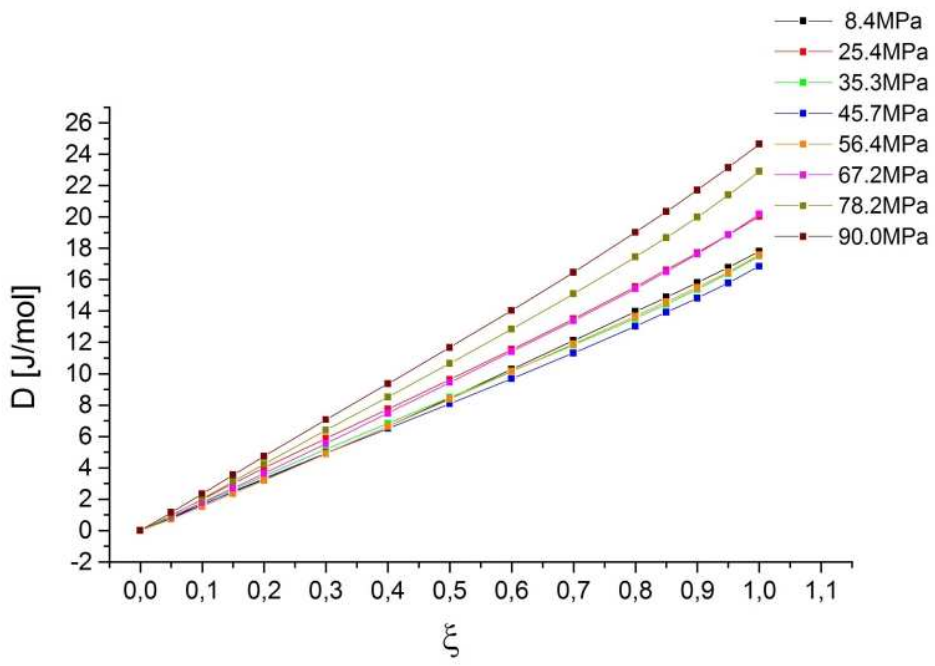

Figure III.17: The dissipated energy vs. martensitic fraction[*]

Let us consider the limit conditions to determine the direction dependence: the dissipative energy is zero at the start of the forward and the reverse transition ($D^{\downarrow}(\xi=0)=0$, $D^{\uparrow}(\xi=1)=0$) and the same amount of energy dissipated in both directions ($D^{\downarrow}(\xi=1)=D^{\uparrow}(\xi=0)$); on the other hand in austenite phase there is no elastic energy in the system ($E^{\downarrow}(\xi=0)=0$, $E^{\uparrow}(\xi=0)=0$) as well as the whole stored elastic energy during the forward transformation is released during the reverse one ($E^{\downarrow}(\xi=1)=E^{\uparrow}(\xi=1)$). In conclusion the next relations can be written:

$$D(\xi) = D^{\downarrow}(\xi) = D^{\uparrow}(1-\xi);\;\; E(\xi) = E^{\downarrow}(\xi) = E^{\uparrow}(\xi) \qquad \text{(III.22)}$$

III.2.2.1.3. Correlation between the differential and integral quantities

According to the section III.1.2. one can examine the evaluation processes performed on the hysteresis and on the DSC curves without any simplifying conditions. In Figs. III.18 and III.19 the open squares mean the values determined from stress free DSC measurement, while the solid ones are were calculated from the hysteresis curves at different stress levels. They show very good accordance, so it can be declared that our model is self-consistent.

[*] See footnote at page 61.

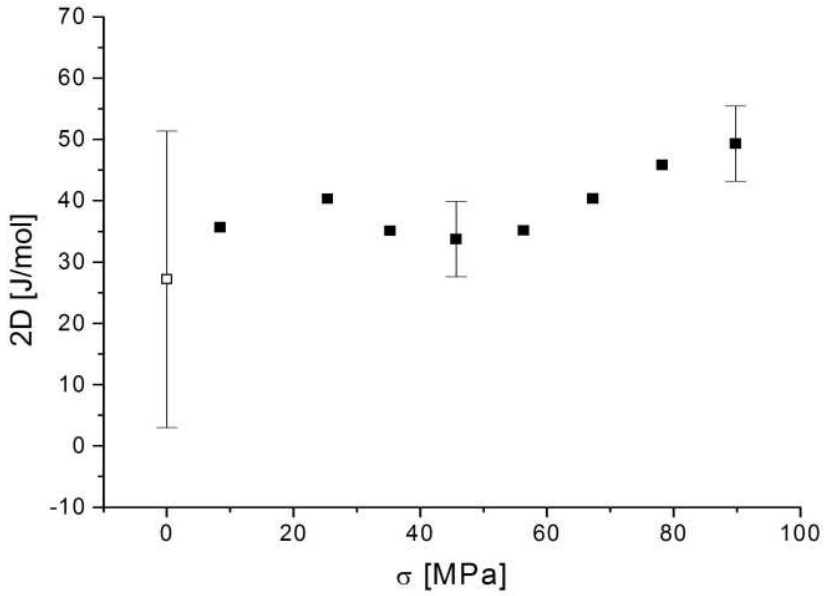

Figure III.18: The full dissipated energy during the complete martensitic (forward and reverse) transformation calculated from DSC (open square) and from hysteresis (solifd squares) measurement[*]

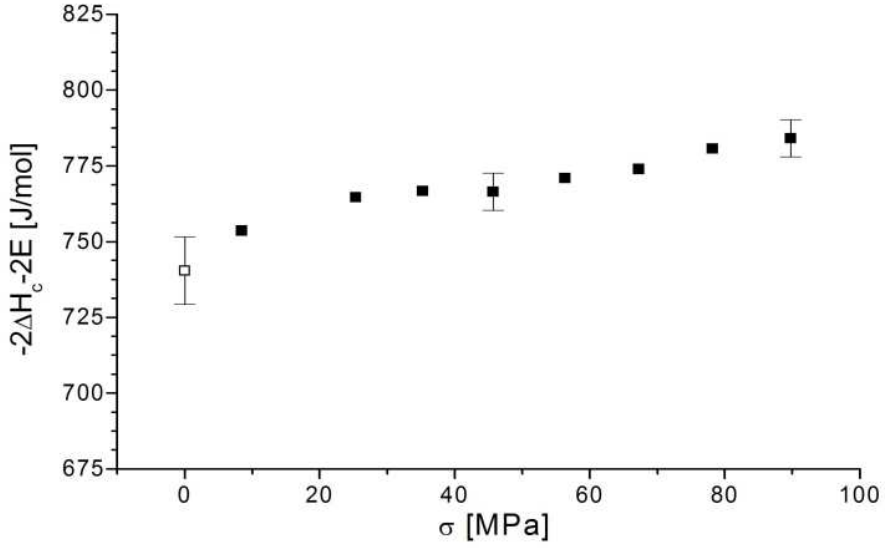

Figure III.19: The minus two times the elastic energy and the free-enthalpy calculated from DSC (open square) and from hysteresis (solid squares) measurement [*]

[*] See footnote at page 61.

III.3. Measurements in single crystalline sample

III.3.1. Anisothermal test under constant stress

As it could be seen the lack of knowing T_0 didn't allow us to determine the exact value of the elastic terms. Salzbrenner and Cohen [S&c79] has already shown that using a single crystalline sample and gradient heating-cooling the martensitic transformation can be guided such a way when only one interface moves along the sample, so in this case the whole sample turns into the same martensitic variant; so elastic energy doesn't store in the system and one receives a hysteresis curve like in Fig. I.2/b, and T_0 is equal to the arithmetic mean of the temperatures of the two perpendicular branches (M_s=M_f and A_s=A_f).

Performing a similar measurement on a single crystalline CuAlNi alloy we can be able to determine the equilibrium transformation temperature. Nevertheless we used a uniform heating and cooling system instead of a gradient one, but we applied uniaxial stress to promote a certain martensitic variant and so to reach that only one variant can form, which should have been led to a rectangular hysteresis loop (Fig. I.2/b).

III.3.1.1. Samples manufacturing

A single crystalline CuAlNi was ordered and we received a cylindrical sample with 50mm length and 5.2mm diameter, its orientation was $[110]_A$. The sample was cut from this rod using an electro discharge machine and the final dimensions were $0.3725mm^2$ in square cross and 45.7mm in length.

III.3.1.2. Experimental set-up

The experiment was performed in the same device (Fig. III.2) like before but now a computer was used for the data acquisition, and so much more points were measured during a cycle like in case of polycrystalline sample. Furthermore the vacuum was changed to N_2 atmosphere. The heating/cooling rate was approximately $5Kmin^{-1}$. The measurement was started at the highest stress level and then the loading force was decreased cycle by cycle.

III.3.1.3. Hysteresis curves

In the Fig. III.20 one can see that the number of measured points allow us to follow the transformation very accurately. As well as there is no shifting between the branches of the elongation-temperature curve. Nevertheless in the resistance-temperature hysteresis loop one can see an artifact, namely the base lines of the austenite and martensite phases are not coincident for heating and for cooling.

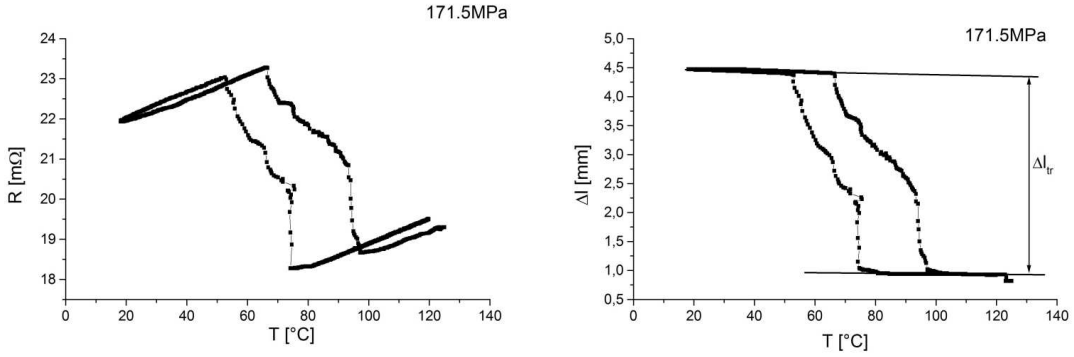

Figure III.20: a) Resistance and b) change of length hysteresis loops at 171.5MPa uniaxial stress (where Δl is the change of length accompanied to the transformation)

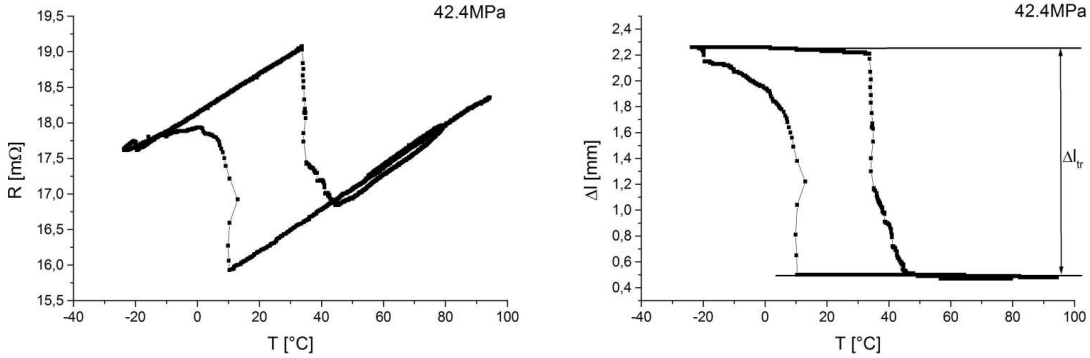

Figure III.21: a) Resistance and b) change of length hysteresis loops at 42.4MPa uniaxial stress (where Δl is the change of length accompanied to the transformation)

Regarding the hysteresis loop measured at the lowest stress level (Fig. III.21) it becomes visible the difference between the high and low stresses. In case of high stress the perpendicular parts can be found at the martensite start and at the austenite finish points, while at low stress levels the vertical parts can be found after the start points of forward and reverse transformation. The explanation of these two different behaviours will be written below.

All measured hysteresis loops can be found in Appendix B.

III.3.2. Evaluation in accordance with B-D model

III.3.2.1. Normalization of hysteresis curves

Like before the measured hysteresis loops had to transform to transformed fraction-temperature plane to perform the evaluation process. The procedure was the same like in case of polycrystalline sample, i.e. firstly the thermal effect was eliminated and then the hysteresis loop was normalized to 1. Although I above mentioned that on the resistance-temperature an artifact could be experienced, after the normalization the two normalized hysteresis showed

very well correspondence (Fig. III.22). So just like before the elongation-temperature curves were taken for the further processes since there is no any unusual effect on them.

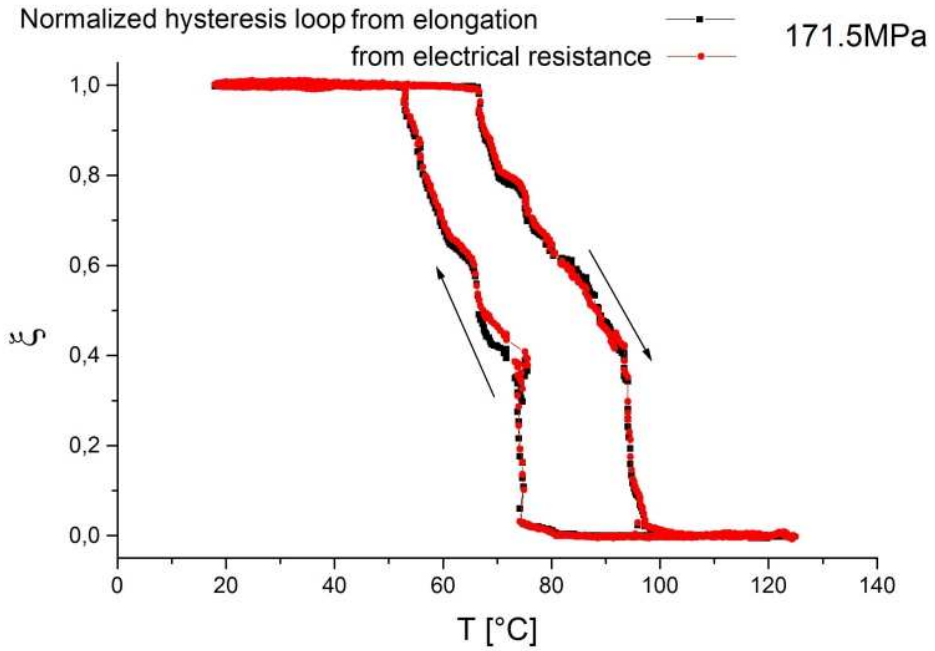

Figure III.22: Correspondence between the normalized hysteresis curves

III.3.2.2. Determination of T_0

III.3.2.2.1. Low and high stress hysteresis loops

The above mentioned difference between the high and low stress curves can be seen on the normalized hysteresis loops (Fig. III.23), namely the forward branches are the same for both stresses: the transformation starts with a perpendicular part and than the branch leans; but the reverse ones are different: the vertical part can be found at the start and at the finish at low and at high stress levels, respectively.

In case of high stress the martensite phase accumulates and grows freely at the beginning of cooling (A→M transition), i.e. there is no any elastic energy storing which is indicated by the perpendicular part as Salzbrenner and Cohen proved [S&C79]; then the product phase cannot grow more freely (in case of multiple nucleus the martensitic plates overlap or the elastic energy cannot run out to the surface and so the system cannot relax), so the elastic energy storing begins and it continuous until the whole sample turns into martensite. During the reverse transformation the releasing of the stored elastic energy helps to accumulate the austenite phase, so first the last martensite plates start to revert, and after the whole elastic energy released the transformation finishes perpendicularly. Practically the high stress hysteresis consists of two parts: the lower part is similar to that described by Salzbrenner and Cohen (see Fig. 1a in Ref. [S&C79]) for a bulk single crystalline specimen with single-interface transformation (thermal gradient heating/cooling), while the upper one resembles to that observed for multiple-interface transformation (uniform heating/cooling)

and it is similar to the hysteresis obtained in polycrystalline sample. Since the rectangular hysteresis indicates that no elastic energy storing or releasing the relation

$$T_0 = \left(M_s + A_f\right)/2 \qquad \text{(III.21)}$$

is a good approximation.

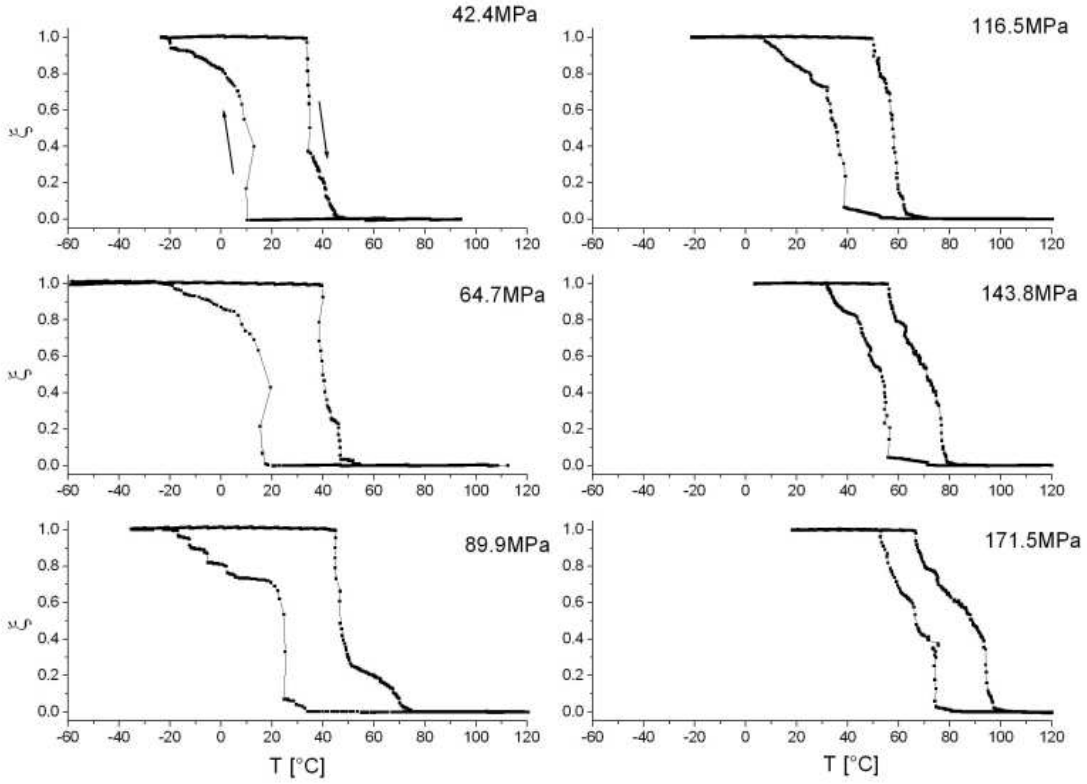

Figure III.23: Normalized hysteresis curves (two cycles were measured at 89.9MPa, both of them can be seen in App. B)

On the other at low stresses the forward transformation takes place the same way, but the reverse transformation starts without any elastic energy releasing; it means the austenite doesn't nuclei where the elastic energy stored, instead the nucleation starts where the first martensite plates appeared during A→M transition. In fact this behaviour can be observed where the chemical energy is much smaller than the other contribution, i.e. the phases start to nuclei in the easy places (e.g. tips, edges), in this case some kind of blocking effect doesn't allow the nucleation of the austenite where the releasing elastic energy would help the transition. So the same part of the specimen begins the forward and the reverse transformation as well as besides the leading force (chemical free energy change) only the dissipative contribution presents and supposing that the derivatives of the dissipative terms are the same in the start points (M_s, A_s) for the equilibrium temperature

$$T_0 = \left(M_s + A_s\right)/2 \qquad \text{(III.22)}$$

is valid.

Between the high and low stress levels there is another distinction which regarding the forming martensite variants, namely there is a limit stress which there is no preferred martensite below, i.e. the martensite accommodate randomly. According to Leclercq and Lexcellent [L&L96] the macroscopic strain of the self accommodated martensite is zero, this demand has to be valid in case of polycrystalline shape memory alloys where the random effect is supported by the randomly oriented austenite grains. However now its value is different from zero (≈4%) (Fig. III.24), so it has to say that in case of single crystal the self-accommodated martensite does its bit from the macroscopic shape change related to the martensitic transformation. Furthermore in Fig. III.24 one can see that the high and low stress curves are distinguished very well and the middle two points seem to be the transition between the two type hysteresis as it can be seen at the normalized hysteresis curves (Fig. III.23); in this region the system was frustrated the self-accommodated and oriented martensite variants compete with each other.

III.3.2.2.2. Accordance with the Clausius-Clapeyron relation

Due to know the equilibrium transformation temperature at each stress levels we can use the Clausius-Clapeyron equation to determine the entropy change between the austenite and martensitic phases since the transformational strain vs. stress function (Fig. III.24) can be determined from the measured hysteresis: $\Delta s_c = -1.169 \times 10^5\ JK^{-1}m^{-3} = -0.843\ Jmol^{-1}$. This value is not equal to the value received for polycrystalline sample but they are in the same order of magnitude; nevertheless the difference is not surprising because the composition of the two samples was different from each other.

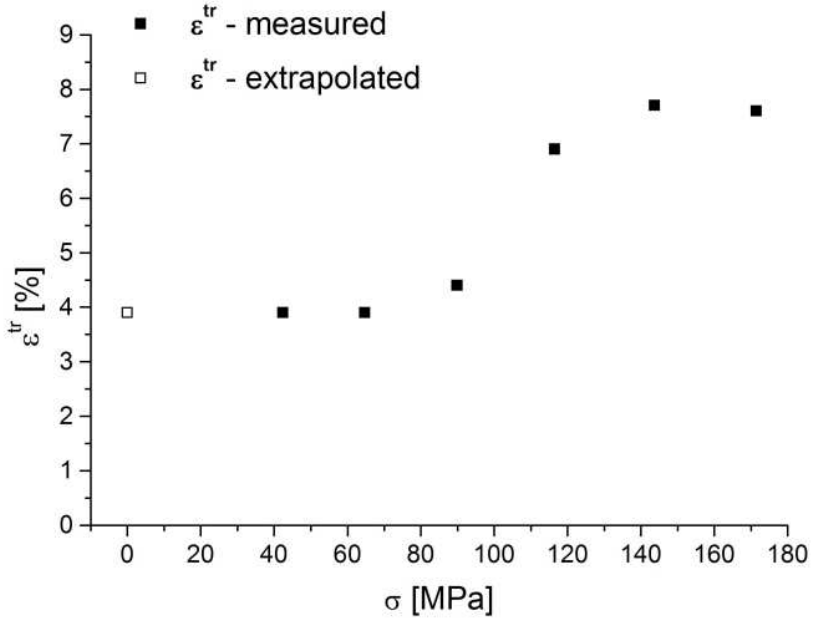

Figure III.24: Transformational strain vs. stress

Now we can calculate the equilibrium transformation temperature (T_0) at all stress levels and even we can determine it in stress free state taking the extrapolated value (open square in Fig. III.24). Taking as a basis the value of T_0 at the highest stress level and using the well

known Clausius-Clapeyron equation one receives a very good accordance between the measured and the calculated values (Fig. III.25).

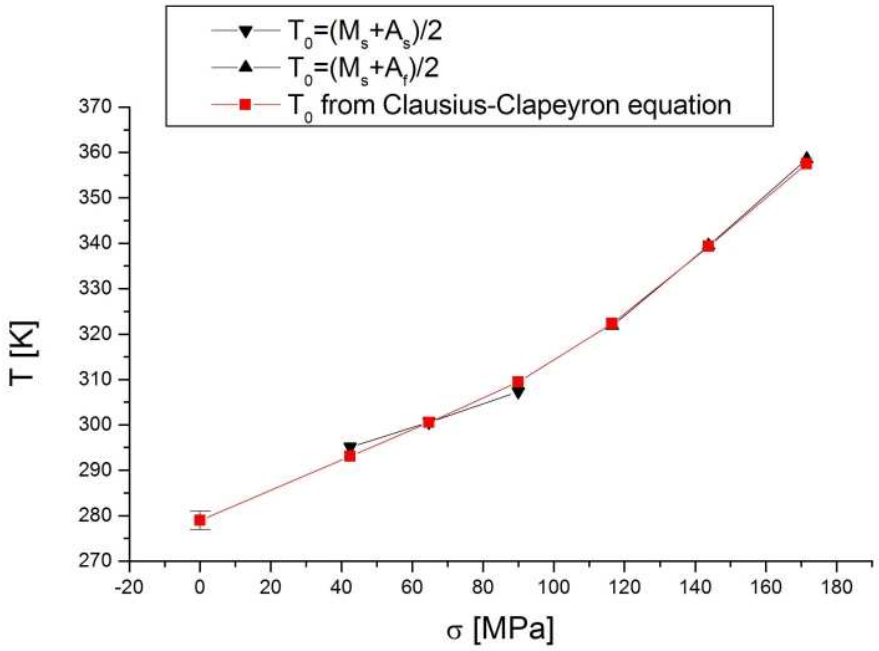

Figure III.25: Measured and calculated equilibrium transformation temperatures

III.3.2.3. Non-chemical energies

Let us perform the same calculation like in case of polycrystalline sample, i.e. from the normalized hysteresis curves the non-chemical energies can be calculated and due to know T_0 even the value of the elastic energy can be given not only its tendency. Nevertheless one has to take into account the differences between the low and high stress hysteresis loops, so these two cases have to be treated separately.

III.3.2.3.1. High stress case

As above firstly the high stress hysteresis curves are evaluated since this case is a little similar to the polycrystalline one, it is so much true that the same simplifier conditions can be used ($d(\xi)=d^{\downarrow}(\xi)=d^{\uparrow}(\xi)$ and $e(\xi)=e^{\downarrow}(\xi)=-e^{\uparrow}(\xi)$).

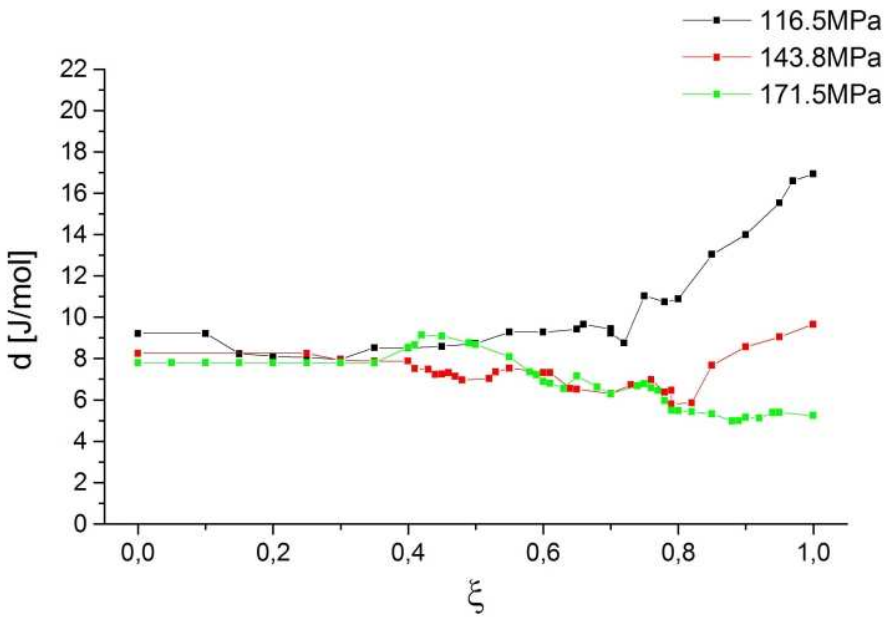

Figure III.26: The martensitic fraction dependence of the derivatives the dissipated energy at three different stress levels

In the Fig. III.26 one can see that the derivatives of the dissipated energy are constant up to ξ=0.7 to a close approximation and then only the 116.5MPa curve start to differ from the constant value significantly which falls into the frustrated region as it was mentioned above. Finally it seems to be a good approximation if one takes the derivatives of the dissipative terms as constant during the martensitic transformation.

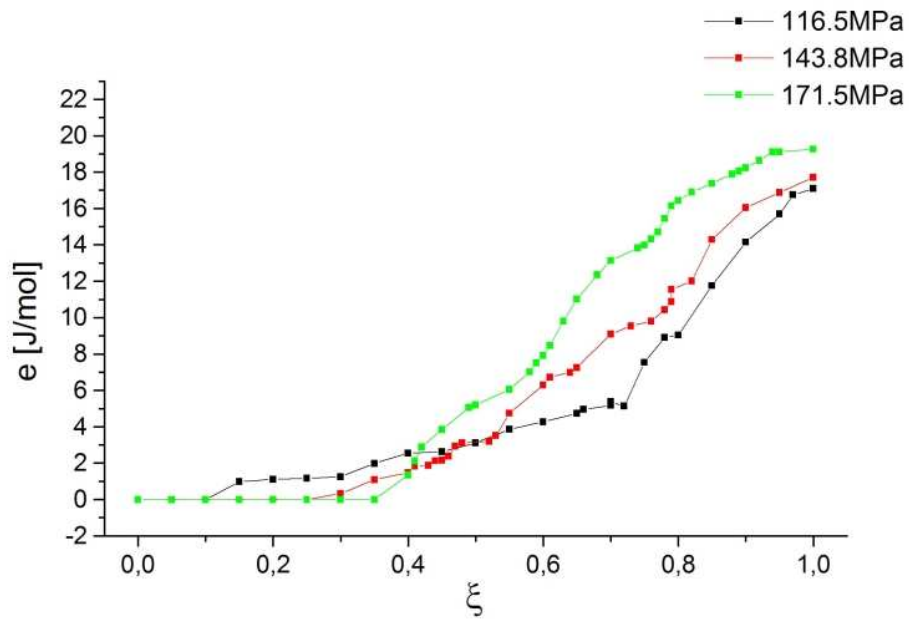

Figure III.27: Derivatives of elastic energy vs. transformed fraction

The derivatives of the elastic contribution (Fig. III.27) show more specified stress dependence. The higher is the applied stress, the bigger is the elastic free region as well as the faster the elastic energy storing and releasing.

III.3.2.3.2. Low stress case

Due to the unusual shape of the low stress hysteresis loops the former simplicity conditions cannot applied, namely they suppose that the hysteresis branches should be approximately parallel to each other which is not true in this case. Instead the branches are investigated separately and a relatively strong condition helps us to perform it. We take the derivative of the dissipative energy as constant and its value is the same for forward and reverse transformation ($d=d^{\downarrow}(\xi)=d^{\uparrow}(\xi)$) – from the polycrystalline measurement and from the result for the high stress case this assumption seems appropriate). This constant can be calculated from the perpendicular parts of the branches. Actually the equality part of this condition was already assumed when the equilibrium transformation temperature was calculated as the arithmetic mean of the martensite start and austenite start temperatures.

Thus $e^{\downarrow}(\xi)$ can be calculated from $(III.6)_1$ (Fig. III.28) and we can see that the elastic energy storing starts at $\xi=0.5$ for all curves, i.e. the half of the sample transforms into martensite freely, then in the case of the two lowest stress $e^{\downarrow}(\xi)$ runs in the same way practically but at 89.9MPa different behaviour is observed which can be explained by that this stress level belongs to the frustrated region (Fig. III.24).

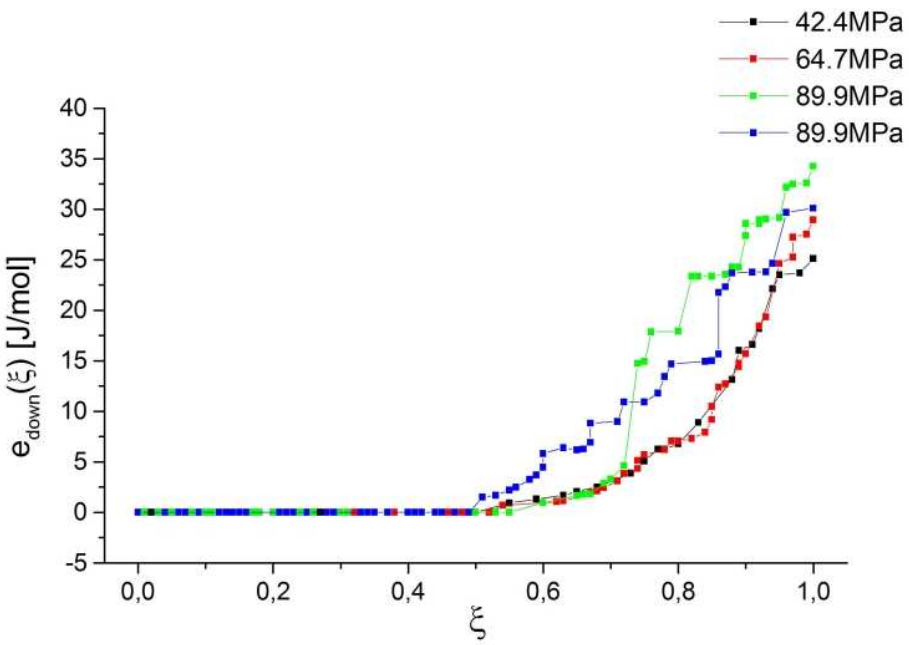

Figure III.28: The derivatives of elastic free energy during forward transformation at low stresses ($e_{down}(\xi)=e^{\downarrow}(\xi)$)

Nevertheless in the case of the reverse branch we have to take into account the above mentioned blocking effect, which is a dissipation-featured term, for this purpose the dissipative can be written as follows for the reverse transformation:

$$d'^{\uparrow}(\xi) = d^{\uparrow}(\xi) + \gamma(\xi) \qquad \text{(III.23)}$$

where $d'^{\uparrow}(\xi)$ means the derivatives of the total dissipated energy, $d^{\uparrow}(\xi)$ is the usual dissipation term which comes mainly from the friction between the habit plane and the lattice defects and $\gamma(\xi)$ represents the blocking effect.

The equation $(III.6)_2$ is modified considering (III.23):

$$T^{\uparrow}(\xi) = T_0 - \frac{d^{\uparrow}(\xi) + \gamma(\xi) + e^{\uparrow}(\xi)}{\Delta s_c} \qquad \text{(III.24)}$$

Regarding this relation both $\gamma(\xi)$ and $e^{\uparrow}(\xi)$ are unknowns. However the elastic contribution can be calculated from $e^{\downarrow}(\xi)$ using a similar assumption like before, whatever the leak of the parallelism of the hysteresis branches denotes that in this condition the transformed fraction will be modified, too. Considering that the forward and reverse transformation start at the same place of the sample we can assume that the whole AM and MA transitions are the mirror images of each other, i.e. for the elastic term

$$e^{\uparrow}(\xi) = -e^{\downarrow}(-\xi) \qquad \text{(III.25)}$$

assumption is acceptable. Thus the derivatives of the blocking effect energy can be calculated from (III.24) (Fig. III.29). A similar case can be observed like by $e^{\downarrow}(\xi)$: between the 42.4MPa and the 64.7MPa curves the correspondence is very good, and the other two ones at 89.9MPa show different tendency.

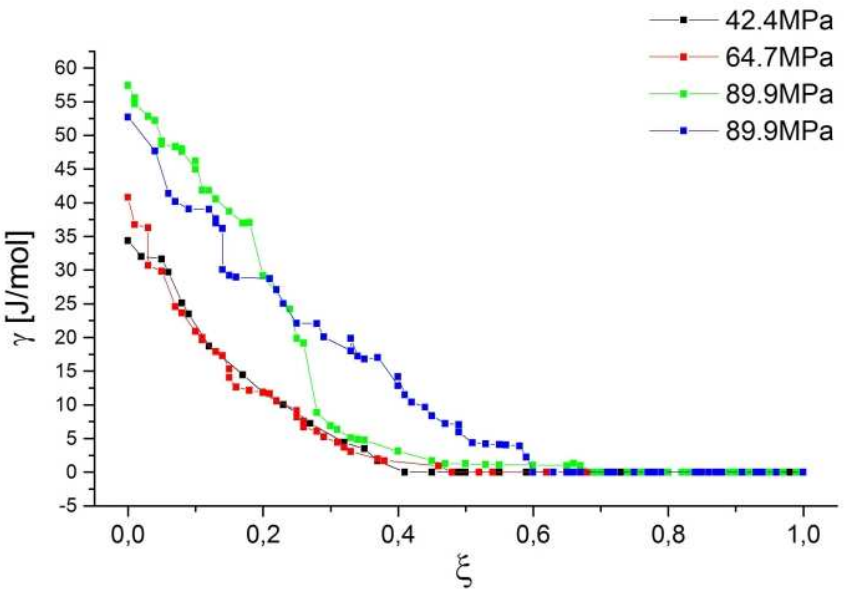

Figure III.29: Calculated γ (related to blocking effect) as a function of ξ

III.3.2.3.3. Stress dependence

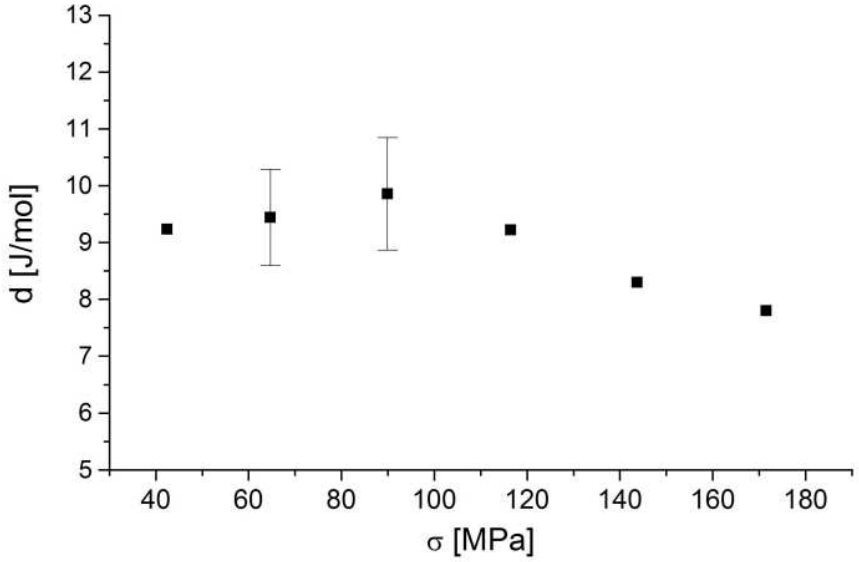

Figure III.30: The constant value of the derivative of the dissipative energy vs. stress

This far the stress dependence appears only in the different shapes of the hysteresis curves. In this section it will be shown how the changing applied stress affects the values of certain quantities and if the different hysteresis loops cause detectable changing.

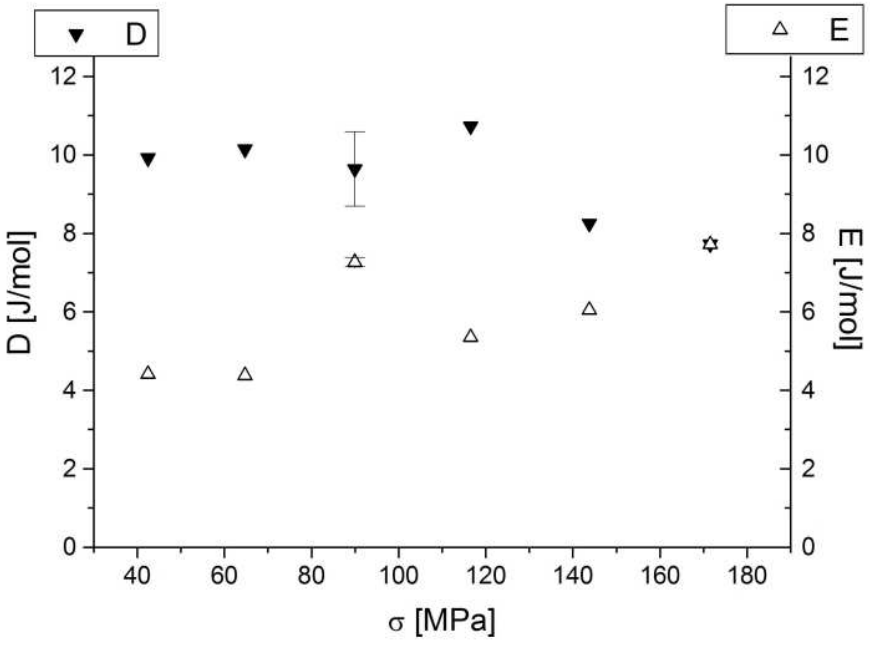

Figure III.31: Stress dependence of the integral quantities

As it was mentioned above it is a good approximation if the derivative of the dissipative energy is considered as a constant during the transformation. From the perpendicular parts the value of this constant can be calculated and in the Fig. 30 one can see these values as a function of applied stress. It shows increasing and decreasing tendencies in the low and the high stress range, respectively.

The full dissipated energy during forward or reverse transformation and the full stored elastic energy in martensitic state can be seen in Fig. III.31 as a function of applied stress. The dissipative energy decreases while the elastic one increases with increasing stress. At 89.9MPa the full stored energy has a jumping point it can come from the above mentioned frustrated state.

Furthermore in Fig. III.32 one can see how the dissipated blocking effect energy (Γ is equal to the integrated of $\gamma(\xi)$ from 0 to 1) changes with the stress. Of course the value of Γ is zero at the highest three stress levels and for the low stresses a constant value can be given except of the 89.9MPa point which is very different from the two others because it belongs to the frustrated region.

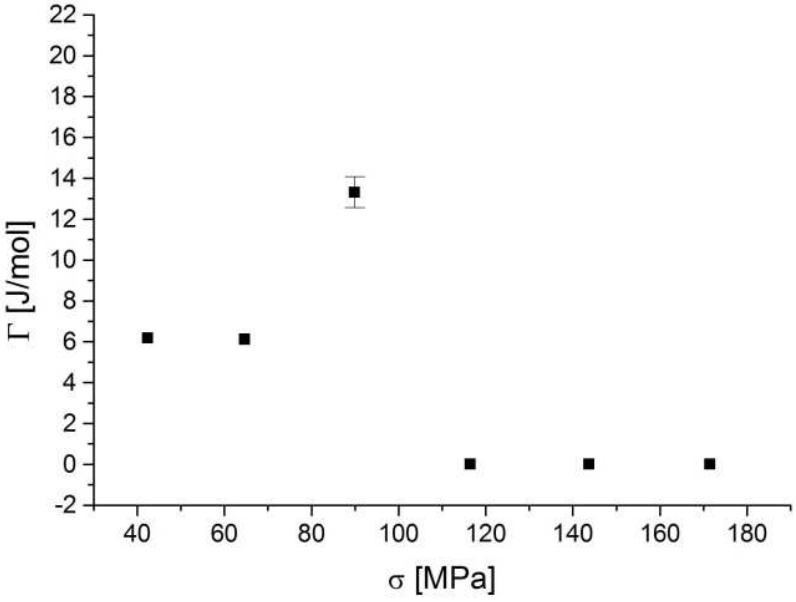

Figure III.32: The dissipated blocking effect energy during the whole reverse transformation

References

[Petal05] Z. Palánki, L. Daróczi and D. L. Beke: *Method for the determination of non-chemical free energy contributions as a function of the transformed fraction at different stress levels in shape memory alloys*, Material Transactions **46/5** (2005) p. 978
[Detal00]L. Daróczi, D.L. Beke, C. Lexcellent and V. Mertinger: *Effect of hydrostatic pressure on the martensitic transformation in CuZnAl(Mn) shape memory alloys*, Scripta materialia **43** (2000) p. 691
[Detal02] L. Daróczi, D.L. Beke, C. Lexcellent, V. Mertinger: *Effect of hydrostatic pressure on the martensitic transformation in near equiatomic Ti–Ni alloys*, Philosophical Magazine B **82/1** (2002) p. 105
[Betal04] D.L. Beke, L. Daróczi, C. Lexcellent, V. Mertinger: *Determination of stress dependence of elastic and dissipative energy terms of martensitic phase transformations in a NiTi shape memory alloy*, Journal de Physique IV France **115** (2004) p. 279
[O&P88] J. Ortín and A. Planes: *Thermodynamic analysis of thermal measurements in thermoelastic martensitic transformation*, Acta Metallurgica **36/8** (1988) p. 1873
[Detal04] L. Daróczi, Z. Palánki, S. Szabó and D. L. Beke: *Stress dependence of non-chemical free energy contributions in Cu-Al-Ni shape memory alloy*, Material Science and Engineering A **378** (2004) p. 274
[Petal89] A. Planes, T. Castán and J. Ortín: *State equation for shape-memory alloys: Application to CuZnAl*, Journal of Applied Physics **66**(6) (1989) p. 2342
[S&C79] R. J. Salzbrenner and M. Cohen: *On the thermodynamics of thermoelastic martensitic transformations*, Acta Metallurgica **27** (1979) p. 739

Chapter IV

Simulation

IV. Simulation

IV.1. Comparison between the models used in Besançon and Debrecen

As it can be seen above the model, which was developed in Debrecen by Beke and Daróczi [Detal00] which was improved by me [Petal05] (from now DE model), is suitable to evaluate the measured hysteresis curves and so determine the non-chemical free energies as well as in case of single crystalline sample the equilibrium transformation temperature. While the R_L model [Retal92], which was improved in Besancon by Lexcellent and Leclercq [L&L96] (from now BE model), is more appropriate to perform simulations on the stress or thermal-induced martensitic transformations. Thus it seems to be a good idea to find out the relations between the two descriptions and so the data evaluated by DE model are used in the calculation of BE one.

IV.1.1. One martensite type

Let us consider firstly the improved DE model. The well known initial point for forward transformation (A→M) is:

$$\frac{\partial\left(\Delta G^{\downarrow}\right)}{\partial z} = \Delta g_c{}^{\downarrow} + e^{\downarrow}(z) + d^{\downarrow}(z) = 0\,. \qquad \text{(IV.1)}$$

The derivative of the free energy change according to the martensitic fraction (z) is zero. Substituting the relation for the chemical energy change (II.4) and using the Clausius-Clapeyron equation (II.9), assuming that the entropy change does not depend on the applied stress, one arrives at:

$$\left(T_0(0) - T\right)\Delta s_c - \sigma\varepsilon^{tr} + d^{\downarrow}(z) + e^{\downarrow}(z) = 0\,, \qquad \text{(IV.2)}$$

A similar relation can be given for the reverse transition (M→A):

$$\left(T - T_0(0)\right)\Delta s_c + \sigma\varepsilon^{tr} + d^{\uparrow}(z) + e^{\uparrow}(z) = 0\,. \qquad \text{(IV.3)}$$

Since currently this model can treat only one type of martensite we should compare it to the R_L model, which consider one martensite, too.

As I above mentioned Raniecki et al [Retal92] started from the Helmholtz free energy of the two-phase system of a unit mass and, neglecting the thermal extension, it can be written as follows :

$$\Phi = u_0{}^1 - Ts_0{}^1 - z\pi_0{}^f(T) + \frac{E}{2\rho}(\varepsilon - z\gamma)^2 + \\ + C_V\left[T - T_0 - T\ln\frac{T}{T_0}\right] + z(1-z)\Phi_{it}\,, \qquad \text{(IV.4)}$$

where u_0^1 and s_0^1 are the internal energy and the entropy of the austenite phase and $\pi_0^f(T)$ is the chemical potential of phase transformation, containing the internal energy and entropy changes of the system due to the evolved martensite phases:

$$\pi_0{}^f(T) = \Delta u^* - T\Delta s^*$$
$$\Delta u^* = u_0{}^1 - u_0{}^2, \qquad \text{(IV.5)}$$
$$\Delta s^* = s_0{}^1 - s_0{}^2$$

It vanishes at the temperature of thermodynamic equilibrium between the austenite and martensite phases:

$$0 = \Delta u^* - T_0(0)\Delta s^* \quad \Rightarrow \quad \pi_0{}^f(T) = (T_0(0) - T)\Delta s^*. \qquad \text{(IV.6)}$$

Let us take the functions (II.51), which describe the transformation-kinetics and are equal to zero for whole cycles, and substitute the expression of π^f (II.42) and replace $\pi_0^f(T)$ by (IV.6):

$$-(T_0(0) - T)\Delta s^* - \frac{\gamma\sigma}{\rho} + (1-2z)\Phi_{it} + k^\alpha(z) = 0 \qquad \text{(IV.7)}$$

where α=1 and 2 means the A→M and M→A transformations, respectively.

Comparing (IV.2) and (IV.3) to (IV.7) we see that the first two terms are the same and somehow the last two ones have to be equal to each other. Nevertheless the relations between the BE and DE models can be given:

$$\Delta s_c = -\rho\Delta s^*; \qquad \gamma = \varepsilon^{tr};$$
$$d^\downarrow(\xi) + e^\downarrow(\xi) = (1-2z)\Phi_{it} + k^1(z) \qquad \text{(IV.8)}$$
$$d^\uparrow(\xi) + e^\uparrow(\xi) = -(1-2z)\Phi_{it} - k^2(z)$$

Let us examine the last two relations: the left sides there are the non-chemical contribution (dissipative and elastic) from DE, while on the right side an interaction component and a function of *z* are present. Using the properties of *k(z)* functions (II.52) one receives the next relations:

$$d^\downarrow(0) + e^\downarrow(0) = \Phi_{it} \qquad d^\downarrow(1) + e^\downarrow(1) = -\Phi_{it} + \infty$$
$$\qquad \text{(IV.9)}$$
$$d^\uparrow(0) + e^\uparrow(0) = \Phi_{it} - \infty \qquad d^\uparrow(1) + e^\uparrow(1) = -\Phi_{it}$$

The interaction component changes its sign at *z=0.5* but such kind of behaviour wasn't supposed and experienced neither for *d(z)* nor for *e(z)* in former experiments. So it can predicated that the *k(z)* function has to eliminate this behaviour somehow.

IV.1.1. Two martensite types

In case of thermally induced martensitic transformation at a constant stress according to BE model two kinds of martensites are distinguished. To achieve the relations as above the DE model has to be improved to take into account the existence of two different martensite types.

Let us suppose that the ratio of the self-accommodated and the stress induced martensite variants is constant during the transformation, so the martensitic fraction can be written as

$$z = z_T + z_\sigma = \eta_T z + \eta_\sigma z\,, \tag{IV.10}$$

where η_T and η_σ denote the thermally and stress induced fraction of the martensite and e.g. $\eta_T=V_{MT}/V_M$, $V_M=V_{MT}+V_{M\sigma}$ and $z=V_M/V$, with $V=V_M+V_A$. Obviously $\eta_T+\eta_\sigma=1$. Since it was assumed that the ratio of the two different martensite variants is constant the possibility of the reorientation process is ruled out.

Indeed, to calculate the derivatives of the elastic and the dissipative contributions related to the different variants, one needs the relation between the $T_T(z_T)$ and $T_\sigma(z_\sigma)$ (inverses of $z_T(T)$ and $z_\sigma(T)$) functions:

$$T(z) = \eta_T T_T(\eta_T z) + \eta_\sigma T_\sigma(\eta_\sigma z)\,. \tag{IV.11}$$

For the elastic and the dissipative terms similar relations can be given:

$$e(z) = \eta_T e_T(\eta_T z) + \eta_\sigma e_\sigma(\eta_\sigma z)\,, \tag{IV.12}$$

$$d(z) = \eta_T d_T(\eta_T z) + \eta_\sigma d_\sigma(\eta_\sigma z)\,. \tag{IV.13}$$

Writing these relations into (IV.2) and (IV.3) regarding the direction of the transformation one receives for A→M

$$\begin{aligned} &(T_0(0) - T_T(\eta_T z))\Delta s_c + d_T{}^{\downarrow}(\eta_T z) + e_T{}^{\downarrow}(\eta_T z) = 0 \\ &(T_0(0) - T_\sigma(\eta_\sigma z))\Delta s_c - \sigma\frac{\varepsilon^{tr}}{\eta_\sigma} + d_\sigma{}^{\downarrow}(\eta_\sigma z) + e_\sigma{}^{\downarrow}(\eta_\sigma z) = 0\,, \end{aligned} \tag{IV.14}$$

and for M→A

$$\begin{aligned} &(T_T(\eta_T z) - T_0(0))\Delta s_c + d_T{}^{\uparrow}(\eta_T z) + e_T{}^{\uparrow}(\eta_T z) = 0 \\ &(T_\sigma(\eta_\sigma z) - T_0(0))\Delta s_c - \sigma\frac{\varepsilon^{tr}}{\eta_\sigma} + d_\sigma{}^{\uparrow}(\eta_\sigma z) + e_\sigma{}^{\uparrow}(\eta_\sigma z) = 0\,, \end{aligned} \tag{IV.15}$$

where

$$\frac{\varepsilon^{tr}}{\eta_\sigma} = \gamma\ \ , \tag{IV.16}$$

i.e. from the $\varepsilon^{tr}(\sigma)$ function and the total pseudoelastic strain (γ) the ratio of the two martensitic variants can be determined.

From the above applied typical assumptions to eliminate the direction dependence ($e^{\downarrow}(\xi)=-e^{\uparrow}(\xi)=e(\xi)\geq 0$ and $d^{\downarrow}(\xi)=d^{\uparrow}(\xi)=d(\xi)\geq 0$) and from (IV.12) and (IV.13) equations similar conditions are received:

$$d_T{}^{\downarrow}(z_T)=d_T{}^{\uparrow}(z_T)=d_T(z_T)\,;\,d_\sigma{}^{\downarrow}(z_\sigma)=d_\sigma{}^{\uparrow}(z_\sigma)=d_\sigma(z_\sigma)$$
$$e_T{}^{\downarrow}(z_T)=-e_T{}^{\uparrow}(z_T)=e_T(z_T)\,;\,e_\sigma{}^{\downarrow}(z_\sigma)=-e_\sigma{}^{\uparrow}(z_\sigma)=e_\sigma(z_\sigma)\,, \qquad \text{(IV.17)}$$

and so from the sums and the differences of the appropriate (IV.14) and (IV.15) equations:

$$d_T(z_T)=-\frac{\Delta s_c}{2}[T_T{}^{\uparrow}(z_T)-T_T{}^{\downarrow}(z_T)]$$
$$e_T(z_T)=-\Delta s_c T_0(0)+\frac{\Delta s_c}{2}[T_T{}^{\uparrow}(z_T)+T_T{}^{\downarrow}(z_T)]\,, \qquad \text{(IV.18)}$$

as well as

$$d_\sigma(z_\sigma)=-\frac{\Delta s_c}{2}[T_\sigma{}^{\uparrow}(z_\sigma)-T_\sigma{}^{\downarrow}(z_\sigma)]$$
$$e_\sigma(z_\sigma)=-\Delta s_c T_0(0)+\sigma\gamma+\frac{\Delta s_c}{2}[T_\sigma{}^{\uparrow}(z_\sigma)+T_\sigma{}^{\downarrow}(z_\sigma)]\,. \qquad \text{(IV.19)}$$

These relations are very similar to the case of one martensite variant. As it can be seen the effect of the constant external stress appears only in the expression of the derivative of the elastic free energy related to the stress induced martensitic variant directly.

As above let us take the Ψ functions (II.72) which are equal to zero for whole external cycles:

$$(T_0(0)-T)\Delta s^*-z_\sigma\Phi_{it}{}^m-(1-2z)\Phi_{it}-k^T{}_\alpha=0 \qquad \text{(IV.20)}$$

$$(T_0(0)-T)\Delta s^*+\frac{\gamma\sigma}{\rho}-z_T\Phi_{it}{}^m-(1-2z)\Phi_{it}-k^\sigma{}_\alpha=0\,, \qquad \text{(IV.21)}$$

where α=f and r means the forward (A→M) and reverse (M→A) transformations, respectively.

Finally, comparing (IV.14), (IV.15) to the previous equations similar relations are received like in case of one martensite variant:

$$\begin{cases} d_T^{\downarrow}(z_T) + e_T^{\downarrow}(z_T) = z_\sigma \Phi_{it}^{\,m} + (1-2z)\Phi_{it} + k^T{}_f \\ d_\sigma^{\downarrow}(z_\sigma) + e_\sigma^{\downarrow}(z_\sigma) = z_T \Phi_{it}^{\,m} + (1-2z)\Phi_{it} + k^\sigma{}_f \\ d_T^{\uparrow}(z_T) + e_T^{\uparrow}(z_T) = -z_\sigma \Phi_{it}^{\,m} - (1-2z)\Phi_{it} - k^T{}_r \\ d_\sigma^{\uparrow}(z_\sigma) + e_\sigma^{\uparrow}(z_\sigma) = -z_T \Phi_{it}^{\,m} - (1-2z)\Phi_{it} - k^\sigma{}_r \end{cases} \qquad \text{(IV.22)}$$

and $\Delta s_c = -\rho \Delta s^*$ is still true.

One can find the same problem like before, i.e. the interaction component changes its sign and the *k* functions have to eliminate this behaviour here, too.

IV.2. Simulation on polycrystalline CuAlNi

Using the measured data on the polycrystalline CuAlNi the *k* functions can be determined after (IV.22) relations and then the correspondence between the measured and the calculated curves can be investigated. Nevertheless, for the sake of simplicity let us neglect the interaction between the martensitic variants ($\Phi_{it}^{\,m}=0$) and the *k* functions depend only on the martensitic fractions explicitly.

IV.2.1. Parameter determination

IV.2.1.1. Thermodynamic constants

Firstly the thermodynamic parameters (Δu^*, Δs^*, $\bar{u}_0$, $\bar{s}_0$) have to be determined from the martensite and austenite start temperatures since at these points the thermodynamic forces are equal to zero:

$$\pi^f(\sigma, M_s{}^\sigma, z=0) = \frac{\gamma\sigma}{\rho} + (\Delta u^* - \bar{u}_0) - M_s{}^\sigma(\Delta s^* - \bar{s}_0) = 0 \qquad \text{(IV.23)}$$

$$\pi^f(\sigma, A_s{}^\sigma, z=1) = \frac{\gamma\sigma}{\rho} + (\Delta u^* + \bar{u}_0) - A_s{}^\sigma(\Delta s^* + \bar{s}_0) = 0\,, \qquad \text{(IV.24)}$$

where ρ (mass density) can be measured and the value of γ is taken from Sittner and Novák [S&N00]. Table IV.1 contains these and the calculated quantities.

γ [%]	ρ [kg/m^3]	Δu^* [J/m^3]	Δs^* [J/Km^3]	$\bar{u}_0$ [J/m^3]	$\bar{s}_0$ [J/Km^3]
6.64	7168	$1.538*10^8$	$4.128*10^5$	$4.419*10^7$	$1.134*10^5$

Table IV.1: Mechanical and thermodynamic parameters

It is worth noting that the values of the entropic change between the two phases calculated form the transformation temperatures (Δs^*) is almost four times bigger than one calculated from the DSC measurement (Δs_c). Probably the difference comes from the fact that

the determination of the transformation temperatures is not so simple and probably the interaction between the martensite variants cannot be neglected.

IV.2.1.2. Kinetic coefficients

To calculate the *k* functions one has to separate the hysteresis curve according to the two different martensite variants. Supposing that the specific resistance of the two martensite types are the same normalizing the resistance-temperature curve the *z(T)* function can be received. As well as the elongation hysteresis curve provides the $z_\sigma(T)$ since the thermally induced martensitic variant does not cause macroscopic shape change and the maximum value of z_σ at a constant stress can be given as $\varepsilon^{tr}(\sigma)/\gamma$. Of course, $z_T(T)$ is equal to their difference. Finally, from their inverses the separated elastic and dissipative terms can be determined according to (IV.18) and (IV.19). To have an exact value of the elastic contribution the $T_0(0)$ has to be known, here it was taken as the ratio of Δu^* and Δs^* according to (IV.6): $T_0(0)$=372.58K; although this value is lower than the lower limit from the previous chapter, the different specific entropy change during the two evaluation processes can cause this discrepancy since it appears in the relation to calculate $T_0(0)$.

As it was mentioned above the *k* functions depend only on the martensitic fractions – the dependence was taken from the one martensite variant case; similar form like (II.53) to fulfil the condition (II.52), i.e. at the beginning of forward transformation the k_f functions have to be equal to zero and at the end they go to infinite as well as for reverse transition the k_r ones are zero at the beginning, too, and they converge to the negative infinite – nevertheless the sign change of the interaction term has to be eliminate, too. So let us take the next formula:

$$
\begin{aligned}
k^T{}_f &= 2\frac{z_T}{\eta_T}\Phi_{it} + a_f{}^T \ln\left(1-\frac{z_T}{\eta_T}\right) = 2\frac{z_T}{\eta_T}\Phi_{it} + f_T(z_T) \\
k^\sigma{}_f &= 2\frac{z_\sigma}{\eta_\sigma}\Phi_{it} + a_f{}^\sigma \ln\left(1-\frac{z_\sigma}{\eta_\sigma}\right) = 2\frac{z_\sigma}{\eta_\sigma}\Phi_{it} + f_\sigma(z_\sigma) \\
k^T{}_r &= 2\left(\frac{z_T}{\eta_T}-1\right)\Phi_{it} + a_r{}^T \ln\frac{z_T}{\eta_T} = 2\left(\frac{z_T}{\eta_T}-1\right)\Phi_{it} + r_T(z_T) \\
k^\sigma{}_r &= 2\left(\frac{z_\sigma}{\eta_\sigma}-1\right)\Phi_{it} + a_r{}^\sigma \ln\frac{z_\sigma}{\eta_\sigma} + b_r{}^\sigma = 2\left(\frac{z_\sigma}{\eta_\sigma}-1\right)\Phi_{it} + r_\sigma(z_\sigma)\,.
\end{aligned}
\qquad \text{(IV.25)}
$$

In Figs. IV.1 and IV.2 one can see how the *f* and *r* functions fit to the curves calculated from the measured data at two different stress levels.

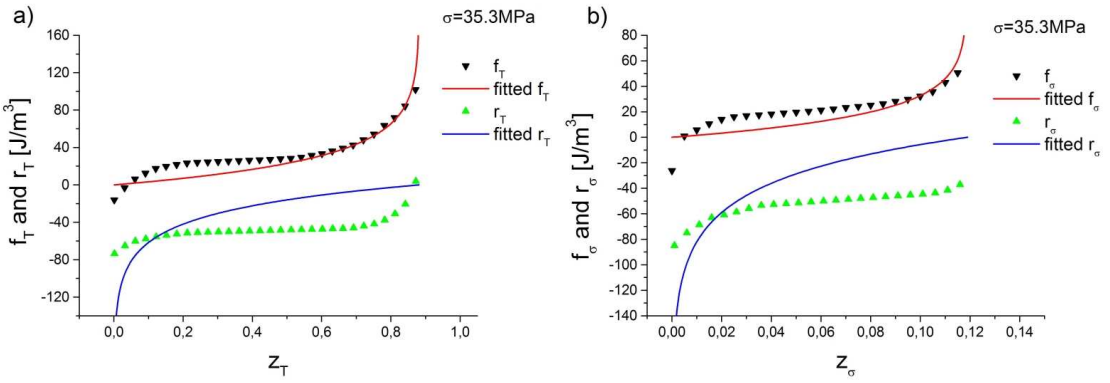

Figure IV.1: The f and r curves and the fitting functions at 35.3MPa

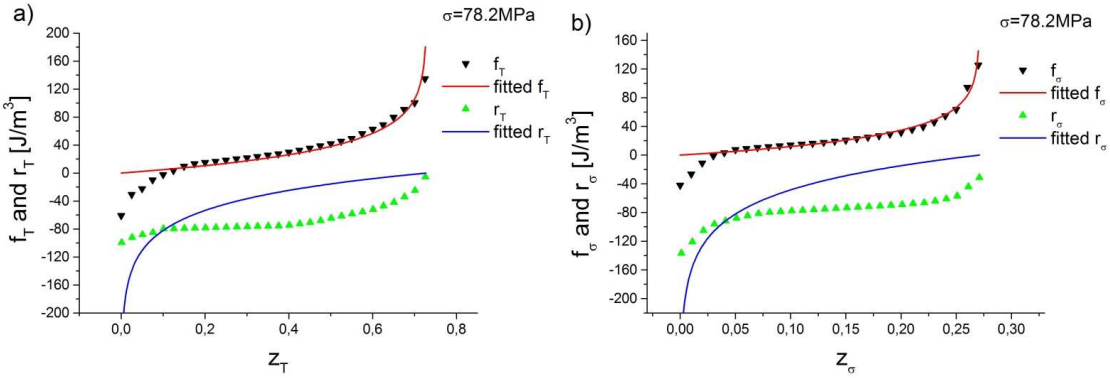

Figure IV.2: The f and r curves and the fitting functions at 78.2MPa

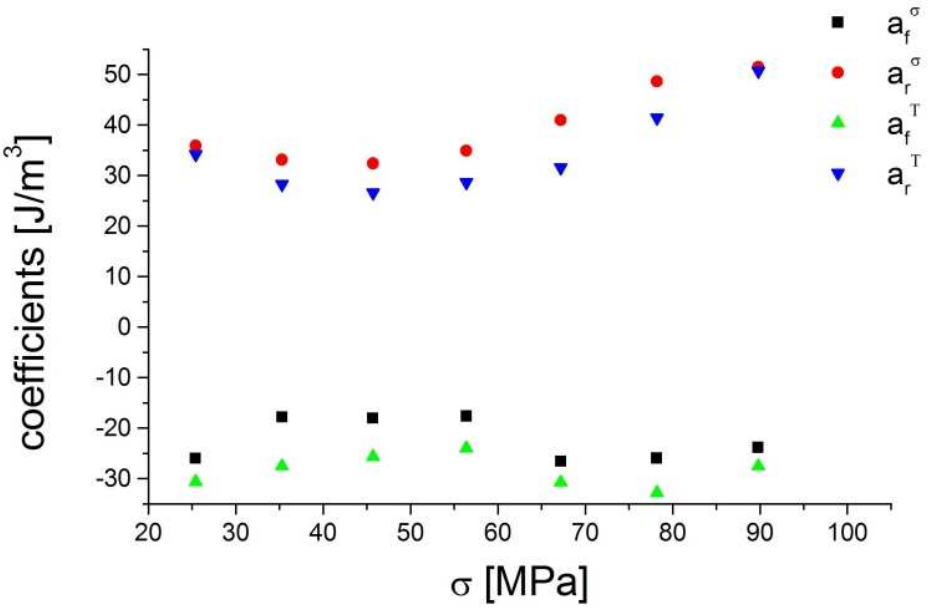

Figure IV.3: Determined coefficients for forward and reverse transitions

As it can be seen the fitting for the forward branches are very good but in the reverse case it is obvious that the formula does not describe well the evolution of the martensitic transformation.

It is worth mentioning that the above *k* formulae are very similar to (II.73-76) except for the temperature dependence. Nevertheless the BE model didn't take the stress dependence of the coefficients into account, but according to the Fig. IV.3 it is not negligible. The forward coefficients do not confirm it since they are almost constant, but the reverse ones slightly increase with the stress.

IV.2.2. Correspondence between the measured and the calculated curves

Finally all the thermodynamic constants and the kinetic coefficients are available to perform the simulation of the hysteresis loops and compare them to measured ones. Figs IV.4 and 5 show the measured and the simulated evolution of the two martensite type in case of two different stress levels. Furthermore in Figs. IV.6 and 7 the comparison of the measured and calculated hysteresis can be seen. (All of these curves can be found in the Appendix C.)

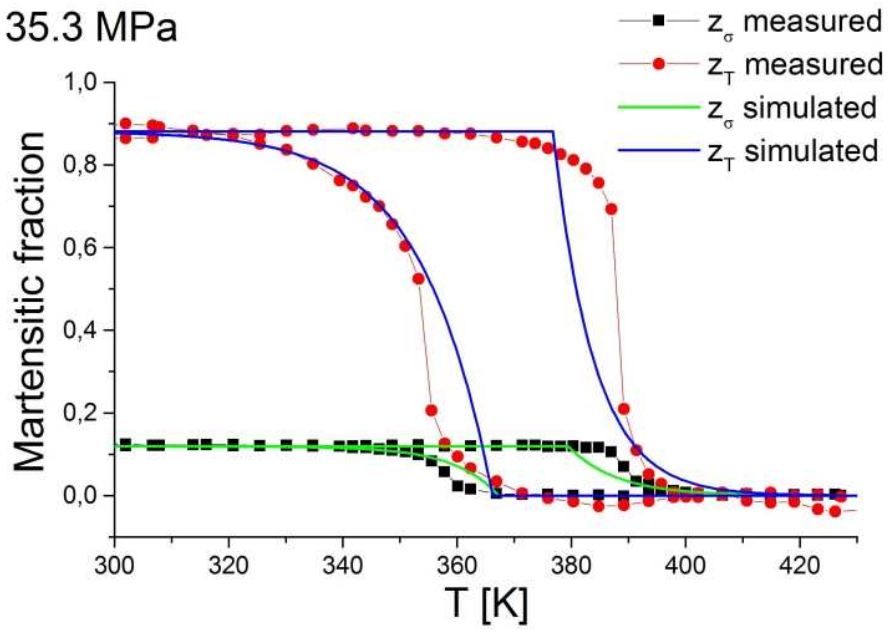

Figure IV.4: Measurement and simulation of the evolution of stress and thermal induced martensite variants at 35.3 MPa

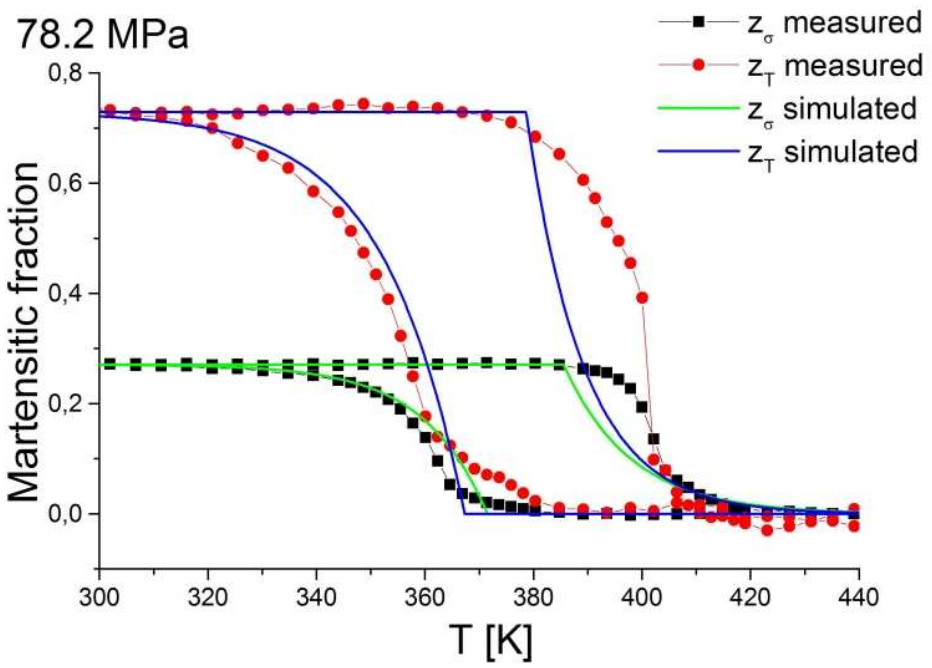

Figure IV.5: Measurement and simulation of the evolution of stress and thermal induced martensite variants at 78.2 MPa

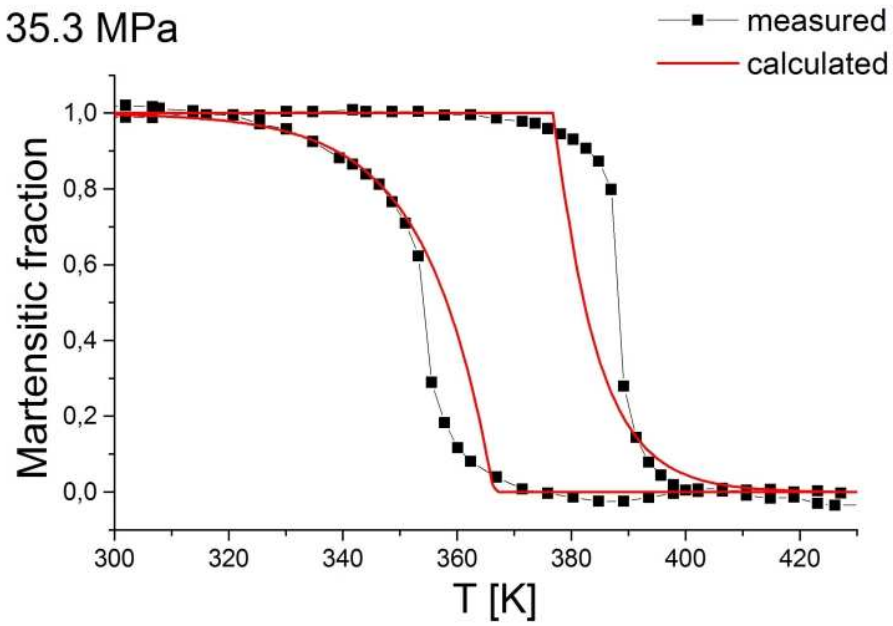

Figure IV.6: Measured and calculated anisothermal hysteresis loops at 35.3MPa

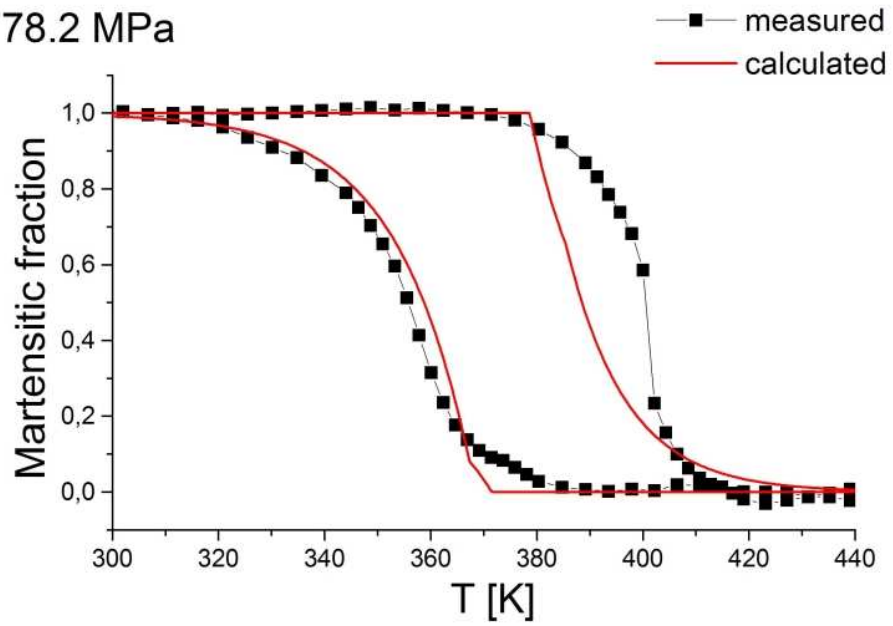

Figure IV.7: Measured and calculated anisothermal hysteresis loops at 78.2MPa

As it was expected from the fitting of the *f* and *r* functions the calculated forward branches show quite good agreements with the measured one especially at high stress; on the contrary for the reverse branches the calculations do not follow the measurements. Nevertheless the start temperatures for both the forward and the reverse transformations were very well reproduced by the calculations.

IV.2.3. Further steps

IV.2.3.1. The case of single crystalline CuAlNi

Elie Gibeau has made calculation on the single crystalline CuAlNi using the BE model. In Figs. IV.8 and 9 the comparison can be seen between the calculation and the measurement. In the low stress case (Fig. IV.8) the agreement is quite good, but at high stress (Fig. IV.4) even the calculated and measured start temperatures are very different to each other. These two cases can not be treated in the same way as it was discussed in the Chapter III.

In fact, the transformation in this single crystalline sample includes jumping steps indicated by perpendicular parts on the measured hysteresis in both directions, i.e. big amount of martensite or austenite phase turns into the other one completely freely without any influence on the elastic field. This behaviour query, if it is well-founded, to use continuous function to describe the transformation kinetics, maybe some kind of probability function should be used.

Furthermore it is worth to consider the possibility that in case of thermal induced martensite type has a not-zero extension, it means only MT martensite can cause macroscopic length change. In this way a new approach can be given: there is a limit stress, below and above which only thermal and stress induced martensite can form during anisothermal test, respectively. So the low and high stress cases can be separated. Nevertheless, this assumption needs further experiments.

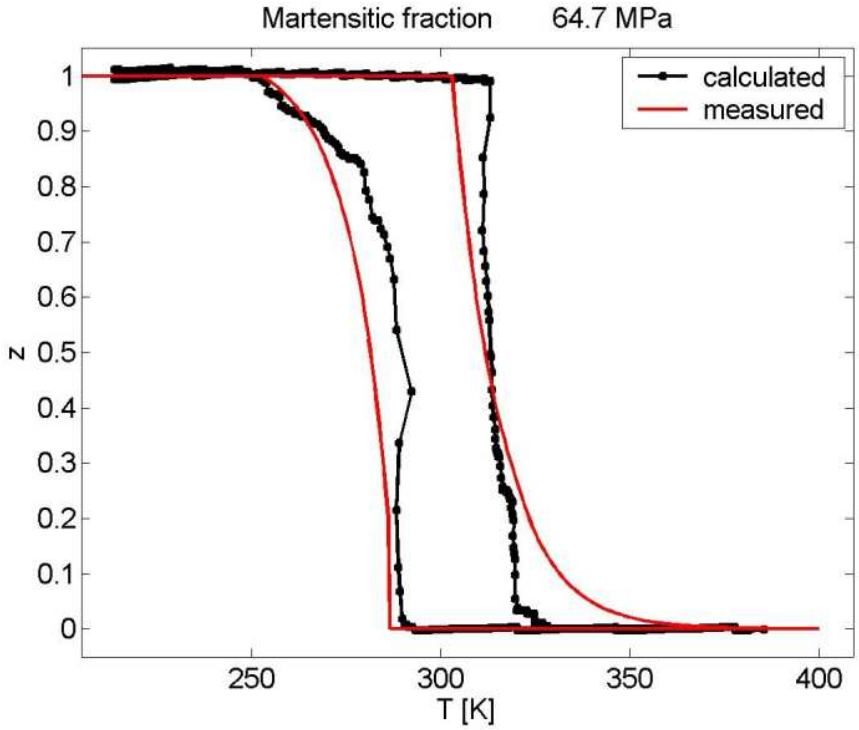

Figure IV.8: Measured and calculated hysteresis curves on single crystalline CuAlNi at 64.7MPa

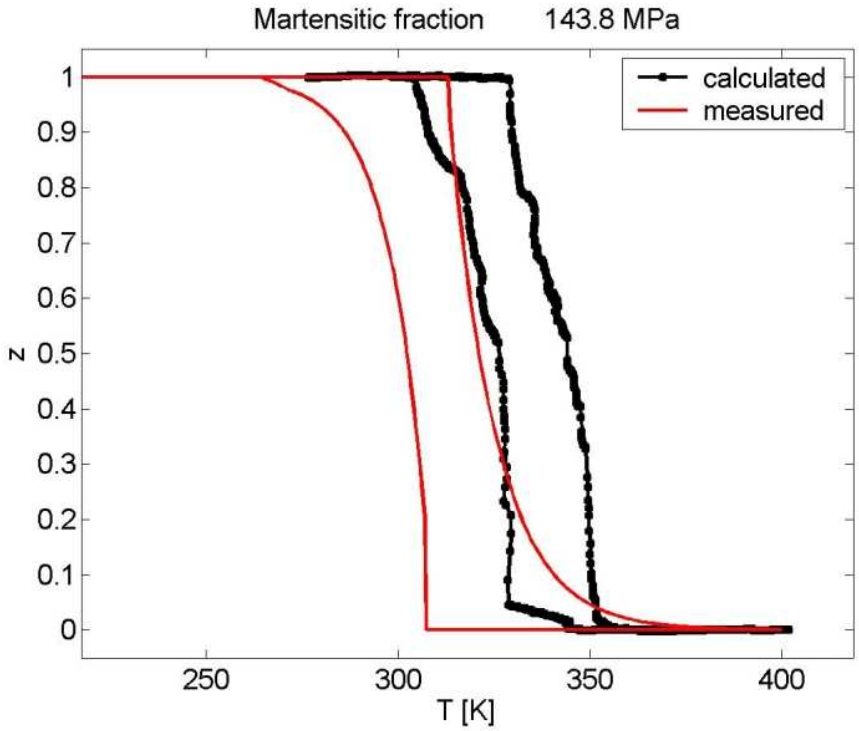

Figure IV.9: Measured and calculated hysteresis curves on single crystalline CuAlNi at 143.8MPa

IV.2.3.2. More reliable simulations

Besides the further test on single crystal it would be worth to measure the anisothermal hysteresis curves with better resolution and to determine the extension related to the martensitic transformation from measured stress-strain curve. In this case all the *k* functions can be calculated and the possibility would be opened to fit them in the whole interval for example with an $ln(p-x)+ln(x)$ function, since both the *f* and *r* functions tend to $-\infty$ and to ∞ at x=0 and at x=p, respectively, as it was written in Ref. [Petal89].

References

[Detal00] L. Daróczi, D.L. Beke, C. Lexcellent and V. Mertinger: *Effect of hydrostatic pressure on the martensitic transformation in CuZnAl(Mn) shape memory alloys*, Scripta materialia **43** (2000) p. 691

[Petal05] Z. Palánki, L. Daróczi and D. L. Beke: *Method for determination of non-chemical free energy contributions as a function of the transformed fraction at different stress levels in shape memory alloys*, Materials Transactions **46**/5 (2005) p. 978

[Retal92] B. Raniecki, C. Lexcellent and K. Tanaka: *Thermodynamics models of pseudoelastic behaviour of shape memory alloys Archives of Mechanics*, **44/3** (1992) p. 261

[L&L96] S. Leclercq and C. Lexcellent: *A general macroscopic description of the thermo-mechanical behavior of shape memory alloys*, Journal of the Mechanics and Physics of Solids **44/6** (1996) p. 953

[S&N00] Petr Sittner and Vacláv Novák: *Anisotropy of martensitic transformations inmodeling of shape memory alloy polycrystals*, International Journal of Plasticity **16** (2000) p. 1243

[Petal89] Antoni Planes, Teresa Castán, Jordi Ortín and Luc Delaey: *State equation for shape-memory alloys: Application to Cu-Zn-AL*, Journal of Applied Physics **66**/6 (1989) p. 2342

Conclusion

Conclusion

1. From measurements of elongation-temperature and resistance-temperature hysteresis curves on Cu–24.0at% Al–2.2at% Ni–0.5at% B polycrystalline shape memory alloy I determined the stress dependence of the derivatives of the elastic and the dissipative energy contributions, according to the transformed fraction, on the austenitic and martensitic side (i.e. in the points of transformation temperatures: M_s, M_f A_s and A_f, where e.g. M_s and M_f are the temperatures related to the appearing of the martensitic and the disappearing of the austenitic phases, respectively). The values of the dissipative terms at the beginning and the end of the martensitic transformation increase with increasing stress. Since the equilibrium temperature, T_0, was not known I could give only the tendency of the elastic energy contribution: in both phases they do not change significantly with the uniaxial stress. Furthermore the derivatives of both the dissipative and the elastic contributions are higher in the martensitic side than in the austenitic one.
2. I extended the evaluation method used in [1] in such a way that it gives the derivatives of the non-chemical free energy contributions not only at the start and the end of the transformations but during the transition (i.e. they can be given as the function of the transformed fraction), too. We showed that these values can be calculated after normalizing of the measured hysteresis loops. Furthermore, I demonstrated that the integral quantities measured in DSC and integrals of the differential ones, received from the measured hysteresis curves, agreed very well, i.e. the analysis is self-consistent. I determined the transformed fraction dependence of the full dissipated energy and the full stored and released elastic energy (calculated as the integral of the appropriate differential quantities) [2, 3].
3. Determination of the equilibrium transformation temperature in single crystalline sample
   a) The analysis mentioned in paragraphs 1. and 2. was extended for single crystalline samples. It was shown that the equilibrium transformation temperature, T_0, can also be determined form such experiments [3]. From the detailed analysis of the data measured we illustrated that it is possible to measure hysteresis loops with vertical parts (perpendicular to the temperature axis) even if we use usual uniform heating-cooling and not a gradient one. As a function of loading we got two different types of hysteresis curves, from which T_0 could be determined by two different ways [4, 5].
   b) Since the elongation-temperature hysteresis was also measured, it allowed calculating the equilibrium transition temperature using the Clausius-Clapeyron equation, too, and they showed really good correspondence with data calculated as described in a). [4, 5]
4. Using the input parameters obtained from the experimental curves on the basis of the extended Debrecen-model (inclusion of two different types of martensitic phases [6]) calculations have been carried out for the hysteretic loops from the Besançon model. In accordance with the experimental data I also assumed that the kinetic parameters in the Besançon-model are not constant but depend on the stress (pressure) as well. The calculated hysteretic curves were compared to the experimental ones and a good agreement was obtained.

Conclusion

1. Des courbes d'hystérésis «élongation-température» et «résistance électrique-température» sur des alliages à mémoire de forme Cu 24.0at%Al 2.2at%Ni 0.5at%B ont été réalisées. Pendant des essais de traction, la dépendance des dérivées des termes d'énergies élastique et dissipative à la fraction de martensite a été quantifiée (i.e. aux températures de transformation: M_s, M_f A_s et A_f). Les valeurs des termes dissipatifs en début et en fin de transformation martensitique augmentent avec la contrainte de traction appliquée. Comme la température d'équilibre T_0, n'est pas connue, j'ai pu seulement suivre l'évolution des termes d'énergie élastique: dans tous les deux phases ils ne changent pas considérablement avec la contrainte uniaxiale. De plus, les dérivées des termes de l'énergie élastique et dissipative sont plus élevées dans la phase martensitique que dans la phase austénitique.
2. La méthode d'évaluation utilisée dans [1] a été étendue, ce qui donne maintenant les valeurs des dérivées des termes d'énergie libre non-chimiques, non seulement, au début et à la fin de transformation martensitique, mais aussi pendant la transition (i.e. elles peuvent être exprimées comme des fonctions de la fraction de martensite). Nous avons montré que ces valeurs pouvaient être calculées grâce à la normalisation des boucles hystérétiques mesurées. De plus, j'ai aussi montré que les quantités intégrales mesurées par DSC et les intégrales extraites des courbes hystérétiques mesurées, sont en bon accord, c'est-à-dire que l'analyse est "auto-cohérente". La dépendance de l'énergie dissipée totale et de l'énergie accumulée ou libérée totale à la fraction de martensite a été déterminée [2, 3].
3. Détermination de la température d'équilibre de la transformation de phase dans les échantillons monocristallins
   a) L'analyse mentionnée dans les 1er et 2ème paragraphes a été étendue aux échantillons monocristallins. Nous avons montré que la température d'équilibre, T_0, peut être déterminée [3]. De l'analyse détaillée des résultats, nous en avons déduit qu'il est possible de mesurer des boucles hystérétiques même avec des parties verticales (perpendiculaire à l'axe de température), même si nous utilisons un système de chauffage-réfrigération uniforme et non avec gradient. Nous avons obtenu deux différents types de courbes hystérétiques fonction du niveau de contrainte appliquée, ainsi T_0 a pu être déterminée par deux façons différentes [4, 5].
   b) Comme la courbe d'hystérésis «élongation-température» a été obtenue expérimentalement, on a pu calculer la température d'équilibre en utilisant l'équation de Clausius-Clapeyron, et il y a un très bon accord avec les valeurs calculées dans a) [4, 5].
4. En utilisant les paramètres déduits des courbes expérimentales sur la base du modèle de Debrecen étendu (deux types de martensites [6]), des calculs avec le modèle de Besançon ont été effectués pour ces courbes hystérétiques. En accord avec les données expérimentales, j'ai présumé que les paramètres cinétiques dans le modèle de Besançon ne sont pas constants mais dépendent de la valeur de la contrainte de traction (compression) appliquée. Les courbes hystérétiques calculées ont été comparées avec celles obtenues expérimentalement et une bonne correspondance a été obtenue.

Befejezés

1. A megnyúlás-hőmérséklet és ellenállás-hőmérséklet hiszterézis görbék méréséből Cu–24.0at% Al–2.2at% Ni–0.5at%B polikristályos alakmemória ötvözetben meghatároztam a rugalmas és disszipatív energiajárulékok átalakult anyaghányad szerinti deriváltjainak feszültség-függését a martenzit és ausztenit oldalon (azaz az M_s, M_f A_s és A_f pontokban, ahol például M_s és M_f martenzit fázis megjelenéséhez illetve eltűnéséhez tartozó hőmérsékleteket jelölik). A disszipatív tagok a martenzites átalakulás kezdetén és végén növekvő feszültség hatására növekednek. A rugalmas energiajárulékonak azonban az egyensúlyi átalakulási hőmérséklet, T_0, ismeretének hiányában csak a menetét tudtam megadni: egyik fázsiban sem változik jelentősen az egytengelyű feszültség hatására. Továbbá mind a disszipativ mind a rugalmas járulékok deriváltjaira az érvényes, hogy a martenzit oldali értékek mindig nagyobbak az ausztenit oldaliaknál. [1,3]
2. Az [1]-ben használt kiértékelési eljárást kibővítettem olyan módon, hogy az ne csak a martenzites átalakulás kezdetén és végén, hanem közben is megadja a rugalmas és disszipatív járulékok átalakult anyaghányad szerinti deriváltjait. Megmutattuk, hogy ezek az értékek a mért hiszterézisgörbék normálása után kiszámolhatók. Továbbá bebizonyítottam, hogy a DSC-ben mért integrális mennyiségek és a hiszterézis hurkokból számolható differenciális mennyiségek jól egyeznek. Meghatároztam a folyamat során disszipálódott, valamint a tárolt és felszabadult rugalmas energiák (mint a differenciális mennyiségek integráltjai) átalakult anyaghányad szerinti függését. [2, 3]
3. Az egyensúlyi átalakulási hőmérséklet meghatározása egykristályos mintákban
   a) Az 1. és 2. pontban említett analízist kiterjesztettük egykristály alakmemória ötvözetre. Megmutattuk, hogy az egyensúlyi átalakulási hőmérsékletet, T_0, is meghatározható ilyen mérésekből [3]. A mérések részletes kiértékelésekor azt kaptuk, hogy szokásos, nem hőmérséklet-gradienst alkalmazó, hűtést/fűtést használva is lehet olyan hiszterézis görbéket mérni, melyeken függőleges szakaszok találhatók. A terhelés függvényében két különböző típusú hiszterézis alakot kaptunk, amelyekből a T_0 kiszámítására más-más módon nyílt lehetőség. [4, 5]
   b) Mivel a megnyúlás-feszültség függvényt is mértem, lehetőség nyílt az átalakulási egyensúlyi hőmérsékleteket a Clausius-Clapeyron egyenletből is kiszámítani, amelyek nagyon jó egyezést mutattak az a) pontban említettekkel. [4, 5]
4. Felhasználva a továbbfejlesztett debreceni modell alapján (kétféle martenzit variáns figyelembe vétele [6]) a kísérleti görbékből kapott bemenő paramétereket számolásokat végeztem a hiszterézis hurokokra a besançoni modell alapján. A mérési adatokból adódóan azt is feltételeztem, hogy a besançoni modellben szereplő kinetikus paraméterek nem konstansok, hanem a feszültség (nyomástól) is függenek. A számított hiszterézis görbéket összevetettem a mért adatokkal, és jó egyezést kaptam.

List of articles:

[1] L. Daróczi, **Z. Palánki**, S. Szabó, D.L. Beke: *Stress dependence of non chemical free energy contributions in Cu-Al-Ni shape memory alloy,* Material Science and Engineering A **378** (2004) pp. 274-277
[2] **Z. Palánki**, L. Daróczi and D.L. Beke: *Method for determination of non-chemical free energy contributions as a function of the transformed fraction at different stress levels in shape memory alloys*, Materials Transactions **46** No.5 (2005) pp.978-982
[3] L. Daróczi, **Z. Palánki** and D.L. Beke: *Determination of the non-chemical free energy terms in martensitic transformations*, Materials Science and Engineering A, **438-440** (2006) pp. 80-84
[4] **Z. Palánki**, L. Daróczi, C. Lexcellent and D.L. Beke: *Determination of the equilibrium transformation temperature (T_0) and analysis of the non-chemical energy terms in CuAlNi single crystalline shape memory alloy*, Acta Materialia **55** (2007) pp. 1823-1830
[5] **Z. Palánki**, L. Daróczi, C. Lexcellent and D.L. Beke: *Determination of the non-chemical energy terms and the equilibrium transformation temperature (T_0) in CuAlNi poly- and single crystalline alloys*, Materials Science and Engineering A, **481-482** (C1-2) (2008) 509-512
[6] D.L.Beke, L. Daróczi, **Z. Palánki** and C. Lexcellent: *On relations between the transformation temperatures, stresses, pressures and magnetic fields in shape memory alloys*, Proceedings of ASM International Conference „Shape memory and superelastic technolgies" held in Tsukuba, Japan, Dec. 3-5 (2007)

Appendices

Appendix A

Measured hysteresis curves on CuAlNi polycristalline sample.

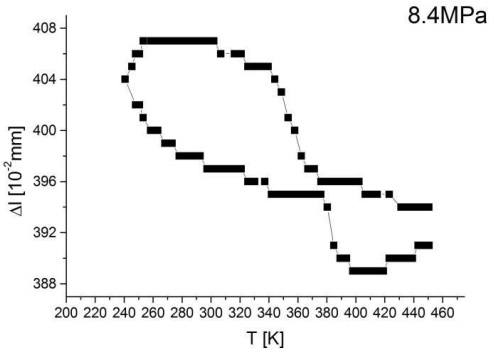

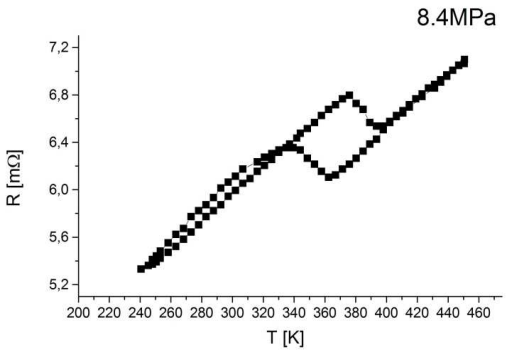

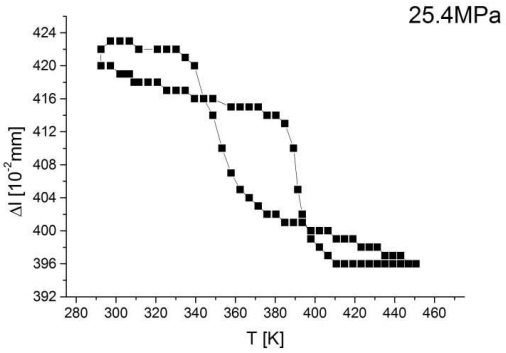

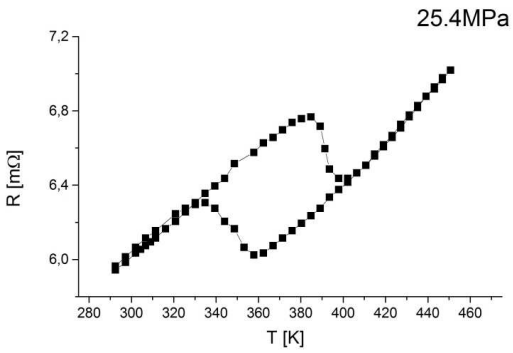

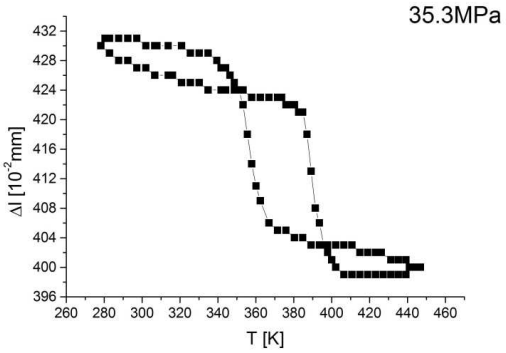

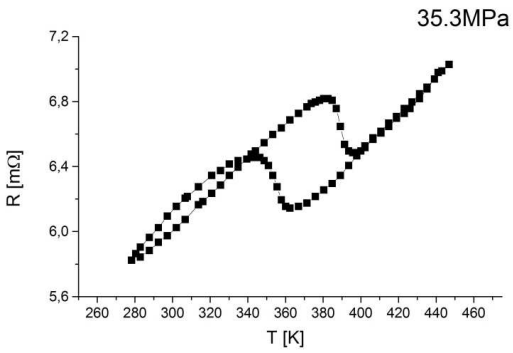

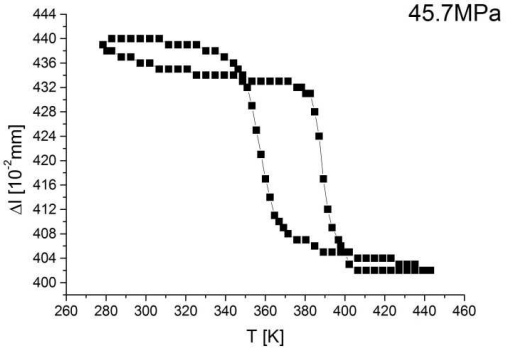
45.7MPa
Δl [10^{-2}mm]
T [K]

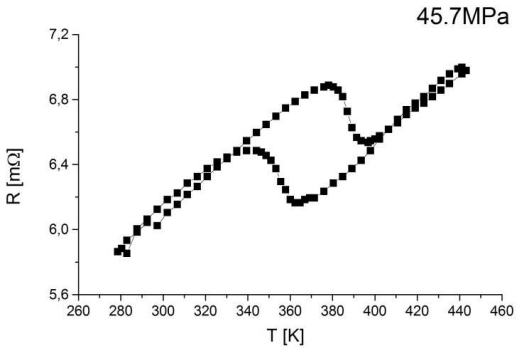
45.7MPa
R [mΩ]
T [K]

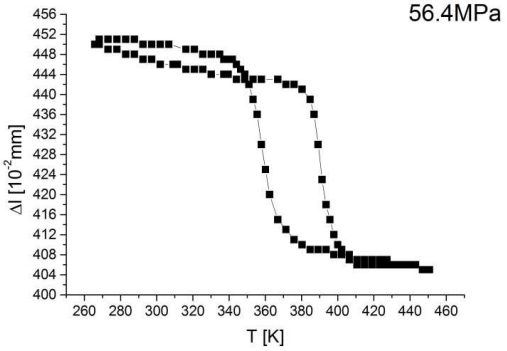
56.4MPa
Δl [10^{-2}mm]
T [K]

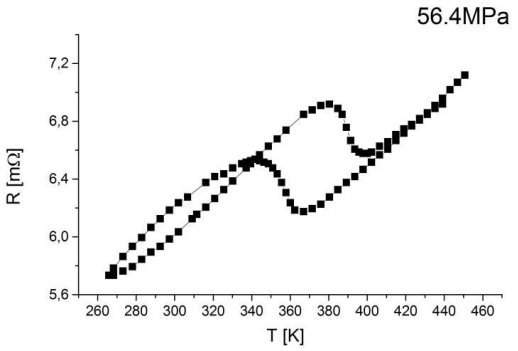
56.4MPa
R [mΩ]
T [K]

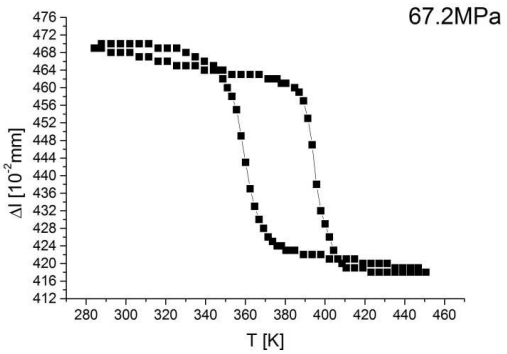
67.2MPa
Δl [10^{-2}mm]
T [K]

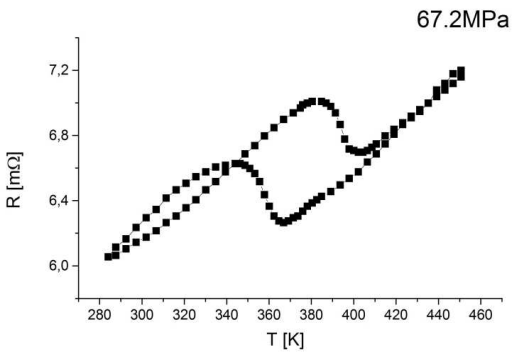
67.2MPa
R [mΩ]
T [K]

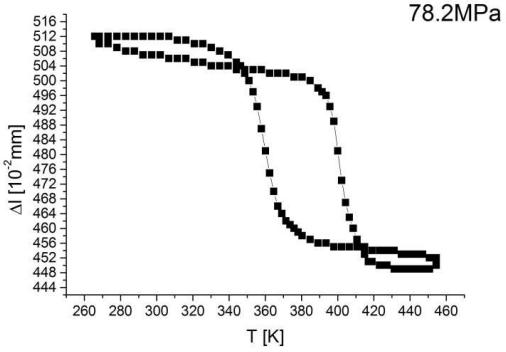
78.2MPa
Δl [10-2mm]
T [K]

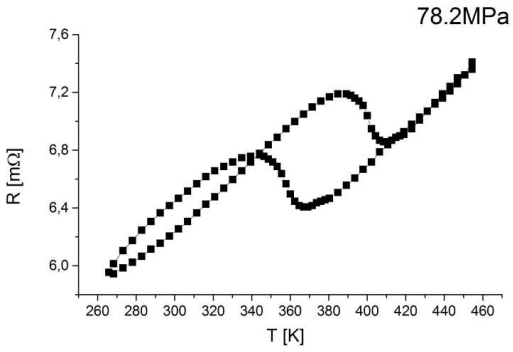
78.2MPa
R [mΩ]
T [K]

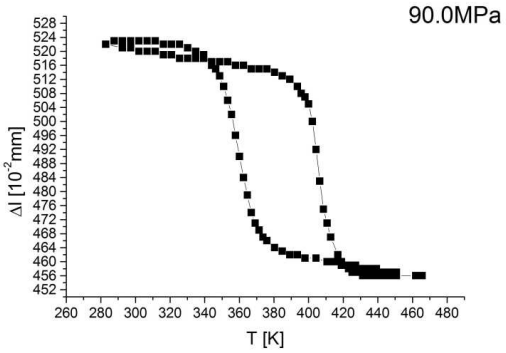
90.0MPa
Δl [10-2mm]
T [K]

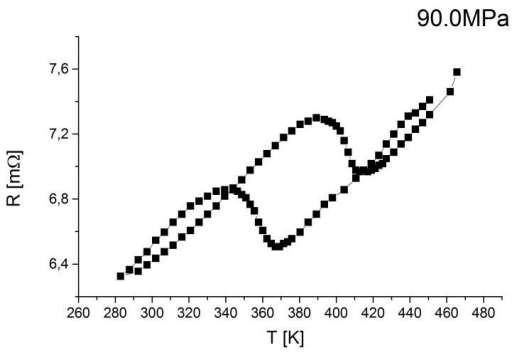
90.0MPa
R [mΩ]
T [K]

Appendix B

Measured hysteresis curves on CuAlNi singlecristalline sample.

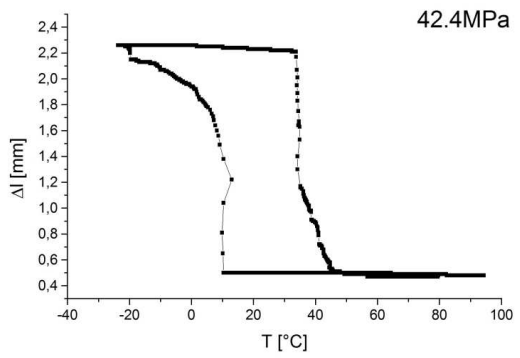

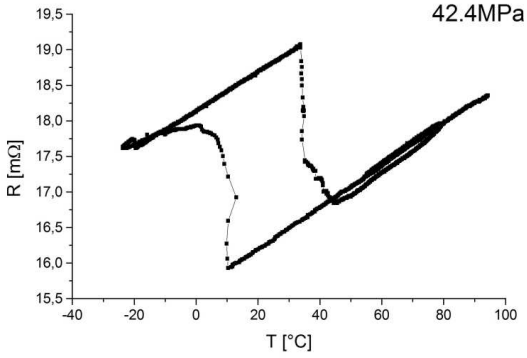

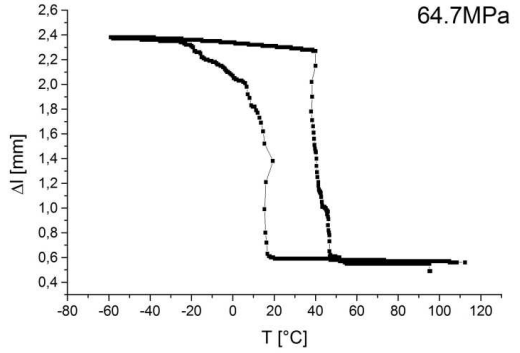

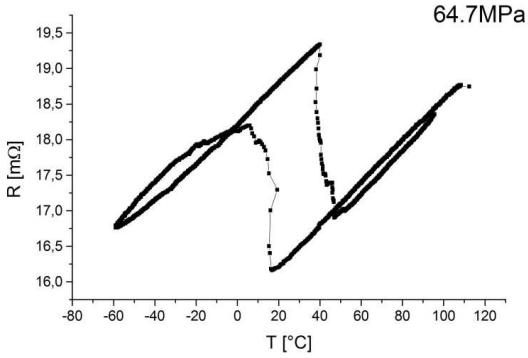

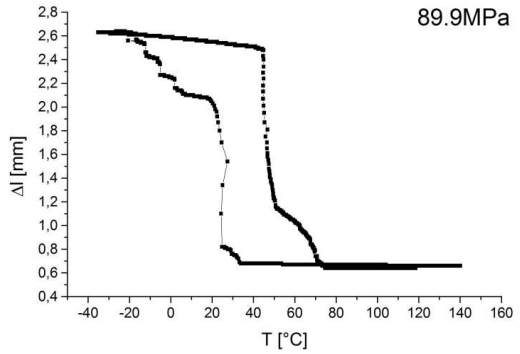

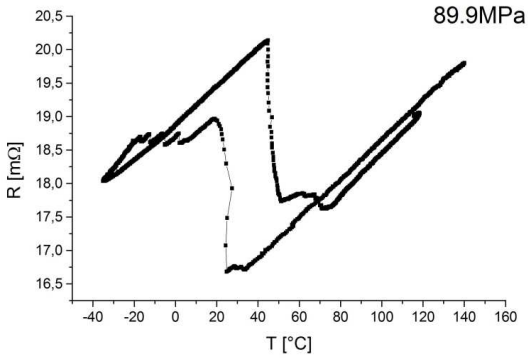

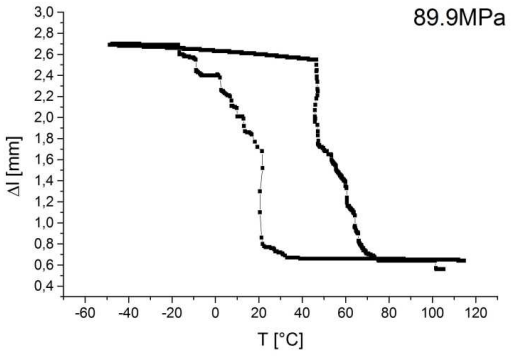
89.9MPa
Δl [mm]
T [°C]

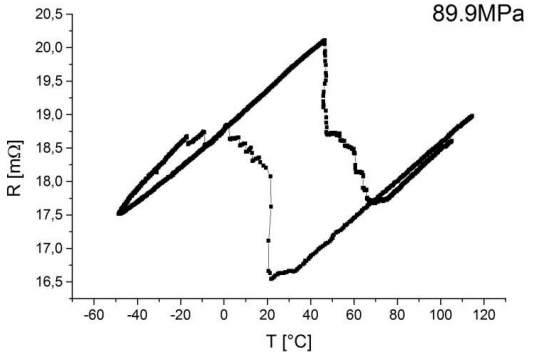
89.9MPa
R [mΩ]
T [°C]

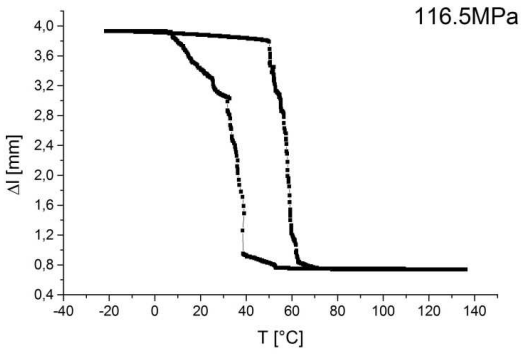
116.5MPa
Δl [mm]
T [°C]

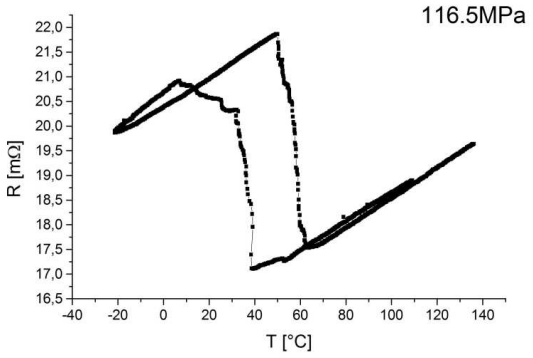
116.5MPa
R [mΩ]
T [°C]

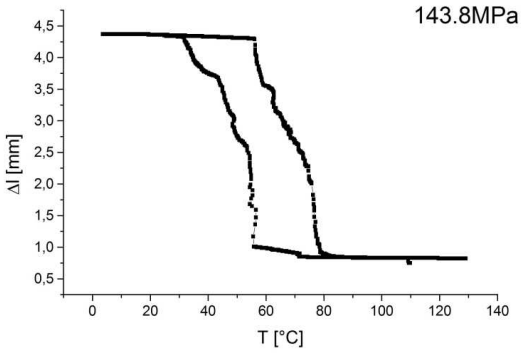
143.8MPa
Δl [mm]
T [°C]

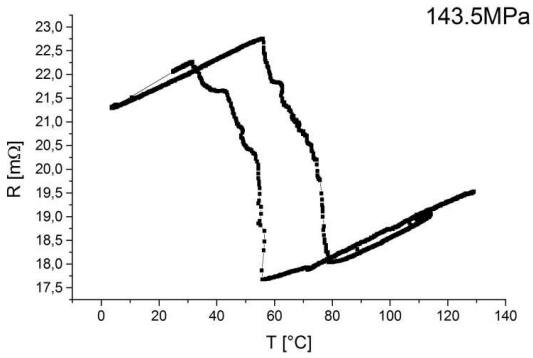
143.5MPa
R [mΩ]
T [°C]

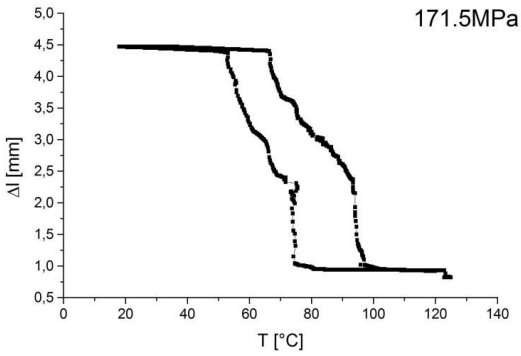
171.5MPa
Δl [mm]
T [°C]

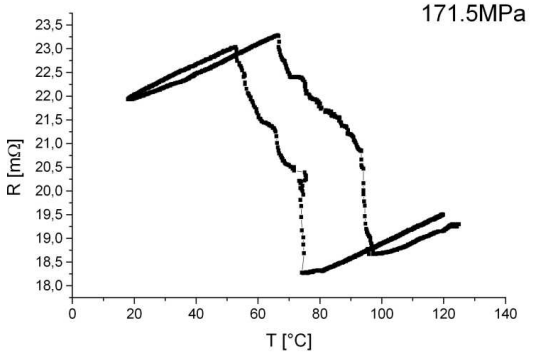
171.5MPa
R [mΩ]
T [°C]

Appendix C

Calculated and measured hysteresis loops of the different types of martensit phases.

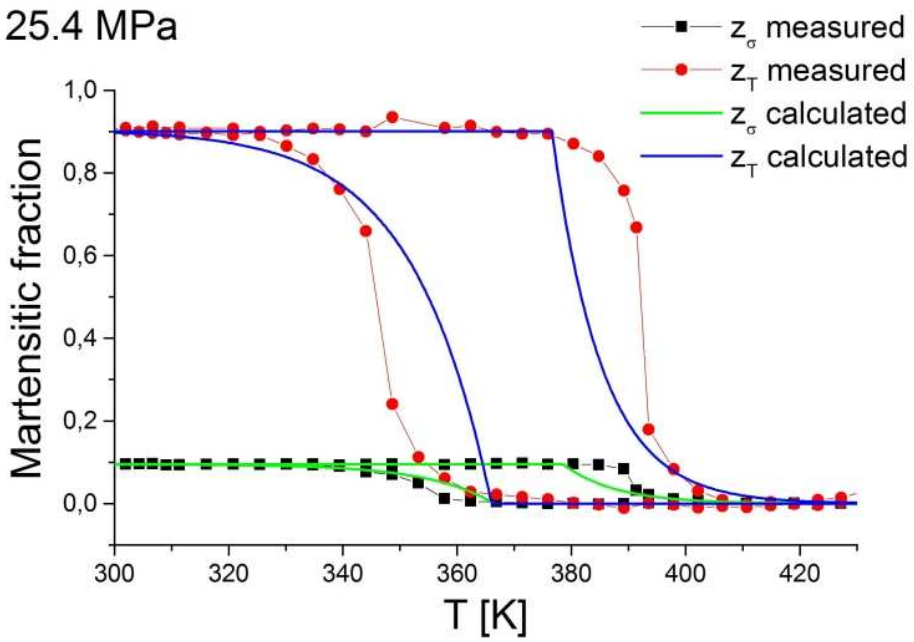

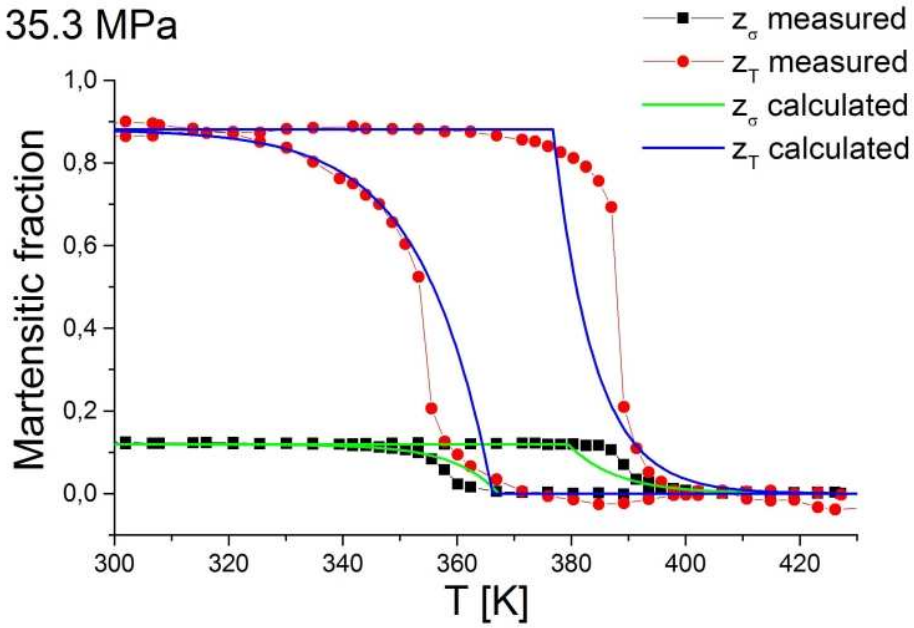

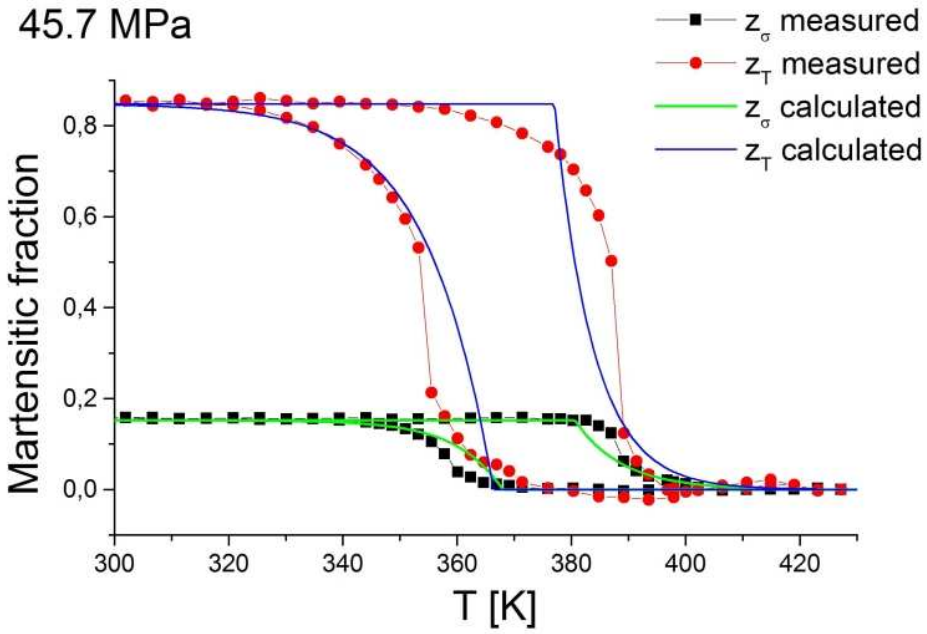
45.7 MPa
z_σ measured
z_T measured
z_σ calculated
z_T calculated
Martensitic fraction
0,0
0,2
0,4
0,6
0,8
300
320
340
360
380
400
420
T [K]

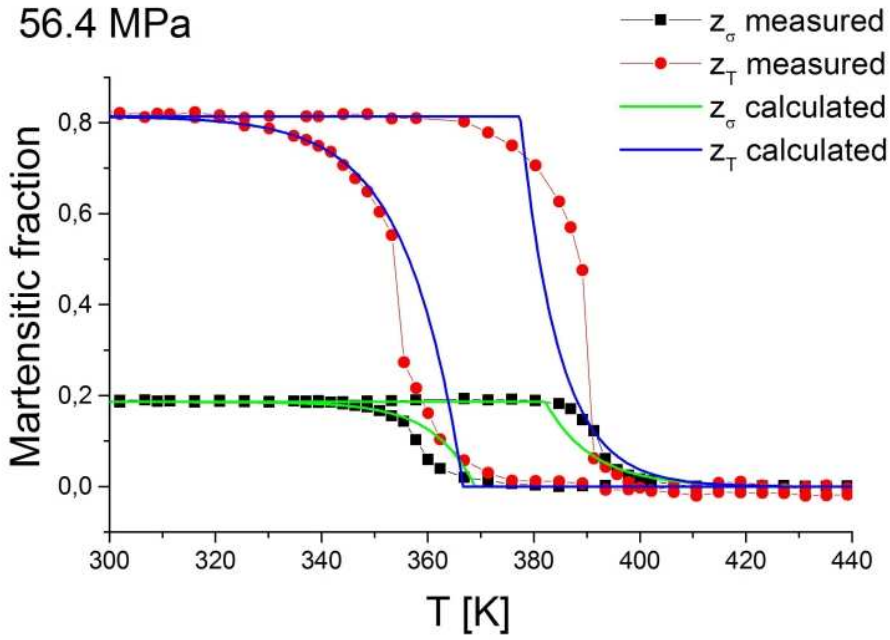
56.4 MPa
z_σ measured
z_T measured
z_σ calculated
z_T calculated
Martensitic fraction
0,0
0,2
0,4
0,6
0,8
300
320
340
360
380
400
420
440
T [K]

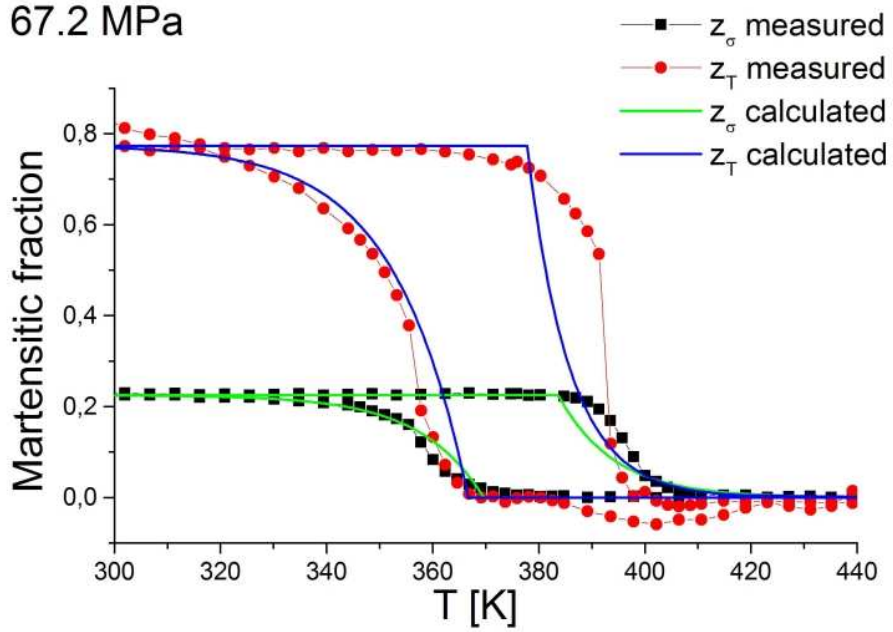
67.2 MPa
z_σ measured
z_T measured
z_σ calculated
z_T calculated
Martensitic fraction
0,0
0,2
0,4
0,6
0,8
300
320
340
360
380
400
420
440
T [K]

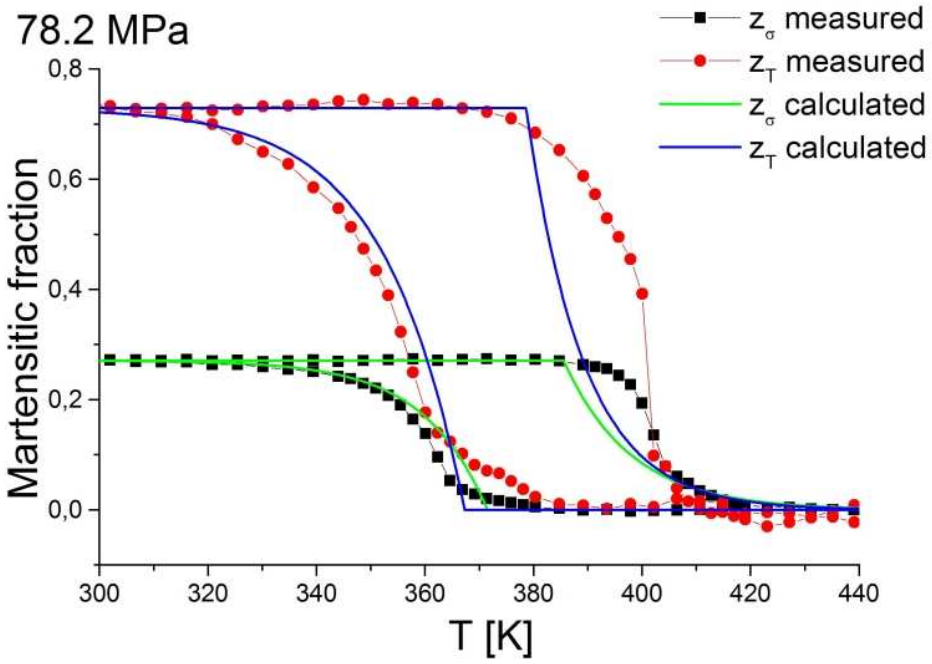
78.2 MPa
z_σ measured
z_T measured
z_σ calculated
z_T calculated
Martensitic fraction
0,0
0,2
0,4
0,6
0,8
300
320
340
360
380
400
420
440
T [K]

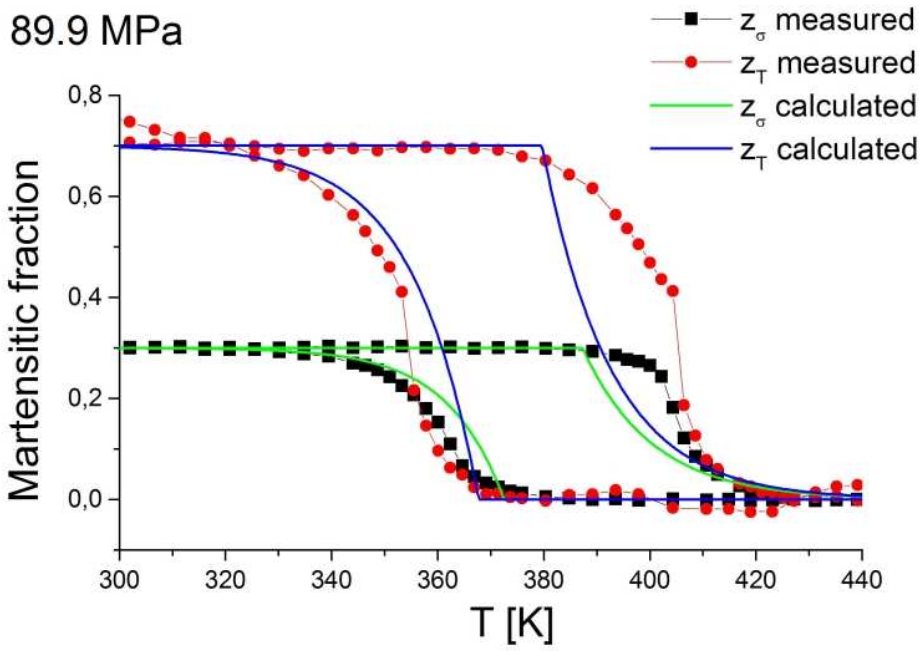
89.9 MPa
z_σ measured
z_T measured
z_σ calculated
z_T calculated
Martensitic fraction
0,0
0,2
0,4
0,6
0,8
300
320
340
360
380
400
420
440
T [K]